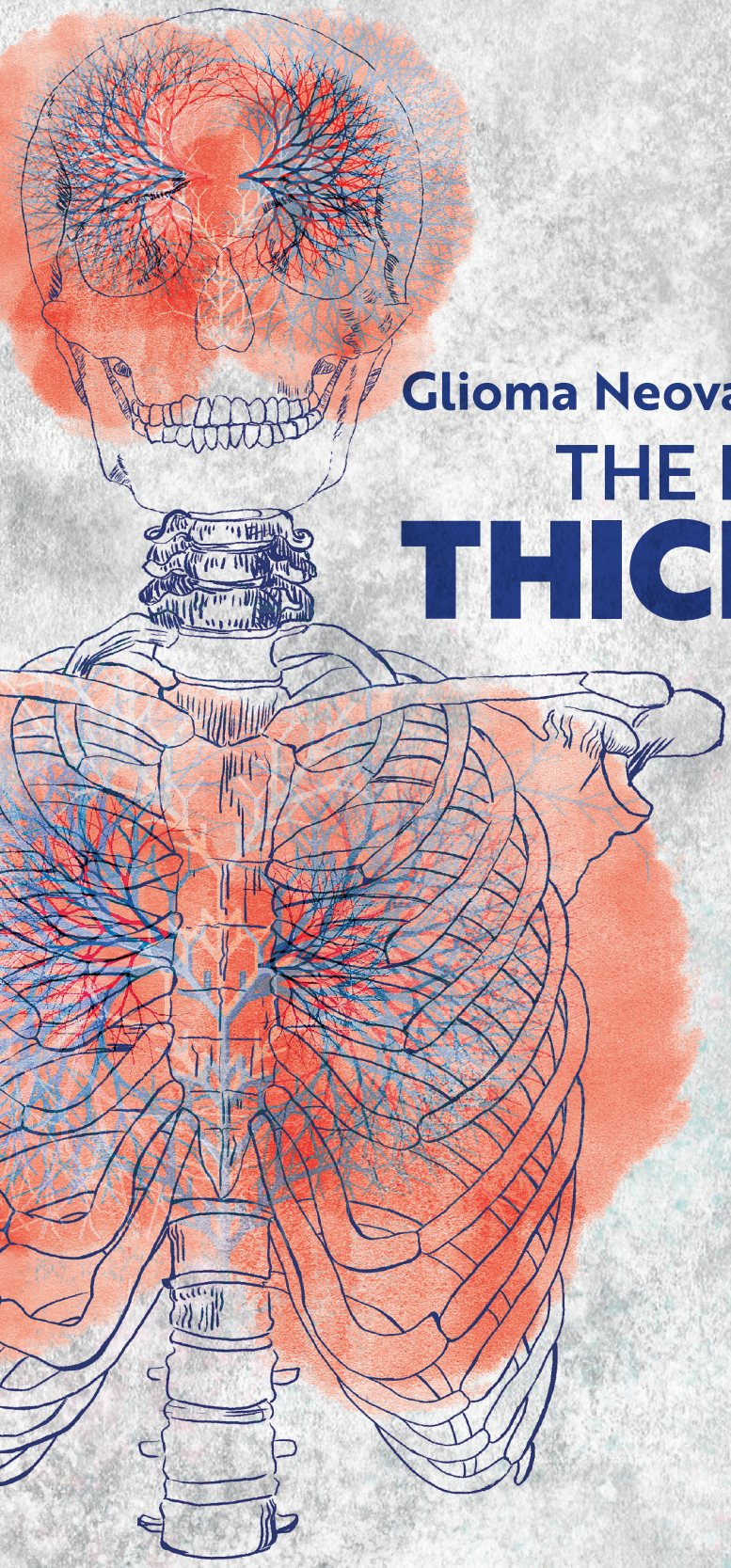

Glioma Neovascularization

THE PLOT THICKENS

KARIN HUIZER

Embargo

Glioma Neovascularization

THE PLOT THICKENS

KARIN HUIZER

Erasmus University Rotterdam

The research described in this thesis was financially supported by the
"Tumor-Immuno Pathologie (TIP)" Laboratory (Support Casper):

https://www.supportcasper.nl/nl/over-support-casper/onderzoek/studies/tumor-immuno-pathologie-laboratorium

ISBN: 978-90-8030-835-0

Cover and Acknowledgements design:
(https://aumenstudios.com/)

Au + Men Studios

Layout and printing:
Jennifer Sanders, Drukkerij Sanders
(https://www.sanders.nl/)

Glioma Neovascularization

THE PLOT THICKENS

KARIN HUIZER

PROEFSCHRIFT

ter verkrijging van de graad van doctor aan de
Erasmus Universiteit Rotterdam
op gezag van de
rector magnificus Prof.dr. R. Engels
en volgens besluit van het College voor Promoties.

De openbare verdediging zal plaatsvinden op

dinsdag 1 december 2020 om 9:30 uur

door

Karin Huizer

geboren te Ridderkerk

PROMOTIECOMMISSIE

Promotor:

Prof. dr. J.M. Kros

Copromotores:

Dr. D.A.M. Mustafa

Dr. A. Sacchetti

Beoordelingscommissie:

Prof.dr. C.M.F. Dirven

Prof.dr. R.A.W. van Lier

Prof.dr. D.J.G.M. Duncker

CONTENTS

CHAPTER 1

IMPROVING THE CHARACTERIZATION OF ENDOTHELIAL PROGENITOR CELL SUBSETS BY AN OPTIMIZED FACS PROTOCOL

PLOS ONE

RESEARCH ARTICLE

Improving the characterization of endothelial progenitor cell subsets by an optimized FACS protocol

Karin Huizer, Dana A. M. Mustafa, J. Clarissa Spelt, Johan M. Kros*, Andrea Sacchetti

Department of Pathology, Erasmus MC, Rotterdam, The Netherlands

* j.m.kros@erasmusmc.nl

Abstract

The characterization of circulating endothelial progenitor cells (EPCs) is fundamental to any study related to angiogenesis. Unfortunately, current literature lacks consistency in the definition of EPC subsets due to variations in isolation strategies and inconsistencies in the use of lineage markers. Here we address critical points in the identification of hematopoietic progenitor cells (HPCs), circulating endothelial cells (CECs), and culture-generated outgrowth endothelial cells (OECs) from blood samples of healthy adults (AB) and umbilical cord (UCB). Peripheral blood mononuclear cells (PBMCs) were enriched using a Ficoll-based gradient followed by an optimized staining and gating strategy to enrich for the target cells. Sorted EPC populations were subjected to RT-PCR for tracing the expression of markers beyond the limits of cell surface-based immunophenotyping. Using CD34, CD133 and c-kit staining, combined with FSC and SSC, we succeeded in the accurate and reproducible identification of four HPC subgroups and found significant differences in the respective populations in AB vs. UCB. Co-expression analysis of endothelial markers on HPCs revealed a complex pattern characterized by various subpopulations. CECs were identified by using CD34, KDR, CD45, and additional endothelial markers, and were subdivided according to their apoptotic state and expression of c-kit. Comparison of UCB-CECs vs. AB-CECs revealed significant differences in CD34 and KDR levels. OECs were grown from PBMC-fractions We found that viable c-kit$^+$ CECs are a candidate circulating precursor for CECs. RT-PCR to angiogenic factors and receptors revealed that all EPC subsets expressed angiogenesis-related molecules. Taken together, the improvements in immunophenotyping and gating strategies resulted in accurate identification and comparison of better defined cell populations in a single procedure.

Citation: Huizer K, Mustafa DAM, Spelt JC, Kros JM, Sacchetti A (2017) Improving the characterization of endothelial progenitor cell subsets by an optimized FACS protocol. PLoS ONE 12(9): e0184895. https://doi.org/10.1371/journal.pone.0184895

Editor: Francesco Bertolini, European Institute of Oncology, ITALY

Received: June 8, 2017

Accepted: September 1, 2017

Published: September 14, 2017

Data Availability Statement: All relevant data are within the paper and its Supporting Information files.

Funding: The authors received no specific funding for this work.

Competing interests: The authors have declared that no competing interests exist.

Introduction

Over the last decades circulating EPCs have been extensively studied in the context of both health and disease. EPCs take part in neovascularization and their levels are used to monitor the effects of therapy [1–4]. Notably, the term EPC is not only used for cells with genuine endothelial lineages, but also for other cell types supporting neovascularization, including

hematopoietic progenitor cells (HPCs) [1, 5–8]. HPCs are bone marrow derived [9] and home to ischemic or neoplastic tissues that secrete chemo-attractants and, following differentiation, contribute to angiogenesis by secreting proangiogenic factors [10–12]. Another subset of circulating EPCs is capable of generating *in vitro* outgrowth endothelial cells (OECs). The *in vivo* equivalent of OECs is believed to contribute to vascular regeneration [7, 13–17]. While most circulating endothelial cells (CECs) are damaged or apoptotic mature endothelial cells with no progenitor potential [18–21], there may well be a small CEC fraction of viable endothelial progenitors from which OECs can be grown. However, the kinship of CECs and OECS has not been proven, mainly because authors used unsorted PBMCs or PBMCs enriched for specific markers using magnetic beads, instead of FACS sorting [1, 7, 20, 22–26]. The accurate identification of EPC subsets, and their subdivision, is challenged by the low frequencies of these cells in the bloodstream, the different ways of their isolation, and the discrepant immuno-phenotypical definitions used [1, 5, 8, 23, 24, 27–31]. The introduction of validated procedures of isolation and work-up would greatly improve accurate comparisons of the various populations and literature data on the EPC subsets, and shed more light on the genuine source of OECs [7, 32].

Here we present a protocol for the accurate identification, characterization, and subdivision of HPCs, CECs and culture-derived OECs from peripheral blood samples of healthy adults (AB) and umbilical cord blood (UCB). The procedure includes the analysis of stem cell markers [32] and RT-PCR on sorted cells allows for the detection of markers beyond cell-surface expression. By following the procedures described we succeeded in demonstrating the similarities between OECs and CECs, suggestive of kinship between these populations. PCR analysis to the distinct EPC subsets and HUVECs for the detection of angiogenic factors and receptors revealed angiogenic capacities of all subsets.

Material & methods

Medical-ethical considerations

This study was approved by the Medical Ethics Committee of the Erasmus Medical Center, Rotterdam, The Netherlands (MEC-2011-313) and carried out in adherence to the Code of Conduct of the Federation of Medical Scientific Societies in the Netherlands (http://www.federa.org/codes-conduct).

Blood samples and preparation

Eighteen samples of adult peripheral blood (24–40 ml) and 15 samples of umbilical cord blood (12 ml) were used for this study. The samples were collected in BD vacutainer EDTA tubes and stored at room temperature in the dark for $\leq$18 hours. Blood was then diluted 1:1 with PBS-0,5 mM EGTA, and PBMCs were isolated using Ficoll Paque plus (GE Healthcare).

FACS analysis and sorting

PBMCs were incubated with 10% mouse serum to block unspecific antibody binding and stained 20' with specific antibodies (S1 Table). To get saturation, OECs/HUVECs were stained with 1 μg Ab/10^6 cells/200 μl, and PBMCs with 1.5 μg Ab/10^7 cells/200 μl. KDR staining was amplified using a 3-step protocol: 1) anti-KDR-APC; 2) anti-APC-biotin; 3) streptavidin-APC. After staining the cells were washed twice and re-suspended in PBS, 10% BSA, 0,1μg/ml Hoechst 3h3258 to mark dead cells. All steps were performed on ice. Live nuclear staining was performed with the cell permeant Hoechst33342 (Sigma-Aldrich), 10μM for 30' at RT. FACS analysis/sorting was performed with a BD FACS Aria III (BD Biosciences, New Jersey, US)

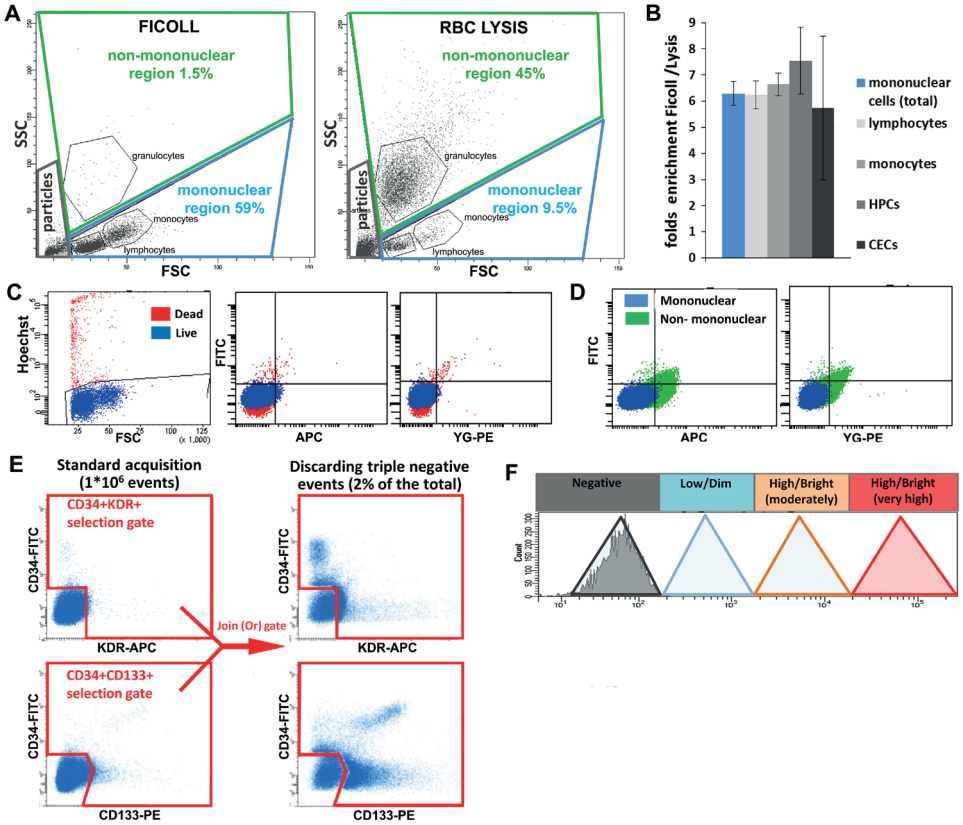

Fig 1. Basic strategies of sample preparation and FACS analysis. A. FACS plots of Ficoll-enriched PBMCs vs. RBC lysis-based preparations. To prevent exclusion of large cells, a large mononuclear-cell gate was applied. **B**. Ratios of enrichment of total live PBMCs, lymphocytes, monocytes, HPCs (as defined in Fig 2) and CECs (as defined in Fig 3) by Ficoll vs. RBC lysis. **C-D**. Examples of reduction of background (auto-fluorescence) by stringent exclusion of dead cells using Hoechst 33258 (C) and (residual) granulocytes (D). **E**. Basic procedure used, in addition to standard acquisition (1x10^6 total events), to enrich for target cells by discarding triple CD34/CD133/KDR negative events. Upper left plot: selection of CD34$^+$ and KDR$^+$ cells; lower left plot: selection of CD34$^+$ and CD133$^+$ cells. Right panels: result of a "Join (Or) gate" in FACS DIVA. KDR$^+$ CD34$^+$ (upper plot) and CD133$^+$ CD34$^+$ (lower plot) populations are better visualized. **F**. Delineation of a scale of FACS-based fluorescence levels. Negative peak = unstained or isotype control; low (dim) = within 1 log from negative; high (bright) = more than 1 log from negative and ranging from moderately high (1st to 2nd log above negative) to very high (3rd log or higher). "Medium" is sometimes used to define populations in between low and high.

https://doi.org/10.1371/journal.pone.0184895.g001

using the parameters listed in (S1 Table). In the FSC/SSC plot, mononuclear cells were selected using a gate for high FSC cells excluding residual granulocytes, cellular debris and small particles (Fig 1 and S1 Fig). In the SSC-H/SSC-W and FSC-H/FSC-W plots single cells were selected and doublets excluded. Avital cells were gated out in a Hoechst-A/FSC-A plot. For the initial setup, fluorescence minus one (FMO) and isotype controls were used for each antibody (S2 Fig).

Annexin V staining

Following immunostaining, 5μl of Annexin-V-FITC (BD) or Annexin-V-biotin (BD), were added to 500,000 PBMCs in Annexin Buffer and left 20' on ice, followed by one washing step. Incubation with Annexin V-biotin was followed by streptavidin-APC staining. The FACS analysis was carried out in Annexin V buffer, 0,1μg/ml Hoechst 33258.

Generation of outgrowth endothelial cells

PBMCs were re-suspended in endothelial cell medium (EGM-2 + BulletKit; Lonza), seeded in culture flasks (Corning, polystyrene) at $2.5x10^6$ cells/cm^2, and incubated at 37˚C, 5% CO2. Medium was changed daily. When OECs reached 80% confluence, cells were passaged using Accutase (Sigma-Aldrich). Gelatin, collagen-I, and fibronectin coating were tested and compared to non-coated plates. Because coating did not significantly affect the generation of OECs we used uncoated plates.

RNA Isolation and RT-PCR

Gene expression was analyzed in HPCs (12 UCB and 10 AB; 2,000–70,000 cells), CECs (2 UCB and 1 AB; 600–2,000 cells), control leukocytes (3 UCB and 6 AB, $CD34^-CD133^-KDR^-CD45^+$), OECs (3 UCB and 1 AB; 500,000 cells), and HUVECs (2 separate cell lines, 500,000 cells). Cells were lysed in RLT buffer (Qiagen RNeasy micro kit) containing 1% β-mercaptoethanol, vortexed for 1' and stored at -80˚C. RNA was isolated using the RNeasy micro kit (Qiagen). cDNA was synthesized using the qScript cDNA SuperMix kit from Quanta. Due to low numbers of sorted HPCs and CECs, the PreAmp cDNA amplification kit (Quanta) was used (up to 100 genes). Amplified cDNA was diluted 20-fold. RT-PCR was performed following manufacturer instructions (Quanta) and 200nM primers. Pre-amplification was extensively validated to determine whether the correct proportion of transcripts was retained. PCR primers are listed in (S1 Table). In order to analyze the cells at functional level, RT-PCR to 10 angiogenic factors and receptors (apelin, PDFDβ, PDGFR, SCF, FGF, EGF, EGFR, VEGFA, Tie-1 and Tie-2) was carried out for all EPC subsets.

Statistical analysis

The non-parametric Mann-Whitney U test in SPSS (version 21.0.0.1) was used to determine differences in HPC and CEC frequencies and in gene expression.

Results

Sample preparation and FACS analysis

The mononuclear cell fraction containing the EPC subsets was on average six times enriched by using Ficoll as compared to standard RBC lysis buffer, thereby leaving the ratios between the PBMCs and EPC subsets unaltered (Panels A and B in Fig 1 and Panel A and B in S1 Fig). The background caused by autofluorescence and unspecific antibody binding was reduced by excluding dead cells by Hoechst 33258 staining (Panel C in Fig 1) and residual non-mononuclear cells (Panel D in Fig 1) by gating them out in a FSC/SSC plot. The mononuclear gate applied was large enough to include CECs eventually present in the high FSC region (Panel A in Fig 1 and Panel C in S1 Fig). Spillover between fluorochromes was minimized by using one fluorescent channel per laser, with the exception of the 405 nm laser (S1 Table). Bright antibodies or signal amplification were used to gain sufficient resolution for each marker. The visualization of rare cells was improved by discarding triple CD34/KDR/CD133 negative events, thereby reducing data overload and enabling the recording of larger sized samples. By

setting a threshold around 2% positive events, the target cells were ~ 50 times enriched (Panel E in Fig 1) and reliable visualization was accomplished for populations with a frequency as low as CECs in AB (~1/1*10^6 PBMCs)[21]. To enable direct visual comparison of fluorescent levels between populations and samples, a common scale of fluorescence intensity based on literature and our own data was applied in all FACS plots (Panel F in Fig 1) [1, 33].

Characterization and quantification of HPCs

Following current definitions [5, 17, 34], HPCs were initially identified as a $CD34^{+/high}$ cluster and refined by gating $CD45^{low}$. Based on the expression intensities for CD133, HPCs were sub-divided in $CD133^{high}$, $CD133^{low}$, and $CD133^{neg}$ cells (Panela A and B in Fig 2) [1, 5, 17, 34]. A bright antibody was necessary to properly visualize different CD133 levels (Panel A in Fig 2). HPCs were located in between lymphocytes and monocytes in the FSC/SSC plot (Panel C in Fig 2). Gating on FSC/SSC converged with CD45-based gating, and provided further purification of HPCs, mainly by cleaning the $CD133^{neg}$ subpopulation. By using both CD45 and FSC/SSC, HPC gating was refined over previous protocols. To verify the identity of the HPCs we tested the expression of CD133 and c-kit by RT-PCR on sorted HPC-fractions. The expression of CD133 was verified by RT-PCR and was at low levels also found in the $CD133^{neg}$ subpopulation (Panel E in Fig 2). mRNA expression for c-kit was found in all three subpopulations (Panel E in Fig 2) and appeared to be high and independent of CD133 levels. Overall, HPCs (calculated as ratio over $CD45^+$ PBMCs) were 5.8 times more frequent in UCB than in AB (Panel F in Fig 2). The frequencies of the three CD133-based subpopulations differed between UCB and AB. $CD133^{high}$ HPCs represented 72% of total HPCs in UCB but only 43% in AB.

Further HPC sub-classification was obtained by simultaneous staining for c-kit and CD133. Four sub-populations of HPCs were distinguished: $CD133^{neg}$c-kit^{high}, $CD133^{low}$c-kit^{high}, $CD133^{high}$c-kit^{high}, and $CD133^{high}$c-$kit^{neg/low}$ (the last only observed in AB samples) (Panels A and B in Fig 3). In addition, the expression of CD34 and CD45 was found to be positively associated with CD133 levels but independent of c-kit levels. $CD133^{neg}$ HPCs have the highest c-kit levels (Panel A in Fig 3 and Panels A-C in S3 Fig). Expression of the endothelial markers KDR, CD144, and CD146 was only observed in sporadic HPCs (Panels C-E in Fig 3). CD105 was expressed at very low levels, only partially crossing the negative gate. Preliminary co-expression analysis revealed that KDR, CD146, CD144, CD105 do not converge to the identification of a single population of EPCs [8], but each marker mostly identifies small independent subpopulations, (Panels D and E in Fig 3 and Panels D-F in S3 Fig).

Characterization and quantification of CECs

CECs were identified as $CD34^+KDR^+$ cells (Panel A in Fig 4) that are negative for CD45 (Panel B in Fig 4). Brightnesss of the staining was essential for proper CEC identification. Visualization of KDR required signal amplification (S1 Table) and the staining intensity of CD45 was crucial for separating $CD45^{neg}$ CECs from sporadic $CD45^{low}KDR^+$ HPCs across the $CD45^{neg}$ gate (Panel B in Fig 4). The frequency of CECs was significantly higher in UCB ($14/10^6$ $CD45^+$ PBMCs) than in AB ($1,9/10^6$ $CD45^+$ PBMCs) (Panels C and D in Fig 4). The CD34 and KDR levels encountered in UCB-CECs (mainly $CD34^{high}KDR^{+/high}$) differed from those in AB-CECs (mainly $CD34^{med}KDR^{low}$) (Panel C in Fig 4). The CECs expressed the endothelial markers CD146, CD144 and CD105 (Panel E in Fig 4 and Panel B in S4 Fig), which largely overlapped with KDR, confirming the endothelial identity of the selected population. Based on our data, CD146 and CD144 can be regarded as good substitutes for KDR in CEC identification, or as additional markers to refine the population. Immunopositivity for CD105 should be

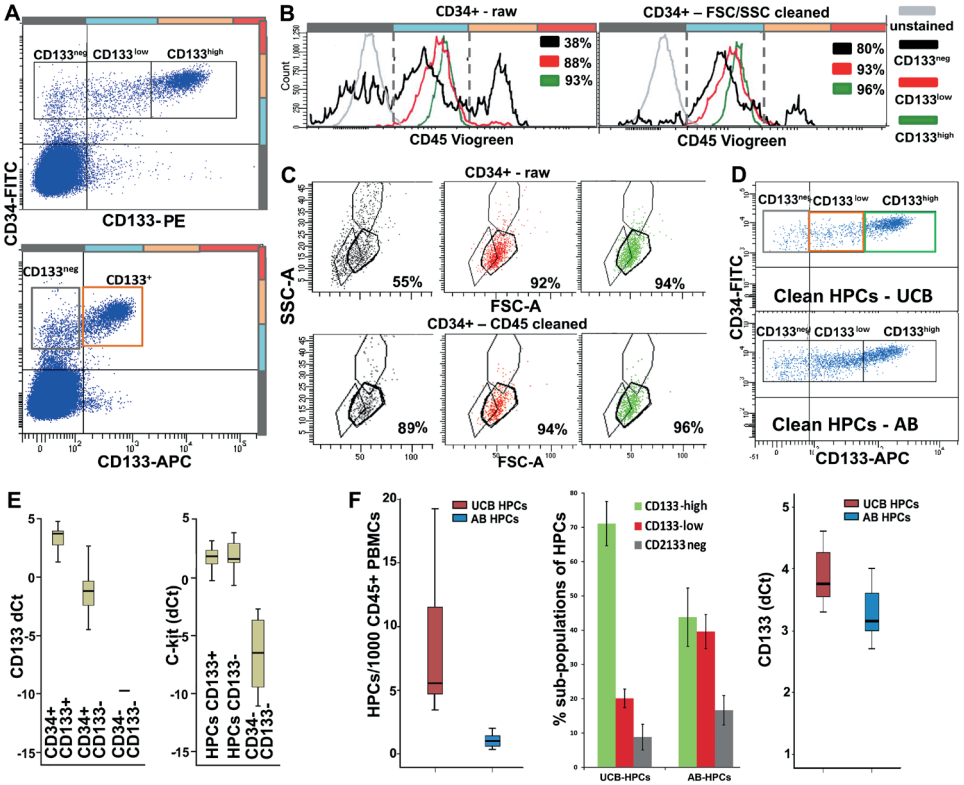

Fig 2. Identification and characterization of HPCs. A. Upper panel: HPCs in UCB and AB are initially selected as $CD34^{+/hi}$ cells and subdivided into $CD133^{hi}$, $CD133^{low}$ and $CD133^{neg}$. Lower panel: discrimination between CD133 levels is partially missed using a less bright antibody. **B**. HPCs are refined by gating a single peak in the $CD45^{low}$ region. Left plot: CD45 gating on raw HPCs ($CD34^{+/hi}$ events). Right plot: CD45 gating on $CD34^{+/hi}$ events pre-refined by FSC/SSC. CD45 levels slightly increase with CD133 expression (see also S3 Fig), still remaining within the "low" gate. The % of match of raw or pre-refined HPCs with the CD45low gate is indicated in the plots for each population. **C**. In a FSC/SSC plot, HPCs appear as a tight cluster in between lymphocytes and monocytes. Upper panel: FSC/SSC gating on raw HPCs ($CD34^{+/hi}$ events). Lower panel: FSC/SSC gating on $CD34^{+/hi}$ events pre-refined by CD45 levels. The % of match of raw or pre-refined HPCs with the FSC/SSC gate is indicated in the plots for each population. Comparison of B (left vs. right plot) and C (upper vs. lower panel) shows that CD45 and FSC/SSC gating converge to the identification of pure HPCs: partial overlapping in HPC cleaning indicates that the two approaches identify the same population, however each approach also provides some independent contribution to HPC purification. The less pure and most affected by cleaning gates appears the CD133neg fraction. **D**. FACS plots showing the distribution of pure HPCs (CD34 vs. CD133 plot) in UCB vs. AB. **E**. CD133 and c-kit RT-PCR in $CD34^{+}CD133^{+}$ cells (n = 22); $CD34^{+}CD133^{-}$ cells (n = 17) and $CD34^{-}KDR^{-}CD133^{-}$ PBMCs (n = 8) isolated from UCB. CD133 mRNA is detected in both $CD133^{+}$ and $CD133^{-}$ HPCs, although at different levels. c-kit mRNA further confirms the HPC identity of the $CD34^{+}CD133^{-}$ cells. **F**. Left panel: median frequency of HPCs in UCB (5,6 in $1*10^{3}$ $CD45^{+}$ PBMCs) and AB (0,97 in $1*10^{3}$ $CD45^{+}$ PBMCs, significantly lower than in UCB, Z = -4,9; p = $1{,}00E^{-06}$). Middle panel: percentage ± SD of the three CD133-based HPC subpopulations in UCB vs. AB. Right panel: RT-PCR confirms higher CD133 expression by total UCB-HPCs than AB-HPCs.

https://doi.org/10.1371/journal.pone.0184895.g002

carefully evaluated since CD105-expressing HPCs (Panel C in Fig 3) that pass the CD45 negative gate may contaminate the CEC population. Notably, KDR yielded the cleanest background on HPCs followed by CD144, and CD146 (Panel C in Fig 3), and the best match (98% vs. only 90% with CD146 and CD144) in CEC-identification (Panel E in Fig 4 and Panel B in S4 Fig).

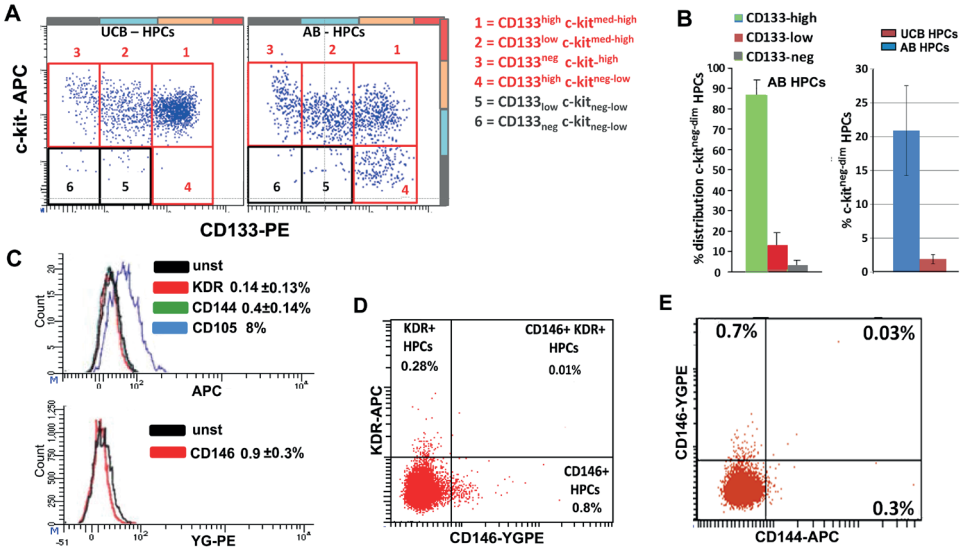

Fig 3. HPCs: Analysis of c-kit and endothelial markers. A. FACS analysis for c-kit vs. CD133 confirms the PCR results and refines HPC subdivision. In UCB, c-kit medium-high levels were observed in all the CD133-based subpopulations (with the exception of sporadic events). In AB, an additional c-kit$^{neg-low}$ cluster was observed within the CD133^{high} subpopulation, while the highest c-kit levels were observed on the CD133^{neg} cells (see also S3 Fig). **B**. Left: distribution of c-kit$^{neg-low}$ cells between the CD133-based subpopulations in AB. Right: quantification of c c-kit$^{neg-low}$ cells in AB vs UCB. Right:. **C**. KDR, CD144, CD146 are sporadically expressed by HPCs. CD105 is dimly expressed but only a fraction of cells crosses the negative gate (8%). The percentages of positive cells are indicated in the plots. **D**. Analysis of KDR vs. CD146 expression in HPCs (UCB): the markers do not match but identify independent subpopulations. For better visualization, we used a UCB sample with high frequency of HPCs and relatively high KDR expression on HPCS (see also Panels D and E in S3 Fig). **E**. Analysis of CD144 vs. CD146 expression in HPCs: the two markers mostly identify independent subpopulations (see also Panel F in S3 Fig).

https://doi.org/10.1371/journal.pone.0184895.g003

RT-PCR confirmed that KDR expression is CEC-specific and absent in HPCs (Panel C in S4 Fig). Because CD31 was expressed at high levels in other cell types, including HPCs, it cannot be considered as a selective marker for CECs. Since CD133 was found to be expressed by few CECs it cannot be regarded as a negative marker for these cells (Panel E in Fig 4). Further subdivision of CECs was obtained by the analysis of c-kit. Around 15% of CECs appeared to be c-kit positive and c-kit expression was associated with higher CD34 and KDR levels. RT-PCR confirmed c-kit expression in CECs. Notably, c-kit mRNA levels were high and comparable to those of HPCs, despite much lower surface protein expression (Panel F in Fig 4), indicative of a discrepancy between mRNA and protein levels or surface expression of this marker.

In order to distinguish nucleated CECs from contaminating non-nucleated events, mainly aggregates of endothelial micro-particles, representative samples were stained with the nuclear dye Hoechst 33342 and all CECs appeared to be nucleated by FACS analysis (Panel A in Fig 5) and post-sorting microscopic inspection. Since CECs are reported to be apoptotic, apoptosis in these cells was assessed by Annexin-V staining. 78 (±4) % of CECs appeared to be apoptotic vs. only 8% of HPCs (Panel B in Fig 5). The pan-caspase inhibitor Z-VAD-FMK, added immediately after blood sampling, did not reduce the apoptotic fraction, which remained on average 80%, indicating that the cells were apoptotic from the time they entered the bloodstream. The expression of c-kit in CECs was associated with lower apoptosis (Panel B in Fig 5).

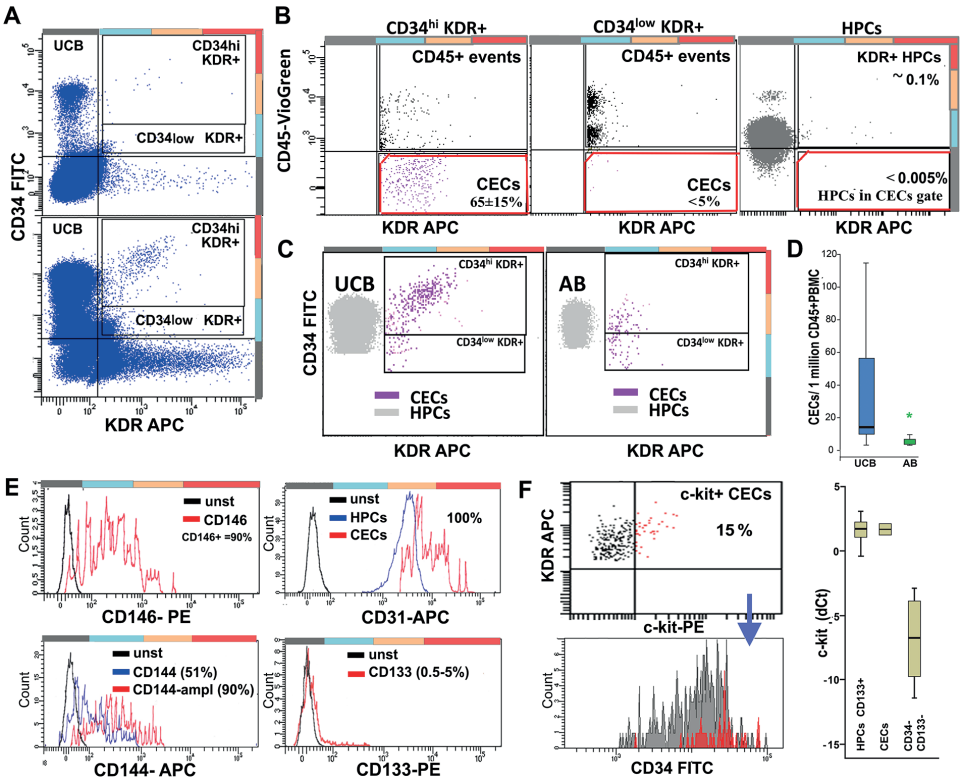

Fig 4. Identification, characterization, and quantification of CECs. A. Initial selection of CECs (UCB) on a CD34 vs. KDR plot ($1x10^6$ events) by gating KDR^+ cells at different CD34 levels. Lower panel: the acquisition of large sized samples was reached by discarding triple CD34/CD133/KDR negative events resulting in better visualization of CECs. **B**. Subsequently, true KDR^+CD45^{neg} CECs are selected in a CD45 vs. KDR plot. Most CECs belong to the CD34 high region (left plot), since KDR^+ $CD34^{low}$ events are almost entirely $CD45^+$ (middle plot). Right plot: the CD45 gate applied efficiently discriminates CECs from sporadic KDR^+ HPCs (selected by CD34 and FSC-SSC). **C**. Comparison of UCB-CECs (left plot) and AB-CECs (right plot). For reference: HPCs are shown in gray. In UCB, most CECs cluster at CD34 levels above HPCs and are KDR^{med-hi}, while in AB CECs have significantly lower CD34 and KDR levels. **D**. Frequency of CECs in UCB ($14/10^6$ $CD45^+$ PBMCs) vs. AB ($1,9/10^6CD45^+$ PBMCs). In AB the levels are significantly lower (Z = -3,6; p = 3,00E-04). **E**. Marker expression by CECs. Upper left: 90% of KDR-selected CECs express CD146. **Lower left**: 90% of CECs express CD144 but only after signal amplification. **Upper right**: CD31 is highly positive in CECs, but does not discriminate CECs from HPCs. **Lower right**: CD133 is expressed by a minority of CECs. **F. Upper left**: Around 15% of the CECs appear positive for c-kit and c-kit positivity correlates with higher KDR and CD34 levels (lower left). **Right panel**: RT-PCR confirms the expression of c-kit by CECs at levels comparable with HPCs (n = 3) despite significantly lower surface expression.

https://doi.org/10.1371/journal.pone.0184895.g004

Generation and characterization of OECs

Following 2–10 days after seeding unsorted PBMCs, adherent spindle-shaped cells matching the morphologic characteristics of "early EPCs" (eEPCs) [1, 35–37] appeared in both AB and UCB at a similar frequency (Panels A and B in S5 Fig). Following 1–3 weeks of culturing, OECs or "late EPCs" appeared in 5 out of 6 UCB samples and 2 out of 10 AB samples (Panel C in S5 Fig). From UCB also more colonies were generated (20 to 30) than from AB (1 and 10) per PBMC sample corresponding to 10 ml of original blood. The OECs displayed the characteristic cobblestone morphology, expressed von Willebrand factor (S5 Fig) and formed tube-

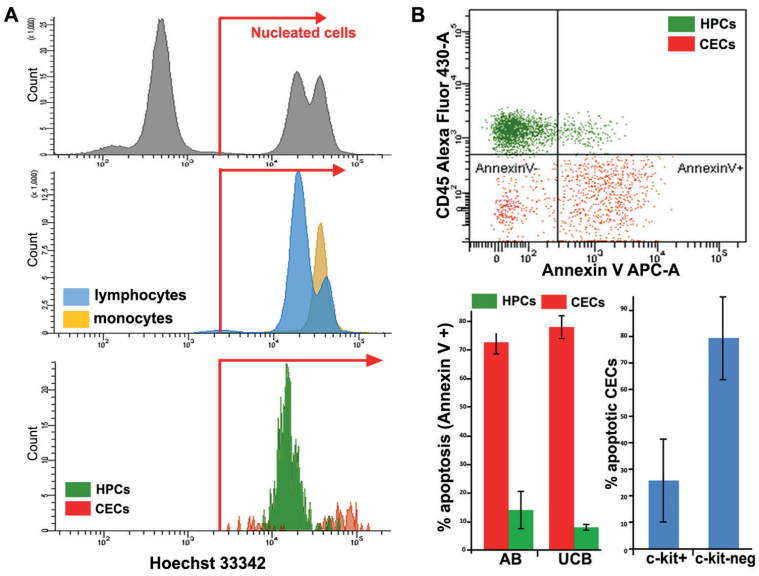

Fig 5. Definition of nucleated events and apoptosis in CECs and HPCs. A. FACS analysis of live nuclear staining with Hoechst 33342. Upper plot: nucleated events are separated from non-nucleated ones using erythrocytes and mononuclear cells as a reference. Medium plot: lymphocytes and monocytes are 100% nucleated. Lower plot: both CECs (red) and HPCs (green) appear as nucleated cells. CECs show a bimodal distribution with a sub-G1 fraction (probably apoptotic, DNA-fragmented cells). **B**. Upper plot: representative Annexin V staining of CECs (selected using CD34-FITC, CD146-PE, CD45-VioGreen) and HPCs (selected using CD34-FITC and CD45-VioGreen) from UCB. Bottom left: percentages of apoptotic CECs and HPCs in AB and UCB. Bottom right: apoptosis in c-kit+ vs c-kit^{neg} CECs.

https://doi.org/10.1371/journal.pone.0184895.g005

like structures after several days. The OECs were harvested and FACS analyzed. HUVECs were used as reference endothelial cells. Both OECs and HUVECs expressed high and stable levels of CD31, CD144, CD146 and CD105 while CD14 and CD45 were not expressed (Panel A in Fig 6 and Panel A in S6 Fig). With the exception of a single outlier, CD133 expression was restricted to $\leq$5% of the OECs (Panel B in Fig 6), matching the CD133 expression in CECs (Panel E in Fig 4). The levels of c-kit, KDR and CD34 were heterogeneous and correlated positively with each other (Panels B and C in Fig 6 and Panels B and C in S6 Fig). Early passage OECs and HUVECs contained a larger fraction of cells expressing high levels of CD34, KDR and c-kit in comparison to the late passage ones (Panel B in Fig 6 and Panels B and D in S6 Fig).

To investigate whether CECs are the source of OECs, we cultured sorted CECs in parallel with sorted and unsorted total PBMCs, using a larger nozzle (100μm) and lower pressure (20 psi) to reduce cell damage. The sorted cells (both CECs and total PBMCs) did not generate OECs, while unsorted PBMCs did. However, spindle-shaped early EPCs were successfully obtained from sorted CD14^{+} cells (Panel B in S5 Fig), or total sorted PBMCs. This confirmed the sound procedure of sample preparation and sorting, and suggested that FACS sorting is too damaging for the vulnerable OEC precursors to generate OECs in culture. No correlation between the yield of OECs and that of eEPCs was noticed in individual samples or in UCB vs.

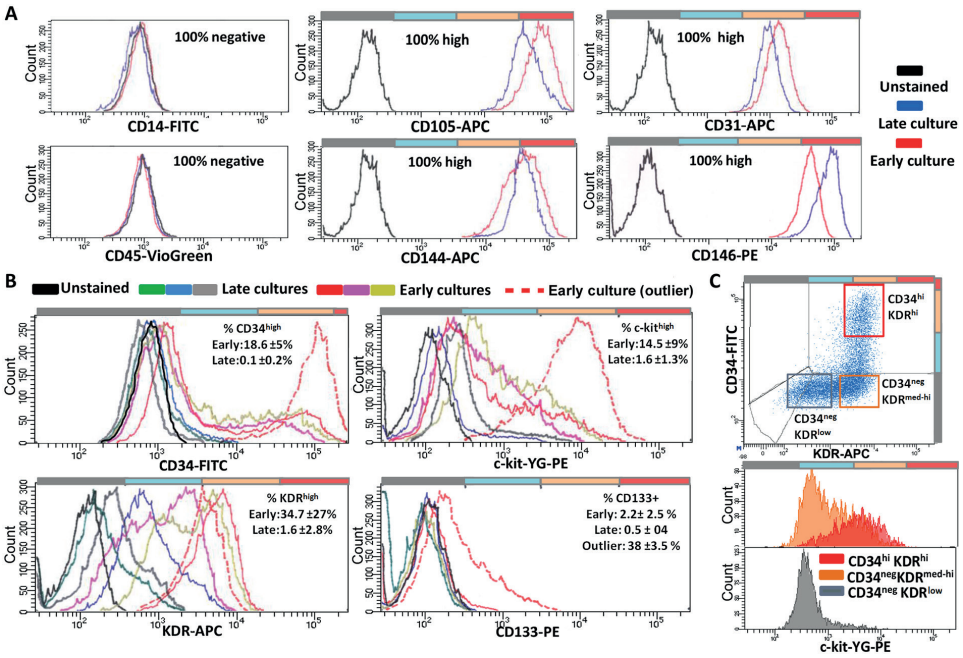

Fig 6. FACS analysis of OECs. FACS analysis of markers with homogeneous/stable **(A)** and heterogeneous/unstable (**B-C**) expression in early (passage 2–3) and late (passage >6) OEC cultures. **A**. No signals for CD45 and CD14. Staining for CD105, CD31, CD144, CD146 was homogeneously high and stable. **B**. CD34, KDR, and c-kit expression was heterogeneous and decreased with ageing of the cultures. The expression of CD133 was sporadic, with the exception of a single outlier, and slightly decreased with time in culture. For each marker, three examples of early and late cultures, and the outlier, are shown. **C**. Example of positive correlation (early passage OECs) between CD34, KDR, and c-kit. The markers define a triple high cluster, which is lost with ageing of the culture.

https://doi.org/10.1371/journal.pone.0184895.g006

AB (S5 Fig), confirming that these two cell types have different circulating precursors [7, 22, 25, 36, 37].

Functional analysis

We analyzed a total of 10 angiogenic factors and receptors (apelin, PDGFβ, PDGFR, SCF, FGF, EGF, EGFR, VEGFA, Tie-1 and Tie-2) by RT-PCR to all distinct EPC subsets and HUVECs. Angiogenic factors appeared to be expressed in all EPC subsets. However, there was variation in the levels of expression of these factors between the various EPC subsets (S7 Fig). The levels of all angiogenic factors and receptors were lowest in HPCs with the exception of EGF. Notably, CECs showed the highest expression of Apelin, PDGFβ, SCF, EGFR, and high expression of Tie-2 as compared to the other cell types. The expressional pattern of OECs and HUVECs almost completely overlapped. Overall, the pattern of OECs was much closer to CECs than to HPCs.

In addition, we added immunohistochemistry for endothelial markers to OECs (vWF, CD31, CD105) (S8 Fig). OECs were positive for all these markers, indicative of their endothelial lineage.

Discussion

In this study we describe a procedure that allows for efficient identification, quantification, and sorting of HPCs and CECs from peripheral blood samples, and culture-generated OECs. Moreover, we improve the characterization of these populations resulting in, for instance, better definition of subpopulations, and identification of a candidate circulating OEC precursor. By using a Ficoll-based density gradient instead of a standard RBC lysis, significant enrichment for PBMCs was achieved with preservation of the relative frequencies of HPCs and CECs over total PBMCs [38, 39]. Ficoll-enrichment, combined with stringent gating out of residual non-mononuclear cells, dead cells and debris, and accurate selection of markers, yielded clean and pure populations meeting the current standards of state-of-the art FACS procedures [40]. The procedure significantly reduced the sample size with preservation of the relative frequencies of HPCs and CECs over total PBMCs, allowing for significantly faster analysis and sorting of the target cells. The visualization and quantification of small populations was improved by selecting the events that were positive for the markers of interest to reduce data overload. This allowed recording the equivalent of ~$50^{*}10^{6}$ $CD45^{+}$ PBMCs within $1^{*}10^{6}$ events (about 10–25 ml of whole blood). Moreover, by avoiding the use of toxic nuclear dyes the cells remain fully viable for subsequent culture experiments and RNA extraction. By using the outlined protocol we were able to identify HPCs and CECs more accurately, and isolate 200 to30.000 cells for RT-PCR analysis from rare populations with frequencies as low as $1/1^{*}10^{6}$ $CD45^{+}$ PBMCs.

Improved characterization of HPCs

The current definition of HPCs is mainly based on a $CD34^{+/high}CD45^{low}$ signature with CD133 expression as an additional marker [5, 17, 34]. In the present analysis HPCs were identified as a $CD34^{+/high}$ $CD45^{low}$ cluster and further cleaned by gating a specific region in FSC/SSC (Panels B and C in Fig 2). Moreover, extending the definition of $CD133^{+}$ and $CD133^{neg}$ HPCs [17, 34], we propose a subdivision of HPCs in $CD133^{high}$, $CD133^{low}$, and $CD133^{neg}$ subpopulations. The HPC-identity of these subpopulations was confirmed by RT-PCR for CD133 and c-kit. By means of additional c-kit staining, HPCs were further subdivided by the demonstration of a $c\text{-}kit^{neg/low}$ subpopulation within the $CD133^{high}$ HPCs that was found only in AB, not UCB. So far, $c\text{-}kit^{neg/low}$ HPCs have not been identified in human blood samples and were only described as a quiescent population in mice [41]. CD133 or c-kit alone are no markers for the identification of HPCs [42, 43], since they range from negative to high. However, our data show that HPCs cannot be negative for CD133 and c-kit at the same time. Simultaneous staining of CD34+ cells (common denominator) for CD133 and c-kit leads to very accurate identification of HPCs as $CD133^{+}$ and/or $c\text{-}kit^{+}$ (Panels A and B in Fig 3). Following CD34, CD133, and-c-kit-based identification, FSC/SSC and CD45 gating can be applied to further purify the HPCs, in particular to exclude residual doublets with other cell types, and other false positives, mainly contaminating CECs.

In line with previous data [1, 27, 44], the frequency of HPCs was significantly higher in UCB than in AB. We observed a prevalence of $CD133^{bright}$ HPCs in UCB vs. AB. This finding fits with the notion that $CD133^{high}$ HPCs are more primitive stem cells serving functions in fetal and post-natal development [43, 45, 46]. We also found positive correlation of CD45 and CD34 expression with CD133 levels, and a negative correlation between c-kit and CD133 levels (S3 Fig). Analysis of the endothelial markers KDR, CD146, CD144, CD105 and CD31 lead to an estimation of the risk of HPC contamination of the CEC population using each single marker. In addition, the endothelial markers highlighted the presence of potentially interesting and rare subpopulations of HPCs like the KDR^{+}HPCs subpopulation that was described by Case et al. [5], and considered as a distinct EPC population by other authors [1, 8, 27–30]. We

show that the percentage of HPCs expressing endothelial markers (KDR, CD146, CD144, CD105) varies significantly and depends on the marker used. We also show that, with the exception of a few sporadic events, the markers are not concurrently expressed (Panels D and E in Fig 3 and Panels D-F in S3 Fig). Therefore, these HPCs expressing endothelial markers represent heterogeneous subpopulations requiring further exploration. Taken together, better identification of HPCs over the previous $CD34^{+/high}CD45^{dim}$ based protocol was reached and better subdivision was achieved by means of a combined CD34, CD133, and c-kit staining.

Identification and characterization of CECs

In addition to the current criteria used for CEC-identification, we aimed at a more precise characterization of these cells, delineation of sub-populations, and sorting for RT-PCR and culture. Since CECs are generally identified as nucleated $CD45^{neg}CD34^{+}$ events that additionally express an endothelial marker, i.e., CD146 or KDR [18, 20, 21, 23], we used the $CD34^{+/high}KDR^{+}CD45^{-}$ profile as a common denominator (Panels A and B in Fig 4). KDR-based CEC identification was confirmed by CD146, CD105 and CD144 staining and by RT-PCR for these markers (Panel E in Fig 4 and Panel C in S4 Fig). Since a single coherent population of CECs was defined by using the endothelial markers, they may substitute KDR in the identification CECs. However, staining for KDR yields the lowest background on HPCs and the best cross-matching score and therefore, is regarded as a marker of first choice, followed by CD146 and CD144 (Panel E in Fig 4 and Panels A and B in S4 Fig). The quality of CD45 staining/gating was crucial for discriminating CECs from contaminating cells, mainly $CD45^{low}$HPCs sporadically expressing KDR, CD146, CD144, and potentially crossing the $CD45^{neg}$ gate (Panel B in Fig 4 and Panel A in S4 Fig). Notably, all the CECs identified by the current procedure were nucleated (Panel A in Fig 5), i.e. not contaminated by (endothelial) micro-particle aggregates and therefore, the use of cell-permeant nuclear dyes like Hoechst or DRAQ5 was not necessary [20, 47, 48]. By avoiding the use of bright and toxic nuclear dyes a fluorescent channel is saved and spillover to other channels minimized, thereby improving the capacity of the detection channels and the sensitivity of the analysis. Moreover, the viability of the cells is well preserved for subsequent culture and RNA extraction.

Besides confirming higher frequency of CECs in UCB vs. AB [1, 7, 21, 22, 32, 44], we found a major difference between CECs in AB as compared to UCB. The CECs in UCB express significantly higher levels of CD34 and KDR (Panel C in Fig 4). Moreover, by means of Annexin-V staining we identified two main subsets of CECs: a viable fraction of ~20%, and an apoptotic fraction of ~80%, equally present in AB and UCB (Panel B in Fig 5). In addition, a $c\text{-}kit^{+}$ subset, expressing higher levels of KDR and CD34, was identified and found to be mainly present in the viable fraction of CECs (Panel F in Fig 4 and Panel B in Fig 5) This subset may well contain OEC-precursor cells. The angiogenic capacities of the CECs were further strengthened by the expression of angiogenic factors (S7 Fig).

Characterization of OECs and prediction of their circulating precursor

The characterization of OECs was improved by various combinations of markers. In addition, comparing early vs. late cultures evidenced the alterations occurring with aging of the cultures and led to the definition of homogeneously high and stable markers (CD146, CD144, CD105, CD31) on the one hand, and heterogeneous and unstable ones on the other (KDR, CD34, c-kit, CD133). The comparisons also enabled us to trace back the OEC precursors to c-kit+ CECs. By combining FACS populations and RT-PCR data we found overlap in the expression of KDR, CD146, CD105, CD144, and CD31 by OECs/HUVECs and CECs. Surface expression of the markers was generally lower in CECs than in OECs/HUVECs. This may be explained by

the fact that OECs/HUVECs are derived from *in vitro* cultures, while CECs are *in vivo* single circulating cells, exposed to different environmental stimuli (lacking, for instance, the adhesion to other endothelial cells, and exposed to the blood microenvironment) and subjected to a potentially stressful purification procedure. Interestingly, the stem cell-marker c-kit was expressed by a significant fraction of early passage OECs and HUVECs and positively associated with KDR and CD34 levels. $CD34^{high}KDR^{high}c\text{-}kit^{high}$ cells decreased with passaging in culture (Panels B and C in Fig 5 and Panels B-D in S6 Fig). This finding points to a triple +/high phenotype ($CD34^{+/high}KDR^{+/high}c\text{-}kit^{+/high}$), which is lost with aging in culture, as the progenitor/founder of both cell types [24, 49]. This view is supported by the recently described $c\text{-}kit^{+}KDR^{+}CD105^{+}CD45^{-}$ 'vascular endothelial stem cells' (VESCs) in the blood vessels of adult mice, which are capable of many cycles of replication and to generate functional blood vessels *in vitro* [50]. Notably, the $CD34^{+/high}KDR^{+/high}c\text{-}kit^{+/high}$ phenotype that we trace back as potential OEC precursor well matches the viable fraction of CECs expressing c-kit and higher levels of KDR and CD34 (Panel F in Fig 4 and Panel B in Fig 5).

The current opinion on the origin of CECs is that these cells are mostly apoptotic, mature endothelial cells without progenitor potential, shed from damaged blood vessels [14, 30, 51]. The present data, however, show that about 20% of circulating CECs are viable and express c-kit (Panel F in Fig 4 and Panel B in Fig 5). The high expression of angiogenic factors by CECs confirmed that these cells contain a fraction potentially contributing to neovascularization and *in vitro* generation of OECs. Unfortunately, we were unable to directly derive OECs from FACS-sorted CECs. These results are in line with results explicitly published by others [23] and with the (implicit) evidence that OECs are reported to be generated from unsorted or immuno-magnetic-bead-sorted PBMC fractions, not FACS-sorted ones [1, 7, 22–26]. The present data, pointing to viable CECs expressing c-kit as OEC precursors, are in line with data obtained from cells purified by antibody-coated beads suggesting that the OEC-founder cells do not originate from bone marrow and express CD34 and CD146, but not CD45 or CD133, a pattern compatible with CECs [7, 22, 23]. The significant higher yield of OECs from UCB (containing more CECs than AB) than from AB further corroborates the view that OECs stem from CECs.

Conclusions

In conclusion, the present FACS-based analysis yields optimal identification, characterization and sub-division of cell populations meeting the current criteria for HPCs, CECs and OECs, and enabled us to propose that the circulating OEC precursors may consist of viable $c\text{-}kit^{+}$ CECs.

Supporting information

S1 Fig. Comparison of the isolated cell fractions between Ficoll vs. RBC treatment.
A. Overview of the distribution of FACS events in the main regions/populations of interest in Ficoll vs. RBC lysis preparations. Besides differences in the mononuclear vs. non-mononuclear regions, a lower amount of small particles and dead cells was observed in the Ficoll samples. **B**. Percentages of white blood cells in the samples treated with RBC lysis buffer. The distribution matches the expected frequencies. **C**. The standard mononuclear gate used encompasses endothelial cells of all sizes including large OECs and BFA (Bovine Foetal Aortic, from CLS).
(TIF)

S2 Fig. Fluorescence minus one (FMO) and isotype controls.
(TIF)

S3 Fig. Characterization of HPCs. Histograms representative of CD34 (**A**) CD45 (**B**), and c-kit (**C**) levels (measured as median fluorescence intensity, MFI) in different HPC subpopulations from UCB and AB. CD34 levels are higher in $CD133^{high}$ HPCs, independently of c-kit levels. CD45 levels are also positively correlated with CD133 expression, and independent of c-kit levels. The highest c-kit levels are in the $CD133^{neg}$ HPCs. **D**-**E**. Additional details relative to KDR vs. CD146 expression in HPCs (see also Panel D in Fig 3). In (E) for each KDR/CD146-based HPC-subpopulation, the frequency vs. total HPCs and total PBMCs (upper panels) is reported. FSC/SSC (medium panels) and CD45 (lower panels) based identification is also shown to confirm HPC identity. FSC/SSC analysis is from CD34+CD45dim selected HPCs, CD45 analysis is from CD34+ FSC/SSC selected HPCs. (**F**) Additional details relative to CD144 vs. CD146 expression in HPCs, (see also Panel E in Fig 3). The frequency of each subpopulation vs. HPCs and total PBMCs is indicated.
(TIF)

S4 Fig. Identification and characterization of CECs. A. Identification of CECs using a CD34 vs. CD146 plot, and subsequent CD45 discrimination. The resulting population is pure and not contaminated by HPCs (red, right plot). **B**. Left: KDR expression in CD34/CD146 selected CECs indicated >98% matching. Right: CD105 expression in CD34/CD146 selected CECs shows significant positivity (>50%). **C**. KDR expression is confirmed at mRNA level by RT-PCR in CECs. HPCs are negative.
(TIF)

S5 Fig. Images of eEPCs and OECs. A. Upper: AB derived eEPCs (total PBMCs, unsorted); lower: UCB derived eEPCs (total PBMCs, unsorted). **B**. eEPCs enriched by sorting out the $CD14^+$ fraction from AB-PBMCs ($0.5x10^6$ CD14+ events/cm^2, 1 week culture). **C**. UCB derived OECs with their typical cobblestone morphology (upper panel: early OEC colony; middle panel: confluent OECs).
(TIF)

S6 Fig. FACS analysis of HUVECs and OECs. A. CD45 and CD14 were invariably 100% negative in HUVECs. CD146, CD144, CD105 were 100% highly expressed and stable. $CD133^+$ cells were sporadic (0.8±0.7%). **B**. CD34, c-kit, and KDR were heterogeneously expressed, with higher levels in early (passage 2–4) compared with late cultures (passage ≥10). **C**. Positive correlation between CD34, KDR and c-kit in early HUVEC. **D**. Quantification of CD34, KDR, and c-kit high cells in early vs. late cultures of OECs and HUVECs.
(TIF)

S7 Fig. RT-PCR results to angiogenic factors and receptors in the EPC subsets. A. Bar diagrams of expressional levels of the genes measured. (mean values and standard deviations). **B**. Differential expressed genes between HPCs and CECs calculated based on two-tailed T-test (Z = standard deviation). **C**. Differential expressed genes between HPCs and OECs calculated based on two-tailed T-test (Z = standard deviation).
(TIF)

S8 Fig. Immunohistochemistry of endothelial markers in OECs. vWF = von Willebrand Factor.
(TIF)

S1 Table. Upper Left panel: FACS settings used. **Upper Right panel**: list of the antibodies used for co-expression analysis in HPCs, CECs and OECs. Details on the staining procedure are reported in Methods. **Lower panel**: primers used for RT-PCR and relative product size.

HPRT1 was used low expressed housekeeping gene, B2M as highly expressed housekeeping gene. Additional details are in Methods.
(DOCX)

Acknowledgments

We thank Dr. C. Cheng for useful comments and providing some of the antibodies used in this study.

Author Contributions

Conceptualization: Dana A. M. Mustafa, Johan M. Kros.

Data curation: Karin Huizer, Dana A. M. Mustafa, J. Clarissa Spelt, Andrea Sacchetti.

Formal analysis: Karin Huizer, Dana A. M. Mustafa, J. Clarissa Spelt, Andrea Sacchetti.

Funding acquisition: Johan M. Kros.

Investigation: Karin Huizer, J. Clarissa Spelt, Andrea Sacchetti.

Methodology: Karin Huizer, Andrea Sacchetti.

Project administration: Johan M. Kros.

Software: Andrea Sacchetti.

Supervision: Dana A. M. Mustafa, Johan M. Kros.

Validation: Dana A. M. Mustafa, Andrea Sacchetti.

Visualization: Dana A. M. Mustafa, Andrea Sacchetti.

Writing – review & editing: Dana A. M. Mustafa, Johan M. Kros, Andrea Sacchetti.

References

1. Fadini GP, Losordo D, Dimmeler S. Critical reevaluation of endothelial progenitor cell phenotypes for therapeutic and diagnostic use. Circ Res. 2012; 110(4):624–37. Epub 2012/02/22. https://doi.org/10.1161/CIRCRESAHA.111.243386 PMID: 22343557.
2. George AL, Bangalore-Prakash P, Rajoria S, Suriano R, Shanmugam A, Mittelman A, et al. Endothelial progenitor cell biology in disease and tissue regeneration. J Hematol Oncol. 2011; 4(1):24. Epub 2011/05/26. https://doi.org/10.1186/1756-8722-4-24 PMID: 21609465.
3. Mayr M, Niederseer D, Niebauer J. From bench to bedside: what physicians need to know about endothelial progenitor cells. Am J Med. 2011; 124(6):489–97. Epub 2011/05/25. https://doi.org/10.1016/j.amjmed.2011.01.015 PMID: 21605723.
4. Ackermann BL, Berna MJ, Murphy AT. Recent advances in use of LC/MS/MS for quantitative high-throughput bioanalytical support of drug discovery. Curr Top Med Chem. 2002; 2(1):53–66. PMID: 11899065.
5. Case J, Mead LE, Bessler WK, Prater D, White HA, Saadatzadeh MR, et al. Human CD34+AC133+VEGFR-2+ cells are not endothelial progenitor cells but distinct, primitive hematopoietic progenitors. Exp Hematol. 2007; 35(7):1109–18. Epub 2007/06/26. https://doi.org/10.1016/j.exphem.2007.04.002 PMID: 17588480.
6. Schmidt-Lucke C, Fichtlscherer S, Rossig L, Kamper U, Dimmeler S. Improvement of endothelial damage and regeneration indexes in patients with coronary artery disease after 4 weeks of statin therapy. Atherosclerosis. 2010; 211(1):249–54. Epub 2010/03/10. https://doi.org/10.1016/j.atherosclerosis.2010.02.007 PMID: 20211468.
7. Tura O, Skinner EM, Barclay GR, Samuel K, Gallagher RC, Brittan M, et al. Late outgrowth endothelial cells resemble mature endothelial cells and are not derived from bone marrow. Stem Cells. 2013; 31(2):338–48. Epub 2012/11/21. https://doi.org/10.1002/stem.1280 PMID: 23165527.

8. Schmidt-Lucke C, Fichtlscherer S, Aicher A, Tschope C, Schultheiss HP, Zeiher AM, et al. Quantification of circulating endothelial progenitor cells using the modified ISHAGE protocol. PLoS One. 2010; 5 (11):e13790. Epub 2010/11/13. https://doi.org/10.1371/journal.pone.0013790 PMID: 21072182.
9. Alvarez P, Carrillo E, Velez C, Hita-Contreras F, Martinez-Amat A, Rodriguez-Serrano F, et al. Regulatory systems in bone marrow for hematopoietic stem/progenitor cells mobilization and homing. Biomed Res Int. 2013; 2013:312656. Epub 2013/07/12. https://doi.org/10.1155/2013/312656 PMID: 23844360.
10. Rafii S, Lyden D, Benezra R, Hattori K, Heissig B. Vascular and haematopoietic stem cells: novel targets for anti-angiogenesis therapy? Nat Rev Cancer. 2002; 2(11):826–35. https://doi.org/10.1038/nrc925 PMID: 12415253.
11. Takakura N, Watanabe T, Suenobu S, Yamada Y, Noda T, Ito Y, et al. A role for hematopoietic stem cells in promoting angiogenesis. Cell. 2000; 102(2):199–209. Epub 2000/08/16. PMID: 10943840.
12. Mayani H, Alvarado-Moreno JA, Flores-Guzman P. Biology of human hematopoietic stem and progenitor cells present in circulation. Arch Med Res. 2003; 34(6):476–88. Epub 2004/01/22. https://doi.org/10.1016/j.arcmed.2003.08.004 PMID: 14734087.
13. Peters BA, Diaz LA, Polyak K, Meszler L, Romans K, Guinan EC, et al. Contribution of bone marrow-derived endothelial cells to human tumor vasculature. Nat Med. 2005; 11(3):261–2. Epub 2005/02/22. https://doi.org/10.1038/nm1200 PMID: 15723071.
14. Becher MU, Nickenig G, Werner N. Regeneration of the vascular compartment. Herz. 2010; 35(5):342–51. Epub 2010/09/16. https://doi.org/10.1007/s00059-010-3360-0 PMID: 20842474.
15. Sieveking DP, Buckle A, Celermajer DS, Ng MK. Strikingly different angiogenic properties of endothelial progenitor cell subpopulations: insights from a novel human angiogenesis assay. J Am Coll Cardiol. 2008; 51(6):660–8. Epub 2008/02/12. https://doi.org/10.1016/j.jacc.2007.09.059 PMID: 18261686.
16. Popa ER, Harmsen MC, Tio RA, van der Strate BW, Brouwer LA, Schipper M, et al. Circulating CD34+ progenitor cells modulate host angiogenesis and inflammation in vivo. J Mol Cell Cardiol. 2006; 41 (1):86–96. Epub 2006/06/20. https://doi.org/10.1016/j.yjmcc.2006.04.021 PMID: 16780869.
17. Mund JA, Shannon H, Sinn AL, Cai S, Wang H, Pradhan KR, et al. Human proangiogenic circulating hematopoietic stem and progenitor cells promote tumor growth in an orthotopic melanoma xenograft model. Angiogenesis. 2013; 16(4):953–62. Epub 2013/07/24. https://doi.org/10.1007/s10456-013-9368-3 PMID: 23877751.
18. Dome B, Timar J, Ladanyi A, Paku S, Renyi-Vamos F, Klepetko W, et al. Circulating endothelial cells, bone marrow-derived endothelial progenitor cells and proangiogenic hematopoietic cells in cancer: From biology to therapy. Crit Rev Oncol Hematol. 2009; 69(2):108–24. Epub 2008/09/05. https://doi.org/10.1016/j.critrevonc.2008.06.009 PMID: 18768327.
19. Shaked Y, Bertolini F, Emmenegger U, Lee CR, Kerbel RS. On the origin and nature of elevated levels of circulating endothelial cells after treatment with a vascular disrupting agent. J Clin Oncol. 2006; 24 (24):4040; author reply -1. Epub 2006/08/22. https://doi.org/10.1200/JCO.2006.07.1175 PMID: 16921064.
20. Kraan J, Sleijfer S, Foekens JA, Gratama JW. Clinical value of circulating endothelial cell detection in oncology. Drug Discov Today. 2012; 17(13–14):710–7. Epub 2012/02/07. https://doi.org/10.1016/j.drudis.2012.01.011 PMID: 22306349.
21. Kraan J, Strijbos MH, Sieuwerts AM, Foekens JA, den Bakker MA, Verhoef C, et al. A new approach for rapid and reliable enumeration of circulating endothelial cells in patients. J Thromb Haemost. 2012; 10 (5):931–9. Epub 2012/03/06. https://doi.org/10.1111/j.1538-7836.2012.04681.x PMID: 22385979.
22. Timmermans F, Van Hauwermeiren F, De Smedt M, Raedt R, Plasschaert F, De Buyzere ML, et al. Endothelial outgrowth cells are not derived from CD133+ cells or CD45+ hematopoietic precursors. Arterioscler Thromb Vasc Biol. 2007; 27(7):1572–9. Epub 2007/05/15. https://doi.org/10.1161/ATVBAHA.107.144972 PMID: 17495235.
23. Mund JA, Estes ML, Yoder MC, Ingram DA Jr., Case J. Flow cytometric identification and functional characterization of immature and mature circulating endothelial cells. Arterioscler Thromb Vasc Biol. 2012; 32(4):1045–53. Epub 2012/01/28. https://doi.org/10.1161/ATVBAHA.111.244210 PMID: 22282356.
24. Delorme B, Basire A, Gentile C, Sabatier F, Monsonis F, Desouches C, et al. Presence of endothelial progenitor cells, distinct from mature endothelial cells, within human CD146+ blood cells. Thromb Haemost. 2005; 94(6):1270–9. Epub 2006/01/18. https://doi.org/10.1160/TH05-07-0499 PMID: 16411405.
25. Urbich C, Heeschen C, Aicher A, Dernbach E, Zeiher AM, Dimmeler S. Relevance of monocytic features for neovascularization capacity of circulating endothelial progenitor cells. Circulation. 2003; 108 (20):2511–6. Epub 2003/10/29. https://doi.org/10.1161/01.CIR.0000096483.29777.50 PMID: 14581410.
26. Yoon CH, Hur J, Park KW, Kim JH, Lee CS, Oh IY, et al. Synergistic neovascularization by mixed transplantation of early endothelial progenitor cells and late outgrowth endothelial cells: the role of angiogenic

cytokines and matrix metalloproteinases. Circulation. 2005; 112(11):1618–27. Epub 2005/09/08. https://doi.org/10.1161/CIRCULATIONAHA.104.503433 PMID: 16145003.

27. Ingram DA, Caplice NM, Yoder MC. Unresolved questions, changing definitions, and novel paradigms for defining endothelial progenitor cells. Blood. 2005; 106(5):1525–31. https://doi.org/10.1182/blood-2005-04-1509 PMID: 15905185.

28. Timmermans F, Plum J, Yoder MC, Ingram DA, Vandekerckhove B, Case J. Endothelial progenitor cells: identity defined? J Cell Mol Med. 2009; 13(1):87–102. Epub 2008/12/11. https://doi.org/10.1111/j.1582-4934.2008.00598.x PMID: 19067770.

29. Yoder MC. Defining human endothelial progenitor cells. J Thromb Haemost. 2009; 7 Suppl 1:49–52. Epub 2009/07/28. https://doi.org/10.1111/j.1538-7836.2009.03407.x PMID: 19630767.

30. Blann AD, Pretorius A. Circulating endothelial cells and endothelial progenitor cells: two sides of the same coin, or two different coins? Atherosclerosis. 2006; 188(1):12–8. Epub 2006/02/21. https://doi.org/10.1016/j.atherosclerosis.2005.12.024 PMID: 16487972.

31. Hristov M, Schmitz S, Nauwelaers F, Weber C. A flow cytometric protocol for enumeration of endothelial progenitor cells and monocyte subsets in human blood. J Immunol Methods. 2012; 381(1–2):9–13. Epub 2012/04/28. https://doi.org/10.1016/j.jim.2012.04.003 PMID: 22537800.

32. Khan SS, Solomon MA, McCoy JP Jr. Detection of circulating endothelial cells and endothelial progenitor cells by flow cytometry. Cytometry B Clin Cytom. 2005; 64(1):1–8. Epub 2005/01/26. https://doi.org/10.1002/cyto.b.20040 PMID: 15668988.

33. Schewe M, Franken PF, Sacchetti A, Schmitt M, Joosten R, Bottcher R, et al. Secreted Phospholipases A2 Are Intestinal Stem Cell Niche Factors with Distinct Roles in Homeostasis, Inflammation, and Cancer. Cell Stem Cell. 2016; 19(1):38–51. Epub 2016/06/14. https://doi.org/10.1016/j.stem.2016.05.023 PMID: 27292189.

34. Vroling L, Lind JS, de Haas RR, Verheul HM, van Hinsbergh VW, Broxterman HJ, et al. CD133+ circulating haematopoietic progenitor cells predict for response to sorafenib plus erlotinib in non-small cell lung cancer patients. Br J Cancer. 2010; 102(2):268–75. Epub 2009/12/17. https://doi.org/10.1038/sj.bjc.6605477 PMID: 20010948.

35. Hur J, Yoon CH, Kim HS, Choi JH, Kang HJ, Hwang KK, et al. Characterization of two types of endothelial progenitor cells and their different contributions to neovasculogenesis. Arterioscler Thromb Vasc Biol. 2004; 24(2):288–93. Epub 2003/12/31. https://doi.org/10.1161/01.ATV.0000114236.77009.06 PMID: 14699017.

36. Lopez-Holgado N, Alberca M, Sanchez-Guijo F, Villaron E, Almeida J, Martin A, et al. Short-term endothelial progenitor cell colonies are composed of monocytes and do not acquire endothelial markers. Cytotherapy. 2007; 9(1):14–22. Epub 2007/03/14. https://doi.org/10.1080/14653240601047726 PMID: 17354099.

37. Vaughan EE, O'Brien T. Isolation of circulating angiogenic cells. Methods Mol Biol. 2012; 916:351–6. Epub 2012/08/24. https://doi.org/10.1007/978-1-61779-980-8_25 PMID: 22914952.

38. Smythe J, Fox A, Fisher N, Frith E, Harris AL, Watt SM. Measuring angiogenic cytokines, circulating endothelial cells, and endothelial progenitor cells in peripheral blood and cord blood: VEGF and CXCL12 correlate with the number of circulating endothelial progenitor cells in peripheral blood. Tissue Eng Part C Methods. 2008; 14(1):59–67. Epub 2008/05/06. https://doi.org/10.1089/tec.2007.0251 PMID: 18454646.

39. Mayani H, Guilbert LJ, Janowska-Wieczorek A. Biology of the hemopoietic microenvironment. Eur J Haematol. 1992; 49(5):225–33. Epub 1992/11/01. PMID: 1473584.

40. Tung JW, Heydari K, Tirouvanziam R, Sahaf B, Parks DR, Herzenberg LA. Modern flow cytometry: a practical approach. Clin Lab Med. 2007; 27(3):453–68, v. Epub 2007/07/31. https://doi.org/10.1016/j.cll.2007.05.001 PMID: 17658402.

41. Matsuoka Y, Sasaki Y, Nakatsuka R, Takahashi M, Iwaki R, Uemura Y, et al. Low level of c-kit expression marks deeply quiescent murine hematopoietic stem cells. Stem Cells. 2011; 29(11):1783–91. Epub 2011/09/08. https://doi.org/10.1002/stem.721 PMID: 21898688.

42. Jaatinen T, Hemmoranta H, Hautaniemi S, Niemi J, Nicorici D, Laine J, et al. Global gene expression profile of human cord blood-derived CD133+ cells. Stem Cells. 2006; 24(3):631–41. Epub 2005/10/08. https://doi.org/10.1634/stemcells.2005-0185 PMID: 16210406.

43. Bissels U, Wild S, Tomiuk S, Hafner M, Scheel H, Mihailovic A, et al. Combined characterization of microRNA and mRNA profiles delineates early differentiation pathways of CD133+ and CD34+ hematopoietic stem and progenitor cells. Stem Cells. 2011; 29(5):847–57. Epub 2011/03/12. https://doi.org/10.1002/stem.627 PMID: 21394831.

44. Ingram DA, Mead LE, Tanaka H, Meade V, Fenoglio A, Mortell K, et al. Identification of a novel hierarchy of endothelial progenitor cells using human peripheral and umbilical cord blood. Blood. 2004; 104 (9):2752–60. Epub 2004/07/01. https://doi.org/10.1182/blood-2004-04-1396 PMID: 15226175.

45. Mayani H. Notch signaling: from stem cell expansion to improving cord blood transplantation. Expert Rev Hematol. 2010; 3(4):401–4. Epub 2010/11/19. https://doi.org/10.1586/ehm.10.37 PMID: 21083031.

46. Wagner W, Ansorge A, Wirkner U, Eckstein V, Schwager C, Blake J, et al. Molecular evidence for stem cell function of the slow-dividing fraction among human hematopoietic progenitor cells by genome-wide analysis. Blood. 2004; 104(3):675–86. Epub 2004/04/20. https://doi.org/10.1182/blood-2003-10-3423 PMID: 15090461.

47. Burger D, Touyz RM. Cellular biomarkers of endothelial health: microparticles, endothelial progenitor cells, and circulating endothelial cells. J Am Soc Hypertens. 2012; 6(2):85–99. Epub 2012/02/11. https://doi.org/10.1016/j.jash.2011.11.003 PMID: 22321962.

48. Lanuti P, Santilli F, Marchisio M, Pierdomenico L, Vitacolonna E, Santavenere E, et al. A novel flow cytometric approach to distinguish circulating endothelial cells from endothelial microparticles: relevance for the evaluation of endothelial dysfunction. J Immunol Methods. 2012; 380(1–2):16–22. Epub 2012/04/10. https://doi.org/10.1016/j.jim.2012.03.007 PMID: 22484509.

49. Ingram DA, Mead LE, Moore DB, Woodard W, Fenoglio A, Yoder MC. Vessel wall-derived endothelial cells rapidly proliferate because they contain a complete hierarchy of endothelial progenitor cells. Blood. 2005; 105(7):2783–6. https://doi.org/10.1182/blood-2004-08-3057 PMID: 15585655.

50. Fang S, Wei J, Pentinmikko N, Leinonen H, Salven P. Generation of functional blood vessels from a single c-kit+ adult vascular endothelial stem cell. PLoS Biol. 2012; 10(10):e1001407. Epub 2012/10/24. https://doi.org/10.1371/journal.pbio.1001407 PMID: 23091420.

51. Singh N, Van Craeyveld E, Tjwa M, Ciarka A, Emmerechts J, Droogne W, et al. Circulating apoptotic endothelial cells and apoptotic endothelial microparticles independently predict the presence of cardiac allograft vasculopathy. J Am Coll Cardiol. 2012; 60(4):324–31. Epub 2012/07/21. https://doi.org/10.1016/j.jacc.2012.02.065 PMID: 22813611.

CHAPTER 2

CIRCULATING PROANGIOGENIC CELLS AND PROTEINS IN PATIENTS WITH GLIOMA AND ACUTE MYOCARDIAL INFARCTION:

Differences in Neovascularization between Neoplasia and Tissue Regeneration

Hindawi
Journal of Oncology
Volume 2019, Article ID 3560830, 13 pages
https://doi.org/10.1155/2019/3560830

Research Article

Circulating Proangiogenic Cells and Proteins in Patients with Glioma and Acute Myocardial Infarction: Differences in Neovascularization between Neoplasia and Tissue Regeneration

Karin Huizer,[1] Andrea Sacchetti,[1] Wim A. Dik,[2] Dana A. Mustafa,[1] and Johan M. Kros[1]

[1]*Department of Pathology, Erasmus Medical Center, Wytemaweg 80, 3015GD Rotterdam, Netherlands*
[2]*Department of Immunology, Erasmus Medical Center, Wytemaweg 80, 3015GD Rotterdam, Netherlands*

Correspondence should be addressed to Johan M. Kros; j.m.kros@erasmusmc.nl

Received 25 January 2019; Accepted 6 May 2019; Published 21 July 2019

Academic Editor: Pashtoon M. Kasi

Although extensive angiogenesis takes place in glial tumors, antiangiogenic therapies have remained without the expected success. In the peripheral circulation of glioma patients, increased numbers of endothelial precursor cells (EPCs) are present, potentially offering targets for antiangiogenic therapy. However, for an antiangiogenic therapy to be successful, the therapy should specifically target glioma-related EPC subsets and secreted factors only. Here, we compared the EPC subsets and plasma factors in the peripheral circulation of patients with gliomas to acute myocardial infarctions. We investigated the five most important EPC subsets and 21 angiogenesis-related plasma factors in peripheral blood samples of 29 patients with glioma, 14 patients with myocardial infarction, and 20 healthy people as controls, by FACS and Luminex assay. In GBM patients, all EPC subsets were elevated as compared to healthy subjects. In addition, HPC and KDR^+ cell fractions were higher than in MI, while $CD133^+$ and KDR^+CD133^+ cell fractions were lower. There were differences in relative EPC fractions between the groups: KDR^+ cells were the largest fraction in GBM, while $CD133^+$ cells were the largest fraction in MI. An increase in glioma malignancy grade coincided with an increase in the KDR^+ fraction, while the $CD133^+$ cell fraction decreased relatively. Most plasma angiogenic factors were higher in GBM than in MI patients. In both MI and GBM, the ratio of $CD133^+$ HPCs correlated significantly with elevated levels of MMP9. In the GBM patients, MMP9 correlated strongly with levels of all HPCs. In conclusion, the data demonstrate that EPC traffic in patients with glioma, representing neoplasia, is different from that in myocardial infarction, representing tissue regeneration. Glioma patients may benefit from therapies aimed at lowering KDR^+ cells and HPCs.

1. Introduction

Although gliomas are among the most vascularized tumors, results of antiangiogenic therapies have been disappointing [1]. Antiangiogenic drugs like Bevacizumab act against VEGF and address sprouting angiogenesis (i.e., the formation of new branches from existing blood vessels). There are various reasons why VEGF blockers like Bevacizumab fail in stopping tumor progression. One reason is that these drugs act against a single step in the complex process of neovascularization that can be compensated for by employing alternative routes of vessel formation [2]. Simultaneously, targeting these alternative routes may result in more successful antiangiogenic therapeutic strategies. Apart from sprouting angiogenesis, circulating endothelial progenitor cells (EPCs) stimulate neovascularization by vasculogenesis, i.e., de novo formation of blood vessels [3–6]. Although these circulating cells are interesting targets for antiangiogenic strategies, there are only scarce data on their frequencies in glioma patients [7]. Since EPCs are involved in physiological tissue repair, therapeutic interventions should ideally not intervene with the normal function of EPCs. EPCs are mobilized by factors secreted by ischemic or neoplastic tissues [8]. Chemoattractants guide EPCs to their target tissues, where they exit from blood vessels and fuel angiogenesis by secreting proangiogenic factors. A subset of EPCs differentiates into endothelial cells and becomes part of the vessel wall [9].

EPCs aid significantly in physiologic tissue regeneration [4]. Following acute myocardial infarction (MI) for instance, EPC subsets are mobilized by the release of proangiogenic factors and chemoattractants [10–13]. HPCs and $CD133^+$ cells are engaged in tissue repair following the acute stage of MI [14–16]. In cancer, EPCs participate in tumor vascularization [17, 18], are associated with tumor progression [19], and may diminish the effects of chemotherapy, while blood EPC levels correlate negatively with survival [20]. In the peripheral circulation of both acute MI and (high grade) glioma patients, increased levels of circulating EPCs were demonstrated [7]. While various circulating EPC subsets were studied in the context of MI, limited studies concerning glioma patients are available [7, 21]. Moreover, there are only scarce data correlating the frequency of circulating EPC subsets and the levels of neovascularization-related plasma factors in situations of tissue regeneration and neoplasia [22, 23].

In the present study, we aimed to find new targets for antiangiogenic strategies for glioma patients that would minimally interfere with normal tissue repair. To that aim, we compared the frequency of circulating EPC subsets and plasma levels of a set of chemoattractants, mobilization factors, and angiogenic factors involved in neovascularization in patients with glioma and in patients who suffered from a recent MI. The reason we chose patient with MI to represent the EPC response in acute ischemic tissue repair is the availability of ample literature showing a significant increase in circulating EPCs in this group of patients. We considered including patients with ischemic stroke as a model for EPC response in acute ischemia, but since the literature is much less abundant in this patient group, and since the EPC response in ischemic stroke patients is not unequivocally elevated [7, 24], we decided against this. Blood from healthy adults was used as control. We used an optimized, highly sensitive four-marker-based FACS protocol, allowing for the accurate determination of the EPC subsets [25]. We investigated the frequencies of HPCs ($CD34^+CD133^{+/-}CD45^{dim}$), KDR^+ cells ($KDR^+CD34^-CD133^-$), $CD133^+$ cells ($CD133^+CD34^-KDR^-$), KDR^+CD133^+ cells ($KDR^+CD133^+CD34^-$), and circulating endothelial cells (CECs; $CD34^{bright}KDR^+CD45^-CD133^-$).

In addition, we distinguished between $CD133^{bright}$ HPCs, a more primitive phenotype of HPCs that is linked with higher proangiogenic capacity [23, 26, 27], and $CD133^-$ HPCs [11].

2. Material & Methods

This study was approved by the Medical Ethics Committee of the Erasmus Medical Center, Rotterdam, The Netherlands (MEC-2011-313), and performed in adherence to the Code of Conduct of the Federation of Medical Scientific Societies in the Netherlands (http://www.federa.org/codes-conduct).

2.1. Blood Sampling and Handling. Based on a previous study from our group, we anticipated to require between 10 and 25 subjects in each patient and control group to determine statistically significant changes in the frequency of circulating EPC subsets [7]. Since our current study uses more stringent inclusion criteria (treatment-naïve patients with a new diagnosis of glioblastoma, grade II/III astrocytoma, myocardial infarction patients within 1-10 days after acute myocardial infarction) and a much more advanced and fine-tuned FACS protocol [25], we expected that fewer inclusion would suffice to determine statistically significant changes between EPC subsets. For this reason, we aimed to include between 10 and 20 patients in each group of patients and controls.

Blood samples of treatment-naïve patients with radiologically suspected first-episode malignant intracranial tumors were obtained from the Department of Neurosurgery, Erasmus MC. The blood was sampled prior to (diagnostic) surgery and chemo- or radiotherapy. Only patients with a histologically confirmed diagnosis of glioma were included in the current study. In retrospect, out of 38 patients with radiologically suspect malignant intracranial tumors included for FACS analysis, 20 patients received a definitive diagnosis of glioblastoma (GBM), 5 patients of astrocytoma grade II/III (AII/III). Nine patients were diagnosed with brain metastases and 4 patients with various other diagnoses (these 13 patients were excluded from our study). One GBM patient was excluded because of radiotherapy prior to blood sampling and surgery, and one GBM patient was excluded due to technical problems during FACS analysis.

We chose not to group together astrocytoma grade II/III and glioblastoma patients due to the differences between these tumor entities in neovascularization. While in astrocytoma neovascularization is not or only modestly increased and blood vessels are histologically largely similar to normal blood vessels, in glioblastoma there is an extremely high density of blood vessels (up to the point that glioblastomas are among the most vascularized solid tumors), which are haphazardly organized and histologically anomalous ("microvascular proliferation"). We expected that because of this: we could find large differences in the role and frequency of EPCs in the circulation of astrocytoma and glioblastoma patients.

Blood samples from patients who had suffered a recent MI (1-10 days prior to sampling) were received from the Department of Cardiology/Thoracic Center, Erasmus MC. Blood samples from healthy blood donors were obtained via the Sanquin Blood Bank. Age and sex distributions are shown in Tables 1(a) and 1(b). A total of 84 blood samples were included (70 were used for the analysis of chemoattractants and proangiogenic factors and 57 for FACS analysis of EPC subsets). For 43 of the patients, both FACS analysis and plasma marker analysis were carried out. For FACS analysis, we finally included blood samples of 14 MI patients, 18 GBM patients, 5 AII/III patients, and 20 healthy controls (HC). The mean age of GBM patients was 66 years, for MI patients 60 years, and for HC 54 years. GBM patients were significantly older than patients with AII/III (mean ages 66 vs. 45, respectively) reflecting the characteristic age distribution for patients with these tumors.

For each subject, 12-30 ml of venous EDTA blood (BD vacutainer) was collected. Two ml of whole blood was immediately centrifuged at 400 rcf for 10 minutes to isolate platelet-rich plasma (PRP). Next, PRP was centrifuged at 3,000 rcf for 15 minutes. Platelet-poor plasma (PPP) was

Table 1: Blood samples used for (a) FACS analysis and (b) Luminex analysis. A total of 84 blood samples were included in the study. For 43 of these samples, both FACS and Luminex analyses were done.

(a)

FACS				*Age*		*Sex*
Samples	*N*	*Mean*	*SD*	*Minimum*	*Maximum*	*m/f*
HC	20	54	12	22	69	15/5
MI	14	60	11	38	77	11/3
AII/III	5	45	11	32	58	0/5
GBM	18	66	10	45	79	9/9
Total	57					

(b)

Luminex				*Age*		*Sex*
Samples	*N*	*Mean*	*SD*	*Minimum*	*Maximum*	*m/f*
HC	20	59	7	38	69	15/5
MI	14	60	11	38	77	11/3
AII/III	7	53	12	35	69	2/5
GBM	29	65	9	45	81	16/13
Total	70					

isolated and stored at -80°C. Blood samples were stored at room temperature in the dark no longer than 18 hours before further FACS analysis.

2.2. FACS Analysis. HPCs and CECs were analyzed by FACS as described before [25]. Additional gates were set to identify $KDR^+CD34^-CD133^-$ cells, $CD133^+CD34^-KDR^-$ cells, and $KDR^+CD133^+CD34^-$ cells. In brief, peripheral blood mononuclear cells (PBMCs) were isolated from whole blood using Ficoll Paque plus (GE Healthcare). PBMCs were incubated with 10% mouse serum on ice to block aspecific antibody binding. CD34-FITC (Southern Biotech), CD133-PE (MACS Miltenyi), KDR-APC (MACS Miltenyi), and CD45-Viogreen (MACS Miltenyi) were used to stain PBMCs. Cells were washed twice to remove excess antibody and resuspended in FACS sorting buffer (PBS+10% BSA). Hoechst was used as viability dye to exclude dead cells from the analysis. For FACS analysis, we used the BD FACS Aria III. For the initial setup, we analyzed positive control samples using fluorescence minus one as well as isotype controls for every antibody used. We acquired the equivalent of $10\text{-}50*10^6$ PBMCs in each analysis using our previously published strategy for the detection of rare cells [25]. We gated the following populations: $CD34^+CD133^{+/-}CD45^{dim}$cells (HPCs), which we subdivided into $CD133^{negative}$, $CD133^{dim}$, and $CD133^{bright}$ subpopulations. In addition, $CD34^{bright}KDR^+CD45^-CD133^-$ cells (CECs) were gated as described in detail in [25]. In addition, $CD133^+$ cells (gated as $CD34^-$ and KDR^-), KDR^+ cells (gated as $CD133^-$ and $CD34^-$), and KDR^+CD133^+ cells (gated as $CD34^-$) were analyzed (setup and gating strategy similar to [25]). To quantify subtypes of EPCs, each population was represented as absolute cell numbers in $1*10^6$ $CD45^+$ PBMCs. The nonparametric Mann–Whitney U test (SPSS version 24) was used to analyze differences between the groups. Extreme outliers were excluded from the analysis (Figure 1).

2.3. Measuring Plasma Chemoattractants and Angiogenic Factors. The concentrations of 21 plasma factors related to EPC biology and neovascularization were measured. The plasma factors were selected based on their key functions in EPC-mediated neovascularization: mobilization and chemotactic factors (CXCL12, CSF2, and CSF3), de-adhesion and invasion factors (MMP2, MMP9), and proangiogenic factors/microenvironment regulators (VEGFA, KITL, vWF, EGF, FGFb, EPO, Ang2, Ang1, BDNF, VCAM1, PDGFBB, tenascin-c, periostin, HGF, and PGF) [22, 28–33]. The angiogenic factors either directly stimulate angiogenesis or represent regulators of angiogenesis like MMP-2, MMP-9, tenascin-c, and periostin that aid in generating a microenvironment favoring neovascularization. The functional delineations are, however, not strict and there is extensive overlap in functions of the factors. The plasma factors were measured in PPP using 3 different custom-mixed magnetic bead-based MAGPIX®-Luminex assays from R&D (see Additional File 1). Analyses were performed on PPP, diluted as recommended by the company (R&D Systems, Abingdon, UK). Because of low concentrations, the levels of CSF2, CSF3, vWF, VEGF, EGF, and CXCL12 were measured by their raw mean fluorescence intensity (MFI) values. In order to determine whether using MFI values yielded reliable statistical results, we compared calculated concentrations of markers with a high concentration, with their corresponding MFI values. This yielded identical statistical results. In addition, the results of the low concentration markers (using their MFI values) fit with preexisting literature [34]. Therefore, the MFI values of these markers were added to the data set. The nonparametric Mann–Whitney U test (SPSS version 24) was used to analyze differences between the groups.

2.4. Correlating Plasma Factors with EPC Frequencies in GBM and MI. To determine if the levels of chemoattractants and mobilization factors were related to EPC and CEC levels, we conducted correlation analyses. Since the frequencies of EPCs display a non-Gaussian distribution and since the correlation between EPC frequencies and plasma factors proved to be nonlinear, we used Spearman's rho to calculate correlation coefficients.

3. Results

3.1. EPC Absolute Frequencies. In all groups HPCs, KDR^+ and $CD133^+$ cells represented the majority of circulating EPCs (Figure 2). In patients with GBM and acute MI, all EPC subsets were higher as compared to HC, except for the HPC fraction in MI (Figures 1 and 3) . In GBM patients, KDR^+ (Z=-2.0; p=0.04) and HPC levels (Z=-1.6; p=0.12) were higher as compared to those in MI patients, while in MI patients $CD133^+$ (Z=-1.3; p=0.19) and KDR^+CD133^+ (Z=-2.0; p=0.02) levels exceeded those in GBM patients.

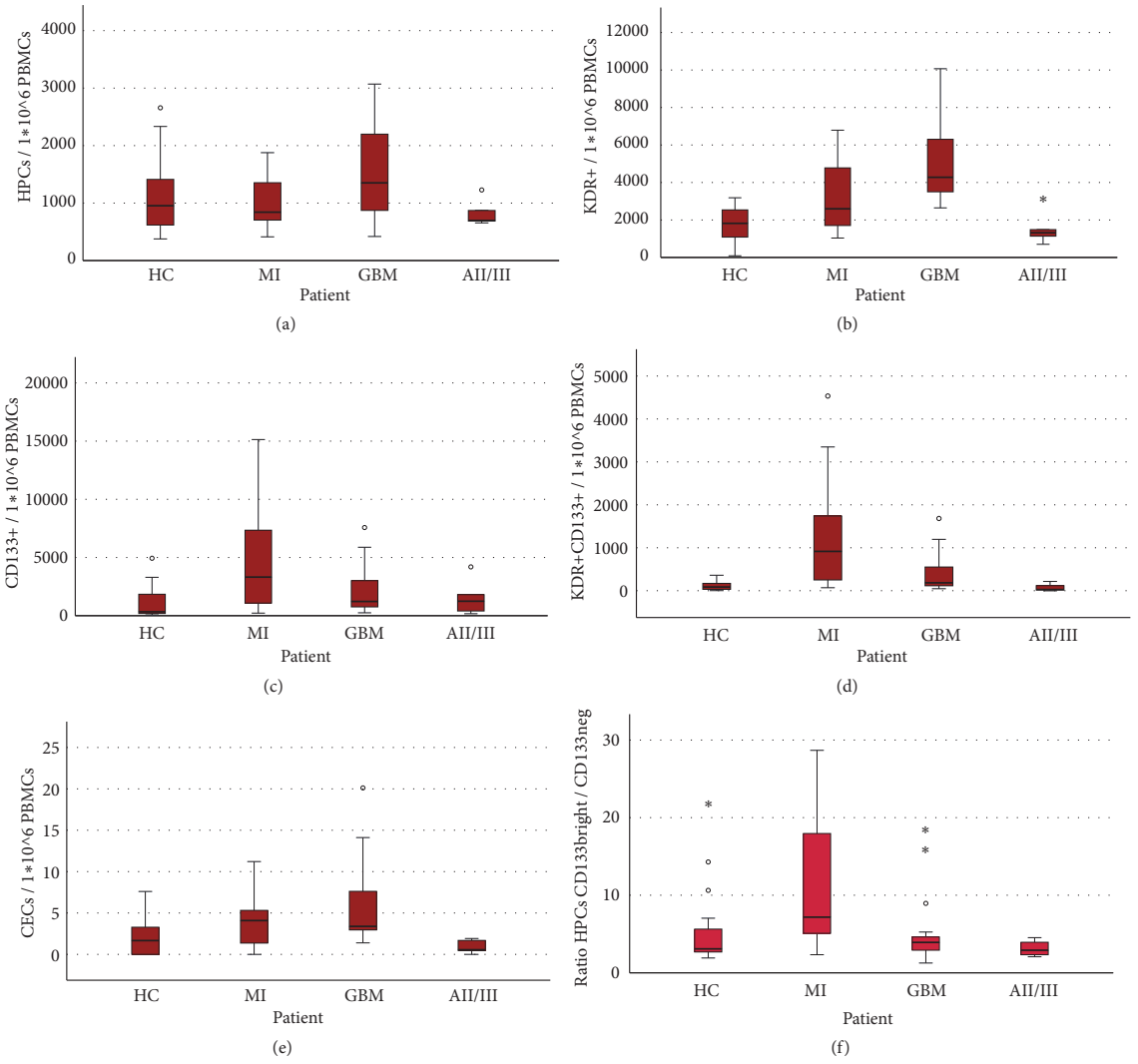

Figure 1: *The frequencies of EPCs in patients included in the study*. Boxplots of frequencies of EPCs (absolute amount in $1*10^6$ PBMCs). Extreme outliers have been excluded from the graphs (extreme outliers excluded: HPCs: 2 (1 MI, 1 GBM); KDR+: 6 (3 MI, 3 HC); CD133+: 2 (1 MI, 1 GBM); KDR+CD133+: 1 GBM). (a) *HPC* levels are the highest in GBM patients. Levels are similar in HC and AII/III patients. (b) KDR^+ levels are the highest in GBM and increased in MI patients. Levels are similar in AII/III and HC. (c) $CD133^+$ cells are the highest in MI patients and elevated in GBM patients. Levels are similar in AII/III and HC. (d) KDR^+CD133^+ cells are the highest in MI patients and elevated in GBM patients. Levels are similar in AII/III and HC. (e) *CECs* are elevated in both MI and GBM patients. They are indistinguishable between HC and AII/III. (f) The ratio of $CD133^{bright}/CD133^-$ *HPCs* is highest in MI patients.

3.2. EPC Relative Fractions. The relative fractions of the EPCs differed in the groups (Figure 2). In GBM, the largest fraction of EPCs was KDR^+ (57%), while in MI patients the largest fraction was $CD133^+$ cells (43%). In addition, in GBM, the HPC fraction was twice as big as in MI, while in MI, the KDR^+CD133^+ fraction was three times larger than in GBM patients. The relative fractions of EPCs in HC were similar to those in GBM. However, the absolute numbers of circulating EPCs are significantly elevated in GBM patients (Figure 1). Noticeably, absolute levels of EPCs in AII/III patients were comparable to HC, while the relative distribution of EPC subsets was very different: in AII/III the fraction of $CD133^+$ cells was significantly larger and that of HPCs was significantly smaller than in HC. Comparing AII/III with GBM, we found the KDR^+ fraction increased along with malignancy grade from 40% in AII/III to 57% in

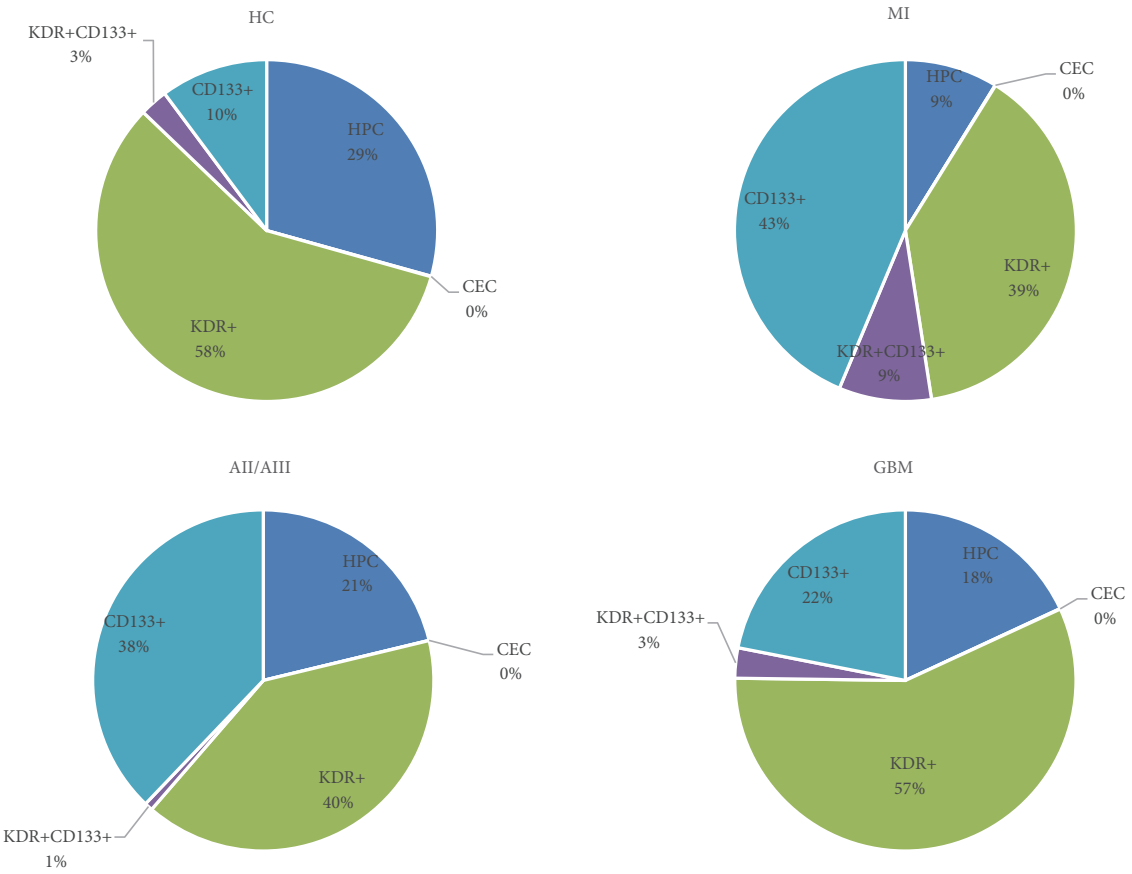

FIGURE 2: *Relative percentages of EPCs.* Relative percentages of EPCs (median values) by patient group are shown in pie charts.

GBM. The $CD133^+$ cell fraction decreased from 38% in AII/III to 22% in GBM.

The KDR^+CD133^+ fraction in all groups was relatively small (for all groups below 10%) and CECs were the smallest population, with percentages below 1% for all groups.

3.3. Plasma Factors. There were considerable differences in the concentrations of the various plasma factors between the groups (Figure 4) . Both in GBM and MI patients, the factors MMP9, HGF, and vWF were elevated in plasma relative to HC. VCAM1 was specifically elevated in GBM, while angiogenin and tenascin-c were specifically elevated in MI, relative to HC. Nine factors were higher in HC than in MI patients and only one factor, CXCL12, was higher in HC than in GBM patients. Most plasma angiogenic factors were higher in GBM than in MI patients. Ang2 and angiogenin levels were higher in MI patients compared to GBM, while CSF2, CSF3, FGFb, EPO, PDGFBB, Angl, and the ratio Angl/Ang2 were all higher in GBM than in MI patients. Interestingly, the concentrations of plasma factors in AII/III patients were indistinguishable from HC, except for CXCL12, which was decreased in AII/III. See Figure 4 .

3.4. Correlations Between Plasma Factors and EPC Frequencies in GBM and MI. The Spearman correlations between EPC subpopulations and plasma factors in patients with gliomas, MI, and HC are shown in Additional File 2. In GBM patients, MMP9 correlated strongly with HPC levels (rho=0.62; p=0.03) and KDR^+ levels correlated with VCAM1 plasma concentration (rho=0.64; p=0.04). In MI patients, HPC levels correlated negatively with plasma concentrations of CSF3 (rho=-0.76; p=0.002), VEGFA (rho=-0.56; p=0.04), and PGF (rho=-0.61; p=0.02). $CD133^+$ levels correlated negatively with MMP2 plasma concentration (rho=-0.59; p=0.03), while tenascin-c concentration correlated positively with both KDR^+CD133^+ levels (rho=0.60; p=0.03) and $CD133^+$ levels (rho=0.57; p=0.03). Significant correlations for GBM and MI are shown in Figure 5 .

GBM vs MI	Z	P (2-tailed)	
KDR+	2.0	0.04	GBM > MI
HPCs	1.6	0.12	
CECs	0.8	0.45	
CD133+	-1.3	0.19	MI > GBM
KDR+CD133+	-2.4	0.02	

GBM vs HC	Z	P (2-tailed)	
KDR+	4.7	≤0.001	GBM > HC
CECs	2.9	≤0.001	
KDR+CD133+	2.3	0.02	
CD133+	2.2	0.03	
HPCs	1.8	0.07	

MI vs HC	Z	P (2-tailed)	
KDR+CD133+	4.0	≤0.001	MI > HC
CD133+	3.0	≤0.001	
CECs	1.8	0.07	
KDR+	2.0	0.04	
HPCs	0.1	0.89	

GBM vs AII/III	Z	P (2-tailed)	
KDR+	3.1	≤0.001	GBM > AII/AIII
CECs	3.0	≤0.001	
KDR+CD133+	2.2	0.03	
HPCs	1.9	0.06	
CD133+	0.7	0.51	

AII/III vs HC	Z	P (2-tailed)	
CD133+	0.7	0.46	AII/AIII > HC
KDR+	-0.4	0.72	HC > AII/AIII
HPCs	-0.6	0.55	
KDR+CD133+	-0.6	0.54	
CECs	-1.0	0.34	

Figure 3: *Differences in EPC frequencies between patients.* EPC levels were represented as absolute cell numbers in $1*10^6$ $CD45^+$ PBMCs. The nonparametric Mann–Whitney U test (SPSS version 24) was used to analyze differences between the groups (p-values are 2-tailed). Direction of Z-score was adjusted as follows: negative to positive when GBM levels were higher than HC/MI/AII/AIII and when MI levels were higher than HC. The heat-maps are based on the levels and directions of Z-scores (red indicated higher levels of EPCs; blue indicated lower levels of EPCs in each comparison). KDR^+: $KDR^+CD34^-CD133^-$ cells. $CD133^+$: $CD133^+CD34^-KDR^-$ cells. KDR^+CD133^+: $KDR^+CD133^+CD34^-$ cells. HPCs: $CD34^+CD133^{+/-}CD45^{dim}$. CECs: $CD34^{bright}KDR^+CD45^-$.

GBM vs MI	Z	P (2-tailed)	
FGFb	2.9	0.004	GBM > MI
CSF3	2.4	0.018	
PDGFbb	2.3	0.021	
EPO	2.3	0.022	
CSF2	2.1	0.040	
Ang1	1.9	0.055	
Angiogenin	-2.0	0.045	MI > GBM
Ang2	-2.5	0.011	

GBM vs HC	Z	P (2-tailed)	
MMP9	4.5	≤0.001	GBM > HC
vWF	3.9	≤0.001	
HGF	2.7	0.008	
VCAM1	2.6	0.008	
CXCL12	-3.8	≤0.001	HC > GBM

MI vs HC	Z	P (2-tailed)	
vWF	4.0	≤0.001	MI > HC
MMP9	3.6	≤0.001	
HGF	3.2	≤0.001	
Angiogenin	2.9	0.004	
Tenascin-C	2.1	0.036	
MMP2	-2.0	0.041	HC > MI
Ang1	-2.1	0.039	
CSF3	-2.1	0.039	
CXCL12	-2.1	0.036	
BDNF	-2.3	0.021	
PDGFbb	-2.3	0.021	
EPO	-2.9	0.003	
FGFb	-3.5	≤0.001	

Figure 4: *Differences in levels of plasma factors between patients.* Z-scores and p-values of differences in the levels of plasma factors between patient and control groups (nonparametric Mann–Whitney U test). Direction of Z-score was adjusted as follows: negative to positive when GBM plasma levels of the factors were higher than MI/HC and when MI levels were higher than HC. The heat-maps are based on the levels and directions of Z-scores (red indicated higher levels of plasma factors; blue indicated lower levels of plasma factors in each comparison).

4. Discussion

We compared circulating EPC populations and plasma factors of patients with GBM and MI to pinpoint potential differences in EPC biology that may lead to the development of new therapeutic strategies directed against glioma-specific neovascularization.

While there was a general elevation of EPC levels in both GBM and MI patients compared to HC, we found differences in specific EPC subsets between GBM and MI patients. In GBM patients, HPCs and KDR^+ cells were elevated compared to MI patients. In MI patients, $KDR^+CD133^+$and $CD133^+$ cells were higher than in GBM patients. Increased levels of CD133+ cells were described before in MI patients [35]. An increase in KDR^+CD133^+ cells was reported following vascular damage due to burns or surgery [36], as well as in GBM and patients with other tumors [19, 37]. Data on circulating $KDR^+(CD34^-CD133^-)$ cells are largely lacking in the literature. Increased levels of circulating KDR^+ bone-marrow-derived EPCs were reported in a cancer mouse model [38], which is compatible with our findings in glioma patients. Increased HPC levels were observed previously in untreated GBM patients [39], while levels seem to normalize

MI (n=14)	CSF3	VEGFA	MMP2	PGF	Tenascin-C
HPCs	-0.76∗∗	-0.56∗		-0.61∗	
KDR^+CD133^+					0.60∗
$CD133^+$			-0.59∗		0.57∗

GBM (n=12)	MMP9	VCAM1
HPCs	0.62∗	
KDR^+		0.64∗

Figure 5: *Correlation between plasma factors and EPC subtypes.* ∗∗Correlation is significant at the 0.01 level (2-tailed). ∗Correlation is significant at the 0.05 level (2-tailed). We used Spearman's rho to calculate correlation coefficients between plasma factor and EPC subtype levels. Figure 5 shows Spearman's rho for significant correlations between EPC levels and plasma factor levels in MI and GBM patients. Blue color indicates a negative correlation between plasma factor and EPC frequency; red indicates a positive correlation. For a complete overview (including $CD133^{bright}$ and $CD133^-$ HPC subtypes and correlations between EPC frequencies and plasma factors in all samples grouped together), see Additional File 2.

and even decrease following treatment [40]. In order to refine the HPC populations, three subgroups of these cells are distinguished: $CD133^-$, $CD133^{dim}$, and $CD133^{bright}$ [25]. In the present study, we found a significant increase in the ratio of $CD133^{bright}/CD133^-$ HPCs in patients with MI, compared to GBM patients (Figure 1(f)). The more primitive phenotype of $CD133^{bright}$ HPCs is reportedly linked with higher proangiogenic capacity of these cells as compared to $CD133^-$ cells [23, 26, 27]. An increase in $CD133^+$ HPCs is seen in acute MI [41], while levels of these cells are low in patients with chronic vascular disease (low $CD133^{bright}/CD133^-$ HPC ratio [26]), suggesting that the rise in $CD133^{bright}/CD133^-$ HPC ratio is linked to acute ischemia.

There are various explanations for the numerical differences in EPC subsets between patients with GBM and MI. Both conditions are associated with increased neovascularization. One explanation is that MI represents a situation of acute injury, followed by programmed regeneration, while in neoplasia such as GBM, acute ischemic events due to, e.g., vessel thrombosis, occur on top of a background of chronic hypoxia and neoplastic vascular remodeling. In acute MI, a time course for EPC and CEC dynamics exists: within hours after MI, a peak in CECs appears in the bloodstream, which declines over the following weeks [36, 42]. Over the course of 3-7 days, $CD133^+$ cells increase, peaking around day 7, a phenomenon that was consistent with the present analysis [35]. Subsequently, somewhat later than $CD133^+$ cells, HPC levels rise [10, 13, 35]. The increase in the levels of both $CD133^+$ cells and $CD133^+KDR^+$ cells in MI patients suggests that these cells are influenced by similar regulatory mechanisms and that these EPC subtypes are particularly important in the early phase of acute ischemia. Elevated levels of $CD133^+$ cells have been described before in MI and GBM and encompass large part of the HPC population, since in these studies no further separation of EPC subtypes was made [35, 43, 44].We found that the absolute levels of EPCs and CECs were increased in MI and GBM, but not in the astrocytomas grade II and III, reflecting the low level of neovascularization in lower-grade gliomas.

The finding of higher levels of CECs in patients with GBM and MI compared to patients with lower-grade gliomas is corroborated by literature on patients with MI and neoplasia, including gliomas [45–53]. The lower levels of CECs in patients with gliomas of lower malignancy grades, in which neovascularization is less abundant, supports the notion that CEC levels correspond with the degree of vessel formation and remodeling in cancer. So far, the presence of CECs was considered to passively reflect vessel wall damage only, but there are indications that a viable subset should be considered as cells with potent proangiogenic and vasculogenic capacities [25, 54]. These cells give rise to outgrowth endothelial cells (OECs) when brought in cell culture and strongly stimulate neovascularization, incorporate in the vessel wall, and home to malignant tumors [55–57]. Increased levels of OEC precursor cells correlate with a better prognosis for patients with MI and coronary artery bypass grafts, illustrative of their proangiogenic capacities [36, 58]. Conversely, higher (viable) CEC levels correspond with a worse prognosis for patients with GBM [50, 51, 59] and other cancers [53, 60, 61]. Therefore, CECs may be considered as potential therapeutic targets in both cancer and infarction.

Limitations to any study on circulating EPCs in human subjects include difficulties of comparing study results to the literature, due to the lack of a clear and comparable definition of EPC subsets and the use of different techniques to determine or isolate EPCs. This makes it challenging to compare findings of different studies into EPCs. For instance, Stamm et al. [62] used magnetic beads to isolate $CD133^+$ cells from bone marrow aspirates of myocardial infarction patients undergoing subsequent coronary artery bypass graft. The $CD133^+$ bone marrow cells would in our study translate into a mixture of $CD133^+$ HPCs, $CD133^+KDR^-CD34^-$ cells and $CD133^+KDR^+CD34^-$ cells. Which of these different subsets will have been accountable for the beneficial effect in the study of Stamm et al. remains to be determined.

The $KDR^+CD34^-CD133^-$ population in the present study was not described before in the literature. However, this population needs to be distinguished from CECs ($CD34^{++}KDR^+CD45^-$) and from $CD133^+KDR^+$ EPCs.

Other studies have found increased levels of CECs and $CD133^+KDR^+$ cells in MI patients [36, 45, 63]. Interestingly, we found low levels of CD34 expression in some $KDR^+CD34^-CD133^-$ sorted populations (data not shown), suggesting that the expression of CD34 may have been too low to detect by FACS and suggesting a relationship with the more frequently described KDR^+CD34^+ EPC population in the literature. In our study, the $KDR^+CD34^-CD133^-$population was exclusively $CD45^+$ indicative of hematopoietic lineage. We also found high expression of proangiogenic factors in these cells (data not shown). Therefore, we believe that the $KDR^+CD34^-CD133^-$ EPC subset stimulates neovascularization just like other EPC subsets. Other confounders to human EPC-related studies are differences in age of subjects included. Younger age is associated with higher levels of circulating EPCs [64]. We do not believe, however, that the slight difference in age has influenced the results in GBM vs. MI patients (Table 1). AII/III patients are younger than GBM and MI patients, reflecting the age difference in the occurrence of these tumors. Young age is associated with higher circulating levels of EPCs. The significantly lower levels of EPCs in AII/III patients vs. GBM and MI patients emphasize the strong effects of underlying pathology on the EPC levels. In addition, sex differences may associate with circulating EPCs levels that vary based on menstrual phase in premenopausal women [65]). Unlike the situation in the glioma group, in the MI group, males predominated. However, since most, if not all, women in this study will have been postmenopausal (based on age), we do not believe that sex will have had a significant influence on the results either. Other confounders like physical exercise status were not controlled for. High-intensity physical exercise may lead to peaks in circulating EPC and CEC levels. This could be an explanation for high EPC level outliers in our study, particularly in the healthy control group. Other explanations for outliers can be time after MI (we included MI patients 1-10 days after myocardial infarction; within this timeframe, the dynamics of EPC and CEC levels can vary), GBM tumor characteristics (size, level of neovascularization), and medication use (e.g., statins can increase the levels of circulating EPCs or normalize previously reduced levels of EPCs in the context of chronic vascular disease and improve their function [66]).

The presence of the blood-brain barrier (BBB) or blood-tumor barrier in the case of GBM is highly unlikely to form an anatomical barrier relevant for EPCs. EPCs do not need to cross the BBB into the brain parenchyma to exert their angiogenic and vasculogenic effects. EPC entrance into the Virchow-Robin space, directly surrounding blood vessels, would suffice for the promotion of angiogenesis through the production of proangiogenic factors. No entrance of EPCs into the brain parenchyma is required for this process. Further, the BBB is severely impaired in glioblastoma, allowing cells to freely enter the brain [67]. Besides, even an intact BBB would allow for the selective entrance of (inflammatory) cells from the periphery into the parenchyma [68].

Since factors secreted by the target tissues are essential for the recruitment and function of EPCs, we investigated a panel of mobilization factors, chemoattractants, and angiogenic factors in plasma along with EPC levels and found significant differences in their mean concentrations between the patient groups and controls. Elevated levels of these factors were previously reported in blood and tumor tissue of patients with GBM [69–75] and of patients with MI [76–83]. Because the levels of vWF, MMP9, VCAM1, angiogenin, and HGF were increased in both GBM and MI patients, but not in the lower-grade gliomas, these factors seem to be necessary for neovascularization in general, both under reactive and high-grade neoplastic conditions. Together with VEGFA, these factors were higher in GBM as compared to the lower-grade gliomas, illustrative of their correlation with tumor grade and level of glioma neovascularization. Increased concentrations of vWF in GBM patients were previously reported [42]. Interestingly, in MI patients, many of the factors were decreased as compared to HC (Figure 4). This may in part be a reflection of chronic cardiovascular disease and vascular dysfunction preceding the acute infarction, as some circulating factors are already reduced in (un)stable angina [84, 85]. An increase in levels when acute ischemia ensues could then still remain below normal levels [86]. The increased levels of tenascin-c, vWF, MMP9, VCAM1, and angiogenin may reflect the response to acute ischemia. Angiogenin increases after MI, but is not elevated in patients suffering from stable cardiovascular disease [82]. Only angiogenin and angiopoietin-2 were increased in MI patients compared to GBM patients, suggestive of their association with the acute onset of ischemia occurring in MI. CXCL12 is one of the main mobilization factors for HPCs and other EPCs. Surprisingly, CXCL12 levels were lower in all patient groups relative to healthy controls. Reduced CXCL12 levels were reported in patients with MI previously [87–89] and also in experimentally induced MI in mice [88]. Our finding of low CXCL12 levels in GBM patients seems to conflict with literature data, where CXCL12 levels allegedly correlate positively with glial tumor progression [37, 50, 90]. The discrepancies may be explained by concurrent treatment, for instance, with antiangiogenic agents [50] in these studies, whilst in our study GBM patients were treatment-naïve.

We correlated the concentrations of mobilization factors and chemoattractants with the levels of EPC subsets in order to investigate a potential relationship between circulating levels of cells and factors. We found various correlations between the plasma factors on the one hand and the EPC subsets on the other hand (Figure 5). Interestingly, in MI patients, tenascin-c levels correlated positively with $CD133^+$ and KDR^+CD133^+ levels. Tenascin-c is a matricellular protein which is upregulated in ischemic myocardial tissue and aids in recruiting EPCs to the infarcted area [91]. Notably, plasma levels of tenascin-c are increased in the acute phase of MI [92, 93] corresponding to the early phase in which $CD133^+$ cells are released. A potential effect of plasma tenascin-c on the mobilization of EPCs, however, remains speculative.

In GBM patients, plasma levels of MMP9 correlated positively with HPC frequencies, which seems in line with data suggesting that MMP9 can mobilize HPCs from the bone marrow [94]. Increased levels of CECs and vWF and VCAM-1 are known to represent vessel damage and activated

endothelial cells, thus explaining their elevation in GBM patients.

How could our findings eventually be translated to novel therapeutic targets for GBM patients? From a therapeutic perspective, several different approaches could be chosen: firstly, by targeting the mobilization factors that lead to higher KDR^+ (and other EPC) levels in GBM patients. We found a strong positive correlation between plasma VCAM1 levels and KDR^+ EPCs in GBM. Should further studies indicate that VCAM1 can act as a mobilization factor for KDR^+ EPCs, anti-VCAM1 antibodies could potentially reduce circulating KDR^+ EPC levels in GBM patients. We found a strong positive correlation between plasma MMP9 levels and circulating HPC levels in GBM patients. From the literature, a causal relationship between the two can be assumed since MMP9 is a known mobilization factor for HPCs (and possibly other EPCs) [94]. Strategies to reduce plasma MMP9 levels could decrease circulating HPC (and possibly other EPC) levels in GBM patients. Likewise, with more of these causal relations between plasma factors and EPC levels coming to light, more therapeutic strategies of a similar nature can be generated.

Contrarily, in MI patients, the same strategies could be used in an opposite fashion: administering mobilization factors with the aim of increasing levels of circulating EPCs (e.g., we found a strong positive correlation between plasma tenascin-C levels and circulating levels of KDR^+CD133^+ and $CD133^+$ EPCs; should tenascin-C prove to act as a mobilization and/or homing factor to these EPCs, increasing the level of circulating and/or myocardial tissue tenascin-C could be beneficial to EPC mobilization and homing to hypoxic myocardial tissue).

Secondly, the homing mechanisms of EPCs to their target tissue can be therapeutically manipulated. In the case of GBM, homing factors such as CXCL12 could be increased in plasma (leading to a reduced gradient of GBM tissue-to-blood CXCL12 levels and potentially reduced homing of EPCs to target GBM tissue; this hypothesis would, obviously, need to be carefully tested in further studies). Another option could be to implant a device that captures KDR^+ (and other) EPCs from the circulation of GBM patients, thereby preventing them from reaching GBM tissue and exerting their proangiogenic effect (a similar strategy is used in preclinical studies in MI patients with EPC-capturing stents to increase neovascularization [95]). To the best our knowledge, this strategy has not been tested with the aim of decreasing circulating levels of EPCs (and decreasing their homing efficiency to tumor tissue) in cancer patients yet, but could be promising.

Thirdly, the ability of EPCs to migrate to GBM tumor tissue means that EPCs themselves could be used as vessels for transport of cancer-blocking agents to the tumor (e.g., radioactive or chemotherapeutic compounds). Whether there is a difference between EPC subsets in their ability to migrate to GBM tumor tissue remains to be determined (e.g., are KDR^+ EPCs better able to home to GBM tissue than other EPCs? If so, this cell type could preferentially be used for this strategy). This hypothesis has been postulated before in the literature [96]. Contrarily, in the case of MI, (KDR^+CD133^+, $CD133^+KDR^-$) EPCs could be altered (in vitro) to, e.g., express higher levels of proangiogenic factors and readministered to MI patients to aid in tissue recovery.

5. Conclusion

In conclusion, while neovascularization in both the context of high-grade neoplasia (GBM) and acute ischemia (MI) is associated with a rise in EPC levels, we found differences in their relative EPC subsets. Our findings indicate that the process of EPC-related neovascularization differs between these two diseases. The data are supportive of the development of EPC targeted therapeutic strategies that differ in both contexts. In acute ischemic conditions, stimulation of EPC-induced neovascularization is needed (increasing the circulating levels of KDR^+CD133^+ and $CD133^+$ cells). However, in GBM, inhibition of EPC-induced neovascularization is necessary (specifically focusing on decreasing KDR^+ cells and HPCs).

Abbreviations

AII/AIII:	Astrocytoma grade 2 and grade 3
Angl:	Angiopoietin 1
Ang2:	Angiopoietin 2
BDNF:	Brain-derived neurotrophic factor
CEC:	Circulating endothelial cell
CSF2:	Colony stimulating factor 2
CSF3:	Colony stimulating factor 3
CXCL12:	CXC-motif chemokine ligand 12
EDTA:	Ethylenediaminetetraacetic acid
EGF:	Epidermal growth factor
EPC:	Endothelial progenitor cell
EPO:	Erythropoietin
FACS:	Fluorescence-activated cell sorting
FGFb:	Basic fibroblast growth factor
GBM:	Glioblastoma
HC:	Healthy control
HGF:	Hepatocyte growth factor
HPC:	Hematopoietic progenitor cell
KDR:	Kinaseinsert domain
KITL:	KIT-ligand
MFI:	Mean fluorescence intensity
MI:	Myocardial infarction
MMP2:	Matrix metalloproteinase 2
MMP9:	Matrix metalloproteinase 9
PBMC:	Peripheral blood mononuclear cell
PDGF-BB:	Platelet-derived growth factor BB
PGF:	Placental growth factor
PPP:	Platelet-poor plasma
PRP:	Platelet-rich plasma
VCAM1:	Vascular cell adhesion molecule 1
VEGFA:	Vascular endothelial growth factor A
vWF:	von Willebrand factor.

Data Availability

The datasets used and/or analyzed during the current study are available from the corresponding author upon reasonable request.

Ethical Approval

This study was approved by the Medical Ethics Committee of the Erasmus Medical Center, Rotterdam, The Netherlands (MEC-2011-313), and performed in adherence to the Code of Conduct of the Federation of Medical Scientific Societies in The Netherlands (http://www.federa.org/codes-conduct).

Conflicts of Interest

The authors declare that they have no conflicts of interest.

Authors' Contributions

K. Huizer, A. Sacchetti, D. Mustafa, and J.M. Kros carried out conception and design and interpretation of data. K. Huizer carried out drafting the article. J.M. Kros carried out drafting and critical revision of the article. A. Sacchetti and D. Mustafa carried out critical revision of the article. All authors read and approved the final manuscript.

Funding

This research was funded by the Department of Pathology, Erasmus Medical Center, Rotterdam, The Netherlands.

Supplementary Materials

Additional File 1: Luminex Assays. Luminex Assays (customized) were used in the study. Three separate assays were included. Columns show the factors analyzed, the dilution factor, bead region used, and value (pg/ml) of standard. Type of factor (AF: angiogenic factor, Mob: mobilization factor, Chemo: chemoattractant) is specified. *Additional File 2: Correlation between Plasma Factors and EPC Subtypes.* We used Spearman's rho to calculate correlation coefficients between plasma factor and EPC subtype levels. All samples were analyzed, as well as every group separately. Green highlighted correlations indicate p-values<0.05. *(Supplementary Materials)*

References

[1] M. Ameratunga, N. Pavlakis, H. Wheeler, R. Grant, J. Simes, and M. Khasraw, "Anti-angiogenic therapy for high-grade glioma," *Cochrane Database of Systematic Reviews*, vol. 11, article CD008218, 2018.

[2] R. Tamura, T. Tanaka, K. Miyake, K. Yoshida, and H. Sasaki, "Bevacizumab for malignant gliomas: current indications, mechanisms of action and resistance, and markers of response," *Brain Tumor Pathology*, vol. 34, no. 2, pp. 62–77, 2017.

[3] M. Mayr, D. Niederseer, and J. Niebauer, "From bench to bedside: what physicians need to know about endothelial progenitor cells," *American Journal of Medicine*, vol. 124, no. 6, pp. 489–497, 2011.

[4] A. L. George, P. Bangalore-Prakash, S. Rajoria et al., "Endothelial progenitor cell biology in disease and tissue regeneration," *Journal of Hematology & Oncology*, vol. 4, no. 1, p. 24, 2011.

[5] M. Kioi, H. Vogel, G. Schultz, R. M. Hoffman, G. R. Harsh, and J. M. Brown, "Inhibition of vasculogenesis, but not angiogenesis, prevents the recurrence of glioblastoma after irradiation in mice," *The Journal of Clinical Investigation*, vol. 120, no. 3, pp. 694–705, 2010.

[6] G. J. Madlambayan, J. M. Butler, K. Hosaka et al., "Bone marrow stem and progenitor cell contribution to neovasculogenesis is dependent on model system with SDF-1 as a permissive trigger," *Blood*, vol. 114, no. 19, pp. 4310–4319, 2009.

[7] P.-P. Zheng, W. C. Hop, T. M. Luider, P. A. E. Sillevis Smitt, and J. M. Kros, "Increased levels of circulating endothelial progenitor cells and circulating endothelial nitric oxide synthase in patients with gliomas," *Annals of Neurology*, vol. 62, no. 1, pp. 40–48, 2007.

[8] A. Aicher, S. Dimmeler, and C. Heeschen, "Nonbone marrow-derived endothelial progenitor cells: what is their exact location?" *Circulation Research*, vol. 101, no. 9, p. e102, 2007.

[9] B. A. Peters, L. A. Diaz Jr., K. Polyak et al., "Contribution of bone marrow-derived endothelial cells to human tumor vasculature," *Nature Medicine*, vol. 11, no. 3, pp. 261-262, 2005.

[10] F. Grundmann, C. Scheid, D. Braun et al., "Differential increase of CD34, KDR/CD34, CD133/CD34 and CD117/CD34 positive cells in peripheral blood of patients with acute myocardial infarction," *Clinical Research in Cardiology*, vol. 96, no. 9, pp. 621–627, 2007.

[11] G. P. Fadini, D. Losordo, and S. Dimmeler, "Critical reevaluation of endothelial progenitor cell phenotypes for therapeutic and diagnostic use," *Circulation Research*, vol. 110, no. 4, pp. 624–637, 2012.

[12] R. Botta, E. Gao, G. Stassi et al., "Heart infarct in NOD-SCID mice: therapeutic vasculogenesis by transplantation of human CD34+ cells and low dose CD34+KDR+ cells," *The FASEB Journal*, vol. 18, no. 12, pp. 1392–1394, 2004.

[13] W. Kuliczkowski, R. Derzhko, I. Prajs, M. Podolak-Dawidziak, and V. L. Serebruany, "Endothelial progenitor cells and left ventricle function in patients with acute myocardial infarction: potential therapeutic considertions," *American Journal of Therapeutics*, vol. 19, no. 1, pp. 44–50, 2012.

[14] V. Jeevanantham, M. R. Afzal, E. K. Zuba-Surma, and B. Dawn, "Clinical trials of cardiac repair with adult bone marrow-derived cells," *Methods in Molecular Biology*, vol. 1036, pp. 179–205, 2013.

[15] A. Manginas, E. Goussetis, M. Koutelou et al., "Pilot study to evaluate the safety and feasibility of intracoronary CD133(+) and CD133(-) CD34(+) cell therapy in patients with nonviable anterior myocardial infarction," *Catheterization and Cardiovascular Interventions*, vol. 69, no. 6, pp. 773–781, 2007.

[16] A. C. Senegaglia, L. A. Barboza, B. Dallagiovanna et al., "Are purified or expanded cord blood-derived CD133+ cells better at improving cardiac function?" *Experimental Biology and Medicine*, vol. 235, no. 1, pp. 119–129, 2010.

[17] A. S. Arbab, S. D. Pandit, S. A. Anderson et al., "Magnetic resonance imaging and confocal microscopy studies of magnetically labeled endothelial progenitor cells trafficking to sites of tumor angiogenesis," *Stem Cells*, vol. 24, no. 3, pp. 671–678, 2006.

[18] X.-T. Sun, X.-W. Yuan, H.-T. Zhu et al., "Endothelial precursor cells promote angiogenesis in hepatocellular carcinoma," *World Journal of Gastroenterology*, vol. 18, no. 35, pp. 4925–4933, 2012.

[19] X. Le Bourhis, R. Romon, and H. Hondermarck, "Role of endothelial progenitor cells in breast cancer angiogenesis: from fundamental research to clinical ramifications," *Breast Cancer Research and Treatment*, vol. 120, no. 1, pp. 17–24, 2010.

[20] J. M. Roodhart, M. H. Langenberg, J. S. Vermaat et al., "Late release of circulating endothelial cells and endothelial progenitor cells after chemotherapy predicts response and survival in cancer patients," *Neoplasia*, vol. 12, no. 1, pp. 87–94, 2010.

[21] G. A. Alexiou, G. Vartholomatos, A. Karamoutsios, and S. Voulgaris, "The role of circulating progenitor cells in glioma patients," *Journal of Neuro-Oncology*, vol. 110, no. 1, pp. 153-154, 2012.

[22] P. Carmeliet and R. K. Jain, "Angiogenesis in cancer and other diseases," *Nature*, vol. 407, no. 6801, pp. 249–257, 2000.

[23] H. Mayani, "Biological differences between neonatal and adult human hematopoietic stem/Progenitor cells," *Stem Cells and Development*, vol. 19, no. 3, pp. 285–298, 2010.

[24] E. Cuadrado-Godia, A. Regueiro, J. Núñez et al., "Endothelial progenitor cells predict cardiovascular events after atherothrombotic stroke and acute myocardial infarction. a PROCELL substudy," *PLoS ONE*, vol. 10, no. 9, article e0132415, 2015.

[25] K. Huizer, D. A. Mustafa, J. C. Spelt, J. M. Kros, A. Sacchetti, and F. Bertolini, "Improving the characterization of endothelial progenitor cell subsets by an optimized FACS protocol," *PLoS ONE*, vol. 12, no. 9, article e0184895, 2017.

[26] M. L. Estes, J. A. Mund, L. E. Mead et al., "Application of polychromatic flow cytometry to identify novel subsets of circulating cells with angiogenic potential," *Cytometry Part A*, vol. 77, no. 9, pp. 831–839, 2010.

[27] W. Wagner, A. Ansorge, U. Wirkner et al., "Molecular evidence for stem cell function of the slow-dividing fraction among human hematopoietic progenitor cells by genome-wide analysis," *Blood*, vol. 104, no. 3, pp. 675–686, 2004.

[28] P. Carmeliet, "Basic concepts of (myocardial) angiogenesis: role of vascular endothelial growth factor and angiopoietin," *Current Interventional Cardiology Reports*, vol. 1, no. 4, pp. 322–335, 1999.

[29] P. Carmeliet, "Angiogenesis in life, disease and medicine," *Nature*, vol. 438, no. 7070, pp. 932–936, 2005.

[30] P. Carmeliet and R. K. Jain, "Molecular mechanisms and clinical applications of angiogenesis," *Nature*, vol. 473, no. 7347, pp. 298–307, 2011.

[31] P. Carmeliet and A. Luttun, "The emerging role of the bone marrow-derived stem cells in (therapeutic) angiogenesis," *Thrombosis and Haemostasis*, vol. 86, no. 1, pp. 289–297, 2001.

[32] M. Potente, H. Gerhardt, and P. Carmeliet, "Basic and therapeutic aspects of angiogenesis," *Cell*, vol. 146, no. 6, pp. 873–887, 2011.

[33] D. A. Mustafa, L. J. Dekker, C. Stingl et al., "A proteome comparison between physiological angiogenesis and angiogenesis in glioblastoma," *Molecular and Cellular Proteomics*, vol. 11, no. 6, article M111.008466, 2012.

[34] H. Sakai, S. Goto, J.-Y. Kim et al., "Plasma concentration of von Willebrand factor in acute myocardial infarction," *Thrombosis and Haemostasis*, vol. 84, no. 2, pp. 204–209, 2000.

[35] R. G. Turan, M. Brehm, M. Koestering et al., "Factors influencing spontaneous mobilization of CD34+ and CD133+ progenitor cells after myocardial infarction," *European Journal of Clinical Investigation*, vol. 37, no. 11, pp. 842–851, 2007.

[36] M. Gill, S. Dias, K. Hattori et al., "Vascular trauma induces rapid but transient mobilization of VEGFR2(+)AC133(+) endothelial precursor cells," *Circulation Research*, vol. 88, no. 2, pp. 167–174, 2001.

[37] J. P. Greenfield, D. K. Jin, L. M. Young et al., "Surrogate markers predict angiogenic potential and survival in patients with glioblastoma multiforme," *Neurosurgery*, vol. 64, no. 5, pp. 819–826, 2009.

[38] H. Zhu, Q. Shao, X. Sun et al., "The mobilization, recruitment and contribution of bone marrow-derived endothelial progenitor cells to the tumor neovascularization occur at an early stage and throughout the entire process of hepatocellular carcinoma growth," *Oncology Reports*, vol. 28, no. 4, pp. 1217–1224, 2012.

[39] G. A. Alexiou, G. Vartholomatos, A. Karamoutsios, A. Batistatou, A. P. Kyritsis, and S. Voulgaris, "Circulating progenitor cells: a comparison of patients with glioblastoma or meningioma," *Acta Neurologica Belgica*, vol. 113, no. 1, pp. 7–11, 2013.

[40] E. Corsini, E. Ciusani, P. Gaviani et al., "Decrease in circulating endothelial progenitor cells in treated glioma patients," *Journal of Neuro-Oncology*, vol. 108, no. 1, pp. 123–129, 2012.

[41] Y. Iso, S. Yamaya, T. Sato et al., "Distinct mobilization of circulating CD271+ mesenchymal progenitors from hematopoietic progenitors during aging and after myocardial infarction," *Stem Cells Translational Medicine*, vol. 1, no. 6, pp. 462–468, 2012.

[42] A. Regueiro, E. Cuadrado-Godia, C. Bueno-Betí et al., "Mobilization of endothelial progenitor cells in acute cardiovascular events in the PROCELL study: time-course after acute myocardial infarction and stroke," *Journal of Molecular and Cellular Cardiology*, vol. 80, pp. 146–155, 2015.

[43] O. Fortunato, G. Spinetti, C. Specchia, E. Cangiano, M. Valgimigli, and P. Madeddu, "Migratory activity of circulating progenitor cells and serum SDF-1alpha predict adverse events in patients with myocardial infarction," *Cardiovascular Research*, vol. 100, no. 2, pp. 192–200, 2013.

[44] N. Rafat, G. C. Beck, J. Schulte, J. Tuettenberg, and P. Vajkoczy, "Circulating endothelial progenitor cells in malignant gliomas," *Journal of Neurosurgery*, vol. 112, no. 1, pp. 43–49, 2010.

[45] K. Bethel, M. S. Luttgen, S. Damani et al., "Fluid phase biopsy for detection and characterization of circulating endothelial cells in myocardial infarction," *Physical Biology*, vol. 11, no. 1, article 016002, 2014.

[46] C. Li, Q. Wu, B. Liu et al., "Detection and validation of circulating endothelial cells, a blood-based diagnostic marker of acute myocardial infarction," *PLoS ONE*, vol. 8, no. 3, article e58478, 2013.

[47] S. Damani, A. Bacconi, O. Libiger et al., "Characterization of circulating endothelial cells in acute myocardial infarction," *Science Translational Medicine*, vol. 4, no. 126, article 126ra33, 2012.

[48] M. Lampka, Z. Grąbczewska, E. Jendryczka-Maćkiewicz et al., "Circulating endothelial cells in coronary artery disease," *Kardiologia Polska*, vol. 68, no. 10, pp. 1100–1105, 2010.

[49] H. C. de Boer, A. M. van Oeveren-Rietdijk, J. I. Rotmans, O. M. Dekkers, T. J. Rabelink, and A. J. van Zonneveld, "Activated platelets correlate with mobilization of naive CD34(+) cells and generation of CD34(+) /KDR(+) cells in the circulation. A meta-regression analysis," *Journal of Thrombosis and Haemostasis*, vol. 11, no. 8, pp. 1583–1592, 2013.

[50] T. T. Batchelor, A. G. Sorensen, E. di Tomaso et al., "AZD2171, a pan-VEGF receptor tyrosine kinase inhibitor, normalizes tumor vasculature and alleviates edema in glioblastoma patients," *Cancer Cell*, vol. 11, no. 1, pp. 83–95, 2007.

[51] G. Reynés, V. Vila, T. Fleitas et al., "Circulating endothelial cells and procoagulant microparticles in patients with glioblastoma: prognostic value," *PLoS ONE*, vol. 8, no. 7, article e69034, 2013.

[52] P. Mancuso and F. Bertolini, "Circulating endothelial cells as biomarkers in clinical oncology," *Microvascular Research*, vol. 79, no. 3, pp. 224–228, 2010.

[53] M. Ilie, E. Long, V. Hofman et al., "Clinical value of circulating endothelial cells and of soluble CD146 levels in patients undergoing surgery for non-small cell lung cancer," *British Journal of Cancer*, vol. 110, no. 5, pp. 1236–1243, 2014.

[54] S. Fang, J. Wei, N. Pentinmikko, H. Leinonen, P. Salven, and M. A. Goodell, "Generation of functional blood vessels from a single c-kit+ adult vascular endothelial stem cell," *PLoS Biology*, vol. 10, no. 10, p. e1001407, 2012.

[55] M. U. Becher, G. Nickenig, and N. Werner, "Regeneration of the vascular compartment," *Herz*, vol. 35, no. 5, pp. 342–351, 2010.

[56] D. P. Sieveking, A. Buckle, D. S. Celermajer, and M. K. C. Ng, "Strikingly different angiogenic properties of endothelial progenitor cell subpopulations: insights from a novel human angiogenesis assay," *Journal of the American College of Cardiology*, vol. 51, no. 6, pp. 660–668, 2008.

[57] K. Bieback, M. Vinci, S. Elvers-Hornung et al., "Recruitment of human cord blood-derived endothelial colony-forming cells to sites of tumor angiogenesis," *Cytotherapy*, vol. 15, no. 6, pp. 726–739, 2013.

[58] N. Meneveau, F. Deschaseaux, M.-F. Séronde et al., "Presence of endothelial colony-forming cells is associated with reduced microvascular obstruction limiting infarct size and left ventricular remodelling in patients with acute myocardial infarction," *Basic Research in Cardiology*, vol. 106, no. 6, pp. 1397–1410, 2011.

[59] E. Galanis, S. K. Anderson, J. M. Lafky et al., "Phase II study of bevacizumab in combination with sorafenib in recurrent glioblastoma (N0776): a north central cancer treatment group trial," *Clinical Cancer Research*, vol. 19, no. 17, pp. 4816–4823, 2013.

[60] P. K. Y. Goon, G. Y. H. Lip, P. S. Stonelake, and A. D. Blann, "Circulating endothelial cells and circulating progenitor cells in breast cancer: relationship to endothelial damage/dysfunction/apoptosis, clinicopathologic factors, and the Nottingham prognostic index," *Neoplasia*, vol. 11, no. 8, pp. 771–779, 2009.

[61] C. G. Willett, Y. Boucher, E. Di Tomaso et al., "Direct evidence that the VEGF-specific antibody bevacizumab has antivascular effects in human rectal cancer," *Nature Medicine*, vol. 10, no. 2, pp. 145–147, 2004.

[62] C. Stamm, H.-D. Kleine, Y.-H. Choi et al., "Intramyocardial delivery of CD133+ bone marrow cells and coronary artery bypass grafting for chronic ischemic heart disease: safety and efficacy studies," *The Journal of Thoracic and Cardiovascular Surgery*, vol. 133, no. 3, pp. 717–725, 2007.

[63] A. J. Flammer, M. Gössl, R. J. Widmer et al., "Osteocalcin positive CD133+/CD34-/KDR+ progenitor cells as an independent marker for unstable atherosclerosis," *European Heart Journal*, vol. 33, no. 23, pp. 2963–2969, 2012.

[64] E. Rurali, B. Bassetti, G. L. Perrucci et al., "BM ageing: implication for cell therapy with EPCs," *Mechanisms of Ageing and Development*, vol. 159, pp. 4–13, 2016.

[65] C. Lemieux, I. Cloutier, and J.-F. Tanguay, "Menstrual cycle influences endothelial progenitor cell regulation: a link to gender differences in vascular protection?" *International Journal of Cardiology*, vol. 136, no. 2, pp. 200–210, 2009.

[66] C. Briguori, C. Quintavalle, F. D'Alessio et al., "Impact of statin therapy intensity on endothelial progenitor cells after percutaneous coronary intervention in diabetic patients. The REMEDY-EPC late study," *International Journal of Cardiology*, vol. 244, pp. 112–118, 2017.

[67] J. N. Sarkaria, L. S. Hu, I. F. Parney et al., "Is the blood-brain barrier really disrupted in all glioblastomas? A critical assessment of existing clinical data," *Neuro-Oncology*, vol. 20, no. 2, pp. 184–191, 2018.

[68] I. Galea, I. Bechmann, and V. H. Perry, "What is immune privilege (not)?" *Trends in Immunology*, vol. 28, no. 1, pp. 12–18, 2007.

[69] B. J. Xu, Q. A. An, S. S. Gowda et al., "Identification of blood protein biomarkers that aid in the clinical assessment of patients with malignant glioma," *International Journal of Oncology*, vol. 40, no. 6, pp. 1995–2003, 2012.

[70] A. Hormigo, B. Gu, S. Karimi et al., "YKL-40 and matrix metalloproteinase-9 as potential serum biomarkers for patients with high-grade gliomas," *Clinical Cancer Research*, vol. 12, no. 19, pp. 5698–5704, 2006.

[71] P. Mahzouni, F. Mohammadizadeh, K. Mougouei, N. A. Moghaddam, A. Chehrei, and A. Mesbah, "Determining the relationship between "microvessel density" and different grades of astrocytoma based on immunohistochemistry for "factor VIII-related antigen" (von Willebrand factor) expression in tumor microvessels," *Indian Journal of Pathology and Microbiology*, vol. 53, no. 4, pp. 605–610, 2010.

[72] N. O. Schmidt, M. Westphal, C. Hagel et al., "Levels of vascular endothelial growth factor, hepatocyte growth factor/scatter factor and basic fibroblast growth factor in human gliomas and their relation to angiogenesis," *International Journal of Cancer*, vol. 84, no. 1, pp. 10–18, 1999.

[73] K. Lamszus, J. Laterra, M. Westphal, and E. M. Rosen, "Scatter factor/hepatocyte growth factor (SF/HGF) content and function in human gliomas," *International Journal of Developmental Neuroscience*, vol. 17, no. 5-6, pp. 517–530, 1999.

[74] P. L. Kornblith, "Perpetual motion and glioma growth," *Surgical Neurology*, vol. 47, no. 3, pp. 282-283, 1997.

[75] R. Garcia-Navarrete, E. Garcia, O. Arrieta, and J. Sotelo, "Hepatocyte growth factor in cerebrospinal fluid is associated with mortality and recurrence of glioblastoma, and could be of prognostic value," *Journal of Neuro-Oncology*, vol. 97, no. 3, pp. 347–351, 2010.

[76] N. Lamblin, A. Bauters, M. Fertin, P. De Groote, F. Pinet, and C. Bauters, "Circulating levels of hepatocyte growth factor and left ventricular remodelling after acute myocardial infarction (from the REVE-2 study)," *European Journal of Heart Failure*, vol. 13, no. 12, pp. 1314–1322, 2011.

[77] A. Konopka, J. Janas, W. Piotrowski, and J. Stępińska, "Hepatocyte growth factor - The earliest marker of myocardial injury in ST-segment elevation myocardial infarction," *Kardiologia Polska*, vol. 71, no. 8, pp. 827–831, 2013.

[78] R. Madonna, C. Cevik, M. Nasser, and R. de Caterina, "Hepatocyte growth factor: molecular biomarker and player in cardioprotection and cardiovascular regeneration," *Thrombosis and Haemostasis*, vol. 107, no. 4, pp. 656–661, 2012.

[79] A. O. Spiel, J. C. Gilbert, and B. Jilma, "Von Willebrand factor in cardiovascular disease: focus on acute coronary syndromes," *Circulation*, vol. 117, no. 11, pp. 1449–1459, 2008.

[80] J. L. Guo, Y. N. Yang, Y. T. Ma et al., "Values of matrix metalloproteinase-9 in early diagnosis and short-term prognosis of ST-segment elevation myocardial infarction," *Chinese Medical Journal*, vol. 92, no. 38, pp. 2681–2684, 2012.

[81] M. M. Thompson and I. B. Squire, "Matrix metalloproteinase-9 expression after myocardial infarction: physiological or pathological?" *Cardiovascular Research*, vol. 54, no. 3, pp. 495–498, 2002.

[82] A. Tello-Montoliu, F. Marín, J. Patel et al., "Plasma angiogenin levels in acute coronary syndromes: implications for prognosis," *European Heart Journal*, vol. 28, no. 24, pp. 3006–3011, 2007.

[83] K. Tamura, H. Nakajima, H. Rakue et al., "Elevated circulating levels of basic fibroblast growth factor and vascular endothelial growth factor in patients with acute myocardial infarction," *Japanese Circulation Journal*, vol. 63, no. 5, pp. 357–361, 1999.

[84] J. K. Damas, T. Waehre, A. Yndestad et al., "Stromal cell-derived factor-1alpha in unstable angina: potential antiinflammatory and matrix-stabilizing effects," *Circulation*, vol. 106, no. 16, pp. 36–42, 2002.

[85] A. Tahara, M. Yasuda, H. Itagane et al., "Plasma levels of platelet-derived growth factor in normal subjects and patients with ischemic heart disease," *American Heart Journal*, vol. 122, no. 4, pp. 986–992, 1991.

[86] L. Manni, V. Nikolova, D. Vyagova, G. N. Chaldakov, and L. Aloe, "Reduced plasma levels of NGF and BDNF in patients with acute coronary syndromes," *International Journal of Cardiology*, vol. 102, no. 1, pp. 169–171, 2005.

[87] K. Stellos, B. Bigalke, H. Langer et al., "Expression of stromal-cell-derived factor-1 on circulating platelets is increased in patients with acute coronary syndrome and correlates with the number of CD34+ progenitor cells," *European Heart Journal*, vol. 30, no. 5, pp. 584–593, 2009.

[88] A. J. Boyle, Y. Yeghiazarians, H. Shih et al., "Myocardial production and release of MCP-1 and SDF-1 following myocardial infarction: differences between mice and man," *Journal of Translational Medicine*, vol. 9, article 150, 2011.

[89] R. Wyderka, W. Wojakowski, T. Jadczyk et al., "Mobilization of CD34+CXCR4+ stem/progenitor cells and the parameters of left ventricular function and remodeling in 1-year follow-up of patients with acute myocardial infarction," *Mediators of Inflammation*, vol. 2012, Article ID 564027, 11 pages, 2012.

[90] S. R. Moosavi, H. Khorramdelazad, M. Amin et al., "The SDF-1 3'A genetic variation is correlated with elevated intra-tumor tissue and circulating concentration of cxcl12 in glial tumors: a study on iranian anaplastic astrocytoma and glioblastoma multiforme patients," *Journal of Molecular Neuroscience*, vol. 50, no. 2, pp. 298–304, 2013.

[91] V. L. Ballard, A. Sharma, I. Duignan et al., "Vascular tenascin-C regulates cardiac endothelial phenotype and neovascularization," *The FASEB Journal*, vol. 20, no. 6, pp. 717–719, 2006.

[92] I. Niebroj-Dobosz, "Tenascin-C in human cardiac pathology," *Clinica Chimica Acta*, vol. 413, no. 19-20, pp. 1516–1518, 2012.

[93] K. S. Midwood and G. Orend, "The role of tenascin-C in tissue injury and tumorigenesis," *Journal of Cell Communication and Signaling*, vol. 3, no. 3-4, pp. 287–310, 2009.

[94] A. Carion, L. Benboubker, O. Hérault et al., "Stromal-derived factor 1 and matrix metalloproteinase 9 levels in bone marrow and peripheral blood of patients mobilized by granulocyte colony-stimulating factor and chemotherapy. Relationship with mobilizing capacity of haematopoietic progenitor cells," *British Journal of Haematology*, vol. 122, no. 6, pp. 918–926, 2003.

[95] R. Zarpak, O. D. Sanchez, M. Joner, L.-G. Guy, G. Leclerc, and R. Virmani, "A novel "pro-healing" approach: the COMBO dual therapy stent from a pathological view," *Minerva Cardioangiologica*, vol. 63, no. 1, pp. 31–43, 2015.

[96] A. Laurenzana, F. Margheri, A. Chillà et al., "Endothelial progenitor cells as shuttle of anticancer agents," *Human Gene Therapy*, vol. 27, no. 10, pp. 784–791, 2016.

CHAPTER 3

CIRCULATING ANGIOGENIC CELLS IN GLIOBLASTOMA:

Towards Defining Crucial Functional Differences in CAC-induced Neoplastic versus Reactive Neovascularization

Neuro-Oncology Advances
2(1), 1–12, 2020 | doi:10.1093/noajnl/vdaa040 | Advance Access date 1 April 2020

Circulating angiogenic cells in glioblastoma: toward defining crucial functional differences in CAC-induced neoplastic versus reactive neovascularization

Karin Huizer, Andrea Sacchetti, Sigrid Swagemakers, Peter J. van der Spek, Wim Dik, Dana A. Mustafa, and Johan M. Kros

Laboratory for Tumor Immuno-Pathology, Erasmus Medical Center, Rotterdam, The Netherlands (K.H., A.S., D.A.M., J.M.K.); Department of Pathology and Clinical Bio-Informatics, Erasmus Medical Center, Rotterdam, The Netherlands (S.S., P.J.v.d.S.); Department of Immunology, Erasmus Medical Center, Rotterdam, The Netherlands (W.D.)

Corresponding Author: Johan M. Kros, MD, PhD, Laboratory for Tumor Immuno-Pathology, Erasmus Medical Center, Wytemaweg 80, 3015 CN Rotterdam, The Netherlands (j.m.kros@erasmusmc.nl).

Abstract

Background. In order to identify suitable therapeutic targets for glioma anti-angiogenic therapy, the process of neovascularization mediated by circulating angiogenic cells (CACs) needs to be scrutinized.

Methods. In the present study, we compared the expression of neovascularization-related genes by 3 circulating CAC subsets (hematopoietic progenitor cells [HPCs], $CD34^+$, and KDR^+ cells; internal controls: peripheral blood mononuclear cells and circulating endothelial cells) of treatment-naïve patients with glioblastoma (GBM) to those of patients undergoing reactive neovascularization (myocardial infarction (MI). CACs from umbilical cord (representing developmental neovascularization) and healthy subjects served as controls. Fluorescent-activated cell sorting was used to isolate CACs, RT-PCR to determine the expression levels of a panel of 48 neovascularization-related genes, and Luminex assays to measure plasma levels of 21 CAC-related circulating molecules.

Results. We found essential differences in gene expression between GBM and MI CACs. GBM CACs had a higher expression of proangiogenic factors (especially, *KITL*, *CXCL12*, and *JAG1*), growth factor and chemotactic receptors (*IGF1R*, *TGFBR2*, *CXCR4*, and *CCR2*), adhesion receptor monomers (*ITGA5* and *ITGA6*), and matricellular factor *POSTN*. In addition, we found major differences in the levels of neovascularization-related plasma factors. A strong positive correlation between plasma MMP9 levels and expression of *CXCR4* in the CAC subset of HPCs was found in GBM patients.

Conclusions. Our findings indicate that CAC-mediated neovascularization in GBM is characterized by more efficient CAC homing to target tissue and a more potent proangiogenic response than in physiologic tissue repair in MI. Our findings can aid in selecting targets for therapeutic strategies acting against GBM-specific CACs.

Key Points

- Glioblastoma CACs have a more potent homing and angiogenic capacity than controls.
- CACs are programmed in the circulation by target tissue-specific requirements.
- Unique CAC characteristics in different diseases translate to therapeutic targets.

High-grade gliomas are among the most vascularized tumors and are characterized by an abundance of leaky vessels. Despite the high degree of vascularization, anti-angiogenic therapies have remained without the expected success.[1] Anti-angiogenic drugs like bevacizumab interfere with Vascular Endothelial Growth Factor A (VEGFA) and the process of sprouting angiogenesis. However, the contribution of circulating cells engaged in the formation of blood vessels may be overlooked as

Importance of the Study

Prior literature on circulating angiogenic cells (CACs) in glioblastoma (GBM) uncovered their potent proangiogenic effects in vitro/vivo and their increased numbers in GBM patients. Our study is the first to show that GBM CACs are qualitatively different from non-neoplastic CACs (ie, in reactive [myocardial infarction], developmental [umbilical cord blood], and steady-state adult [healthy control] neovascularization). GBM CACs exhibit a gene expression profile compatible with increased tumor-homing capacity (higher expression of *CXCR4*, *CCR2*, *ITGA5*, and *ITGA6*) and a more potent proangiogenic potential (higher expression of *KITL*, *CXCL12*, *JAG1*, *IGF1R*, *TGFBR2*, and *POSTN*). Plasma levels of tumor-derived mobilization factor MMP9 correlate positively with both circulating hematopoietic progenitor cell (HPC) levels and HPC *CXCR4* gene expression in GBM patients, illustrating that GBM tissue is capable of pre-programming CACs. GBM, though non-metastatic, should thus be considered a systemic disease requiring systemic treatment. Our results can be translated toward developing disease-specific therapies targeting CAC-induced neovascularization in GBM.

a significant component of neovascularization in gliomas. This could partially explain the failing of anti-angiogenic therapies in glioma patients. Vasculogenesis is defined as de novo formation of blood vessels by endothelial progenitor cells (EPCs) that differentiate into endothelial cells and become part of the newly formed vessel wall.[2] Although characteristic for embryogenesis, the process of vasculogenesis also contributes to neovascularization in adults.[3] Whereas in embryogenesis differentiation into endothelial cells by EPCs is widespread, this process is limited in adulthood.[4] In adulthood, circulating cells stimulate neovascularization by invading the target tissue and secreting proangiogenic factors that fuel angiogenesis[4]. Since these cells do not differentiate into endothelial cells, they do not fit the definition of EPC and are better termed "circulating angiogenic cells" (CACs). Various stages of CAC-mediated neovascularization exist. CACs are mobilized from the bone marrow by factors secreted by the target tissue and/or bone marrow microenvironment, or in an autocrine fashion by CACs themselves. In the bloodstream CACs migrate towards the target tissue through chemotaxis where they adhere to endothelial cells mediated by integrins and invade the tissue by expressing proteinases such as matrix metalloproteases (MMPs). Once in the target tissue CACs differentiate and start to secrete growth factors thus creating an environment permissive for angiogenesis.

In adulthood, neovascularization is stimulated on demand and is activated during revascularization after trauma or ischemia. In myocardial infarction (MI), a well-described and potent mobilization of CACs is induced early after the ischemic event.[5] Other ischemic states, such as ischemic stroke, have been less extensively studied. The literature on CACs in ischemic stroke shows less consistent results regarding the mobilization of CACs, with some studies showing no increase[6,7] or even a decrease of CACs.[8] Since the CAC response to ischemic brain appears to be far less extensive than to ischemic myocardium,[9] we chose to use MI patients rather than stroke patients as representing CAC-induced neovascularization in response to ischemia.

While in MI revascularization aids in recovery, new blood vessels in tumors are associated with propagation and contribute to the decease of the organism.[10] In patients suffering from MI, CAC-based therapies have been implemented with promising results.[11] In cancer, however, CAC-directed therapies have only been applied in animal studies where significant decreases in tumor sizes were reached.[12] Little is known about functional differences in CAC trafficking and function in the contexts of acute ischemia, cancer, and development. A better understanding of CAC biology in these different situations is necessary to design therapies acting on CAC-related neovascularization in cancer.

Here we compared the expression in CAC subsets of genes involved in neovascularization of glioblastomas (GBMs) and MI. Umbilical cord blood (UCB) and blood from adult healthy controls (HC) served as references for embryonic/fetal and steady-state adult neovascularization, respectively. Genes and 21 circulating plasma factors were chosen based on their functional roles (mobilization, chemo-attraction, homing, and growth factors secretion).[13] The expressional profiles of the respective CACs and the plasma factors of patients with GBM and MI were compared and correlated. The findings show profound differences between CAC-mediated neovascularization in GBM and MI patients.

Material and Methods

This study was approved by the Medical Ethics Committee of the Erasmus Medical Center, Rotterdam, The Netherlands (MEC-2011-313) and carried out in adherence to the Code of Good Conduct of the Federation of Medical Scientific Societies in the Netherlands (http://www.federa.org/codes-conduct). Informed consent was obtained from all subjects.

Blood Samples and Preparation: See Supplementary Materials and Methods.

Selection and FACS Sorting of CAC Subsets: See Supplementary Materials and Methods.

RNA Isolation and RT-PCR and Gene Expression Analysis: *Quality Control:* See Supplementary Materials and Methods.

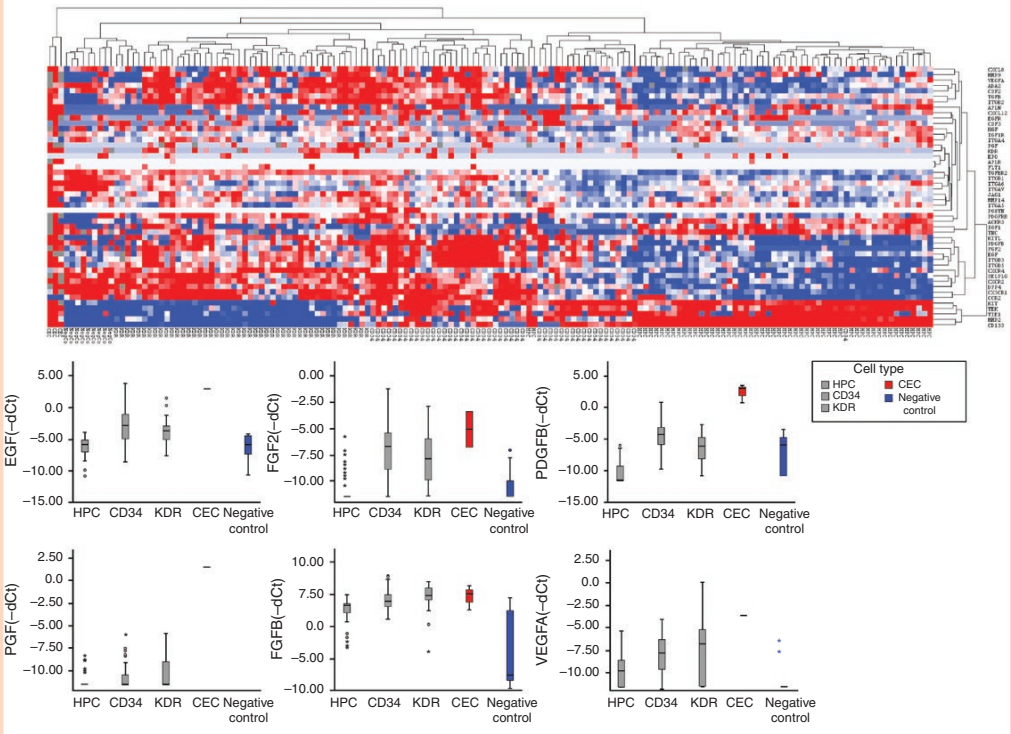

Figure 1. Unsupervised hierarchical cluster analysis of gene expression in all samples and boxplots of expressional levels. *Upper panel*: Unsupervised hierarchical cluster analysis of gene expression in all samples (city block distance with complete linkage). Blue = low expression and red = high expression. Clustering is seen based on CAC type: CECs display the most conspicuous phenotype (high expression). CD34$^+$ cells partially cluster with HPCs and partially with KDR$^+$ cells. Negative control leukocytes cluster with KDR$^+$ cells. The HPC cluster in general shows lower gene expression than the other CACs or CECs. *Lower panel*: Boxplots showing gene expression levels (−dCt) of proangiogenic factors in HPCs ($n = 54$), CD34$^+$ cells ($n = 47$), KDR$^+$ cells ($n = 46$), CECs ($n = 3$), and negative control PBMCs ($n = 9$). Proangiogenic factors overall are expressed highest in CECs and lowest in negative control PBMCs. In general, CD34$^+$ and KDR$^+$ cells express higher levels of proangiogenic factors than HPCs.

RT-PCR Data Analysis: See Supplementary Materials and Methods.

Data Analysis: See Supplementary Materials and Methods.

Results

Hierarchical Cluster Analysis: Gene Expression Patterns of CAC Subsets From All Subjects

The expression patterns of the CAC subsets, negative control peripheral blood mononuclear cells (PBMCs), and circulating endothelial cells (CECs) in the various patient and control groups clustered according to the respective cell types (Figure 1). CECs expressed genes from almost all functional groups at a much higher level than the other CACs, except for chemotactic receptors, which were only expressed at a higher level in CECs compared to hematopoietic progenitor cells (HPCs). HPCs showed relatively low overall expression of neovascularization-related genes. Overall expression levels of the investigated genes were lower in HPCs than in KDR$^+$ cells, CD34$^+$ cells, and CECs. HPCs were most homogenous regarding gene expression, irrespective of the source of the blood samples. CD34$^+$ cells clustered with HPCs for growth factor receptors and *CD133* expression while they resembled KDR$^+$ cells by their high expression of proangiogenic molecules and molecules operative in (de)adhesion and invasion. KDR$^+$ cells clustered with negative control leukocytes for all functional groups, suggesting the closest kinship of all subsets investigated with negative control PMBCs. CACs from GBM patients expressed neovascularization-related genes at a higher level than those from MI patients or HC. Following unsupervised hierarchical cluster analysis on individual CAC subsets, we found that HPCs from UCB and MI clustered together, as opposed to GBM HPCs (Figure 2).

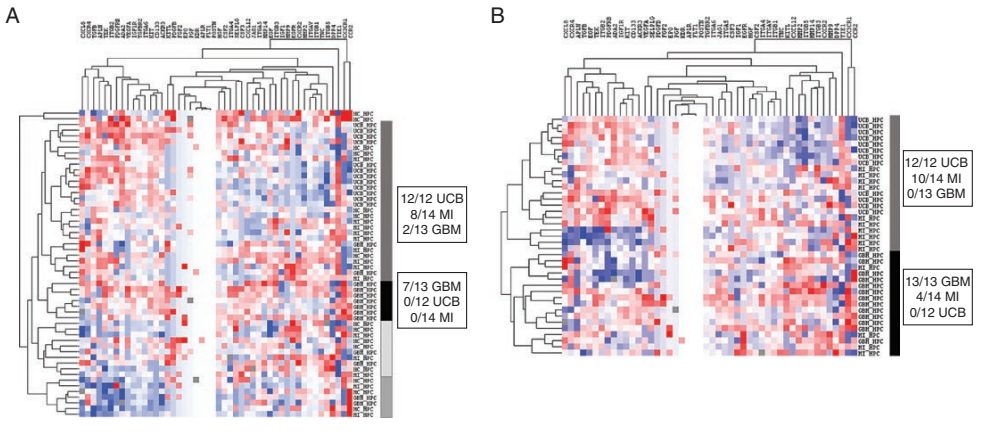

Figure 2. Unsupervised hierarchical cluster analysis of gene expression in HPCs. (A) Unsupervised hierarchical cluster analysis (city block distance, complete linkage) of gene expression in HPCs (all samples). UCB and MI HPCs cluster together, while GBM HPCs are in a separate cluster. There is higher overall gene expression in the GBM HPCs cluster compared to the other clusters. (B) Unsupervised hierarchical cluster analysis of HPCs (city block distance, complete linkage) after removing HC samples from the analysis: clustering of UCB and MI HPCs is more obvious. There is higher gene expression in the GBM HPCs cluster compared to the other clusters.

Differences in Expression of Individual Genes in CACs Between GBM and MI Patients

The genes that showed differential expression in CACs between the GBM and MI group represented all distinct functional groups (Figures 3–5). *CXCR4* and *KITL* were overexpressed in all CAC subsets of GBM patients as compared to patients with MI. Reversely, *IGF1* was underexpressed in GBM compared to MI. Higher RNA levels of *APLN* were detected in MI CACs as compared to GBM, while *CXCL12* and *ITGA5* transcript levels were lower in MI. The activity of some genes was consistently different for all CAC subtypes (eg, *CXCR4* was overexpressed in GMB HPCs, $CD34^+$, and KDR^+ cells as compared to these cells in MI), while the differential activity of other genes appeared to be confined to specific CAC subtypes (eg, overexpression of *JAG1* in GBM vs MI HPCs only, not in $CD34^+$ or KDR^+ CACs (Figures 3–5). Deviations from the reference HC expression levels (whether upregulated or downregulated) consistently followed the direction of UCB gene expression levels with the exception of *KITL* expression in GBM CACs (upregulated in GBM, downregulated in UCB compared to HC (Figures 4 and 5).

Plasma Factors

In GBM patients the overall levels of all plasma factors were higher than those in MI patients and HC subjects. Unsupervised hierarchical cluster analysis of the concentrations of all plasma factors measured in all samples yielded 3 main clusters: one containing only UCB samples, one with the large majority of GBM and HC samples, and one with the large majority of MI samples (lower overall levels of plasma factors) (Figure 6). Spearman correlation analysis between plasma factor concentrations and gene expression in CACs revealed a strong positive correlation between plasma MMP9 levels and the expression of *CXCR4* in HPCs in GBM patients (Spearman's rho = 0.77; $P < .01$). In MI patients no correlation between HPC *CXCR4* gene expression and plasma MMP9 levels was found (Supplementary Figure 3). When lowering the correlation threshold to at least 0.5, multiple significant correlations were detected between CAC gene expression and plasma factor levels (eg, a positive correlation between HPC *CSF2* gene expression and plasma CXCL12 levels; positive correlation significant for both GBM and MI patients, not for HC).

Discussion

In the present study, we investigated alterations in the expression of neovascularization-related genes in circulating CAC subsets between GBM and MI patients and sought correlations with circulating chemo-attractants and mobilization factors. Where in previous studies we observed that levels of circulating CACs differ in GBM patients as compared to HC and patients suffering from recent MIs,[7,14] in the present study we explored the expression of 48 neovascularization-related genes in 3 CAC subsets in these groups. We found major differences in expressional profiles. There was close similarity between the gene expression patterns of HPCs in MI and UCB, indicative of reactivation of embryonal/fetal mechanisms for CAC-mediated neovascularization following acute myocardial ischemia. In circulating CACs from GBM (where neovascularization is disordered and haphazard) this coordinated CAC

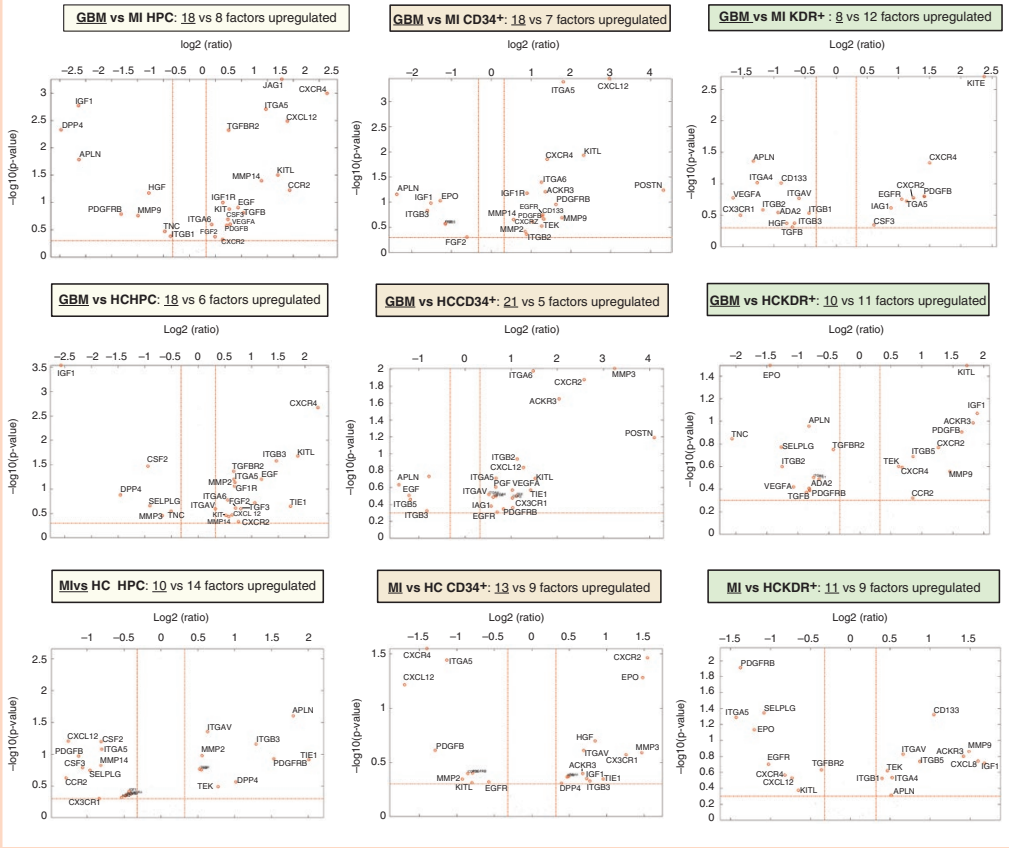

Figure 3. Volcano plots of gene expression differences between patients and controls by CAC subset. *Upper row* (A–C): Volcano plots (–log10 *P*-value vs log2 fold change (FC) with the following cutoff values: FC > |1.25|, $P < .5$) of GBM versus MI CACs. More genes are overexpressed in GBM versus MI CACs. Overexpressed genes belong to all functional groups. Specifically, there is higher expression in GBM versus MI CACs (especially, HPCs and CD34$^+$ cells) of growth factor receptors (GFRs), chemotactic receptors (CRs), and mobilization factors (MFs). There is higher expression in GBM versus MI HPCs of proangiogenic factors (PAFs). *Z*-scores and *P*-values of gene expression in GBM versus MI CACs are given in Figure 5. *Middle row* (D–F): Volcano plots (–log10 *P*-value vs log2 FC with the following cutoff values: FC > |1.25|, $P < .5$) of GBM versus HC CACs. A similar overall pattern of higher gene expression is seen as in the comparison of GBM versus MI CACs. Overexpressed genes belong to all functional groups. Higher expression in GBM versus HC CACs (especially, HPCs and CD34+ cells) of GFRs, CRs, MFs, adhesion factors (ITGs), PAFs. *Lower row* (G–I): Volcano plots (–log10 *P*-value vs log2 FC with the following cutoff values: FC > |1.25|, $P < .5$) of MI versus HC CACs. Overall gene expression is similar/lower in MI CACs versus HC CACs. Lower expression is seen in MI versus HC HPCs for PAFs, CRs, and MFs.

gene expression program was absent. We also discovered significant variations in the concentrations of 21 neovascularization-related plasma factors between GBM and MI patients, reflecting considerable differences in the "microenvironment" of the peripheral circulation, in which circulating CACs reside. Furthermore, we found strong correlations between the levels of specific plasma factors and gene expression levels in CACs. Altogether, these findings suggest that the difference in "blood microenvironment" as a result of MI or neoplastic growth drives alterations in gene expression in circulating CACs.

HPCs are capable of trafficking back and forth between the bone marrow, peripheral blood, (extra)-medullary tissues, and the lymphatic system.[15] We know from the literature that HPCs mobilized to peripheral blood have different gene expression profiles than bone marrow (BM)-resident HPCs.[16] Hypothetically, residing in target tissues will alter HPC (and other CAC) gene expression profiles dependent on target tissue/lesion-specific microenvironments. Hence, another explanation for our findings of altered gene expression patterns in CACs between GBM and MI patients is the reentrance of CACs

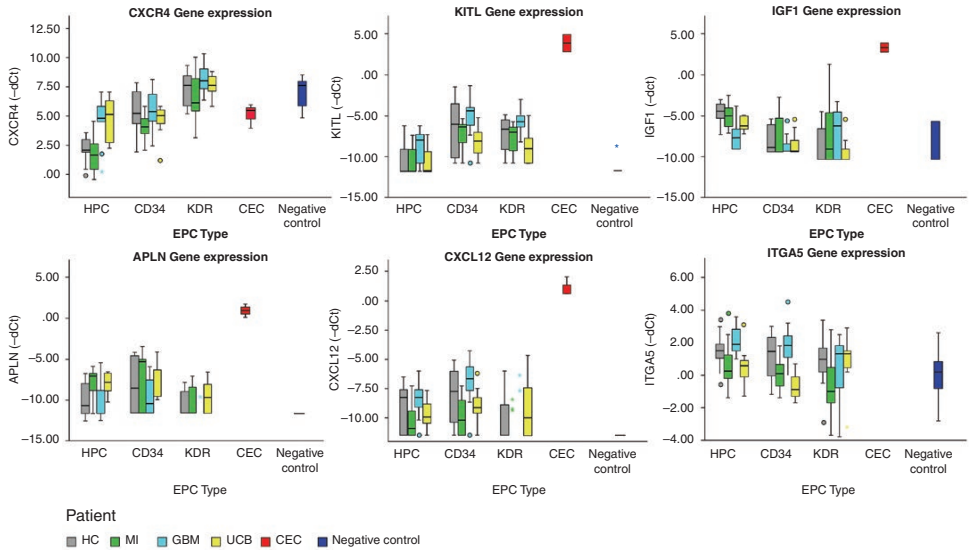

Figure 4. Boxplots of gene expression levels (–dCt) of significantly differentially expressed genes between GBM and MI CACs. Boxplots showing gene expression levels (–dCt) of significantly differentially expressed genes between GBM and MI CACs (data shown for gene expression differences present in ≥2 CAC subsets). *CXCR4* and *KITL* are overexpressed in GBM CACs compared to both MI and HC CACs. *IGF1* is underexpressed in GBM CACs (HPCs and CD34⁺) compared to MI and HC CACs. *ITGA5* is underexpressed in MI CACs compared to GBM and HC CACs. *APLN* is overexpressed in MI CACs compared to GBM and HC CACs. *CXCL12* is underexpressed in MI CACs compared to GBM and HC CACs. Deviations from the reference HC expressions levels (whether upregulated or downregulated) follow the pattern of UCB CAC gene expression levels (except for the overexpression of *KITL* in GBM CACs). For exact *P*-values and *Z*-scores for each CAC subtype, see Figure 5.

that were reprogrammed in such target tissues into the bloodstream. Differences in the trafficking speed of CACs between the bone marrow, peripheral blood, and target tissues can also contribute to changes in particular gene expression patterns[16] and could be another factor contributing to our findings. The trafficking speed is dependent on various circumstances, such as levels of mobilization factors in the circulation and sympathetic innervation of BM.[17] The latter could be altered in the presence of malignant glioma. Various combinations of cues like adhesion/chemotactic receptors, not single molecules themselves, drive the attraction and retention of HPCs to specific niches in the bone marrow.[18,19] It is likely that similar cue patterns govern the attraction and retention of CACs to specific target tissues. We found that these cues differ in the context of GBM and MI, pointing to disease-driven alterations in gene expression in circulating CACs. The CAC gene expression profile in GBM patients suggests that they have a more potent capacity to home to GBM tissue and are capable of a stronger proangiogenic response than CACs in MI. Overall, the influence of GBM tumor tissue on circulating CAC biology justifies the notion that GBM should be considered as a systemic disease, rather than a disease which is limited to the brain.

The expression level of *CXCR4* in GBM CACs was similar to that in UCB CACs, but significantly higher than in MI CACs. CXCR4 is a chemokine receptor expressed on the surface of leukocytes and HPCs.[20] CXCR4 binds to its ligand CXCL12, which acts as a mobilization factor and chemoattractant of CXCR4⁺ cells, including HPCs. Because CXCL12 is highly expressed in GBM tumor cells, endothelial cells, neurons, and white matter we included this protein in our panel of plasma factors.[21–24] We found decreased plasma CXCL12 levels in both GBM and MI patients. The lower CXCL12 levels in MI patients are in line with the existing literature,[25] while in glioma patients elevated, not reduced, plasma levels of CXCL12 have been reported.[26] A technical explanation for the reported elevated levels could be the release of α-granule factors including CXCL12 into plasma following blood sample cooling.[26,27] In our study plasma values represent the free CXCL12 fraction, not the platelet α-granule stored fraction. While high free plasma CXCL12 mobilizes CACs from the bone marrow, homing of CXCR4⁺ cells to target tissues is less efficient due to the lower target tissue-to-plasma CXCL12 ratio.[28,29] Reversely, low plasma CXCL12 levels allow for more efficient homing of CXCR4⁺ cells to CXCL12-expressing target tissues due to a high target tissue-to-plasma CXCL12 ratio.[30] The low plasma level of CXCL12 in GBM patients therefore facilitates homing of CXCR4⁺ cells to CXCL12-expressing GBM tissue.[30,31] The present finding of increased expression of *CXCR4* in UCB HPCs was previously reported in the literature,[32] but increased *CXCR4* expression in GBM HPCs (and other CACs) was not described earlier. Higher expression of *CXCR4* in cultured CACs increases migration triggered by CXCL12 and enhances their capacity to exit blood vessels

	GBM>MI	GBM vs MI						GBM>HC	GBM vs HC						MI>HC	MI vs HC					
	MI>GBM	HPCs		CD34		KDR		HC>GBM	HPCs		CD34		KDR		HC>MI	HPCs		CD34		KDR	
	PAF	Z	p	Z	p	Z	p	PAF	Z	p	Z	p	Z	p	PAF	Z	p	Z	p	Z	p
PAF	APLN	-2.4	0.02	-1.9	0.05	-1.7	0.09	APLN	-0.6	0.54	-1.3	0.20	-1.4	0.15	APLN	2.4	0.02	0.4	0.66	0.8	0.45
	CXCL12	2.8	0.01	3.3	0.00	0.1	0.93	CXCL12	0.6	0.53	1.3	0.19	-0.6	0.56	CXCL12	-1.7	0.08	-1.8	0.07	-0.8	0.41
	CXCL8	-0.2	0.82	-1.3	0.20	-0.8	0.40	CXCL8	1.0	0.34	0.1	0.91	0.2	0.83	CXCL8	1.4	0.15	1.7	0.09	1.3	0.20
	EGF	0.8	0.45	-1.0	0.30	0.2	0.83	EGF	1.4	0.17	-0.9	0.37	1.7	0.09	EGF	0.3	0.74	0.4	0.71	0.5	0.64
	EPO	0.0	1.00	-1.8	0.07	-1.3	0.20	EPO	0.0	1.00	0.9	0.35	-2.2	0.02	EPO	0.1	0.94	2.2	0.03	-1.7	0.09
	FGF2	0.8	0.40	-0.2	0.87	0.6	0.55	FGF2	1.4	0.15	-0.2	0.88	0.5	0.64	FGF2	0.6	0.57	-0.1	0.95	-0.1	0.93
	HGF	-1.8	0.08	0.2	0.82	-1.3	0.19	HGF	-0.6	0.56	1.4	0.17	-0.3	0.74	HGF	1.3	0.21	1.1	0.25	0.7	0.51
	IGF1	-2.9	0.00	-1.3	0.18	0.2	0.82	IGF1	-3.3	0.00	-1.3	0.21	1.7	0.08	IGF1	-1.0	0.30	0.5	0.64	1.1	0.27
	JAG1	3.5	0.00	1.0	0.31	1.2	0.23	JAG1	1.4	0.15	0.6	0.52	0.5	0.64	JAG1	-1.6	0.12	-0.4	0.67	-1.0	0.34
	KITL	2.2	0.03	2.7	0.01	3.0	0.00	KITL	2.3	0.02	1.1	0.29	2.0	0.05	KITL	0.4	0.73	-0.7	0.48	-0.9	0.35
	PDGFB	1.0	0.31	1.7	0.08	1.6	0.11	PDGFB	-0.4	0.68	0.3	0.74	1.6	0.11	PDGFB	-1.3	0.19	-1.2	0.23	0.2	0.85
	PGF	0.1	0.96	1.2	0.22	-0.3	0.76	PGF	1.1	0.28	1.2	0.23	-1.3	0.18	PGF	1.0	0.32	0.1	0.95	-1.1	0.26
	TGFB	1.0	0.33	-0.2	0.81	-0.2	0.88	TGFB	0.2	0.82	-0.1	0.92	-1.1	0.28	TGFB	-0.6	0.54	-0.1	0.95	-0.8	0.40
	VEGFA	1.0	0.30	0.4	0.70	-1.4	0.17	VEGFA	0.6	0.56	1.2	0.22	-1.1	0.28	VEGFA	-0.6	0.58	0.8	0.42	0.4	0.70
		GBM vs MI							GBM vs HC							MI vs HC					
		HPCs		CD34		KDR			HPCs		CD34		KDR			HPCs		CD34		KDR	
	GFR	Z	p	Z	p	Z	p	GFR	Z	p	Z	p	Z	p	GFR	Z	p	Z	p	Z	p
GFR	ADA2	0.3	0.74	0.3	0.74	-1.1	0.28	ADA2	-1.0	0.29	-0.3	0.80	-1.4	0.18	ADA2	-1.2	0.25	-0.9	0.39	0.2	0.87
	APLR	0.0	1.00	0.0	1.00	0.0	1.00	APLR	-0.9	0.35	0.0	1.00	-0.9	0.36	APLR	-1.0	0.33	0.0	1.00	-1.0	0.30
	CXCR4	3.1	0.00	2.4	0.02	1.9	0.06	CXCR4	2.7	0.01	-0.1	0.90	0.9	0.39	CXCR4	-0.7	0.50	-2.1	0.03	-1.1	0.29
	EGFR	0.2	0.81	1.1	0.29	1.4	0.15	EGFR	0.0	0.98	0.5	0.64	0.2	0.88	EGFR	-0.2	0.82	-0.7	0.48	-1.2	0.25
	FLT1	0.0	1.00	-1.1	0.26	-0.4	0.71	FLT1	0.0	1.00	0.0	1.00	1.1	0.27	FLT1	0.0	1.00	1.0	0.30	1.4	0.17
	IGF1R	1.7	0.09	1.9	0.05	0.5	0.60	IGF1R	1.8	0.07	1.2	0.25	0.6	0.57	IGF1R	0.1	0.91	-0.4	0.69	-0.1	0.91
	KDR	1.0	0.30	-0.8	0.43	-0.4	0.66	KDR	0.2	0.88	-0.2	0.86	-0.1	0.94	KDR	-1.0	0.33	0.7	0.47	0.6	0.57
	KIT	1.6	0.11	0.1	0.91	0.3	0.80	KIT	0.7	0.50	0.4	0.72	0.5	0.58	KIT	-0.5	0.63	0.0	1.00	0.1	0.93
	PDGFRB	-1.1	0.27	1.6	0.11	0.8	0.44	PDGFRB	-0.5	0.65	0.6	0.55	-0.1	0.95	PDGFRB	1.6	0.10	-1.1	0.28	-2.6	0.01
	TEK	0.4	0.70	1.0	0.30	0.2	0.81	TEK	1.2	0.22	1.2	0.25	1.2	0.22	TEK	1.0	0.34	-0.2	0.85	1.1	0.27
	TGFBR2	2.7	0.01	1.0	0.30	-0.2	0.88	TGFBR2	2.1	0.04	0.3	0.78	-0.7	0.47	TGFBR2	0.0	0.98	-0.6	0.55	-1.0	0.34
	TIE1	0.4	0.72	0.5	0.58	-0.7	0.51	TIE1	1.3	0.18	1.1	0.28	-1.3	0.21	TIE1	1.2	0.21	0.5	0.60	-0.5	0.58
		GBM vs MI							GBM vs HC							MI vs HC					
		HPCs		CD34		KDR			HPCs		CD34		KDR			HPCs		CD34		KDR	
	CR	Z	p	Z	p	Z	p	CR	Z	p	Z	p	Z	p	CR	Z	p	Z	p	Z	p
CR	ACKR3	0.6	0.54	2.0	0.04	1.5	0.14	ACKR3	0.3	0.80	2.2	0.03	1.6	0.11	ACKR3	-0.6	0.53	0.9	0.38	0.9	0.37
	CCR2	2.0	0.04	0.7	0.48	0.2	0.83	CCR2	1.0	0.32	0.8	0.40	0.6	0.55	CCR2	-1.2	0.25	0.4	0.67	0.8	0.43
	CX3CR1	0.7	0.46	-0.1	0.96	-0.8	0.44	CX3CR1	0.4	0.71	0.8	0.44	-0.5	0.60	CX3CR1	-0.2	0.86	1.5	0.13	0.7	0.46
	CXCR2	0.4	0.70	1.4	0.16	1.3	0.18	CXCR2	0.4	0.68	2.6	0.01	1.5	0.13	CXCR2	0.2	0.86	1.9	0.06	0.0	1.00
	CXCR4	3.1	0.00	2.4	0.02	1.9	0.06	CXCR4	2.7	0.01	-0.1	0.90	0.9	0.39	CXCR4	-0.7	0.50	-2.1	0.03	-1.1	0.29
	SELPLG	0.1	0.94	0.7	0.48	0.4	0.71	SELPLG	1.2	0.24	0.3	0.80	-1.1	0.29	SELPLG	-1.3	0.20	-0.2	0.85	-2.0	0.05
		GBM vs MI							GBM vs HC							MI vs HC					
		HPCs		CD34		KDR			HPCs		CD34		KDR			HPCs		CD34		KDR	
	DIF	Z	p	Z	p	Z	p	DIF	Z	p	Z	p	Z	p	DIF	Z	p	Z	p	Z	p
DIF	DPP4	-2.8	0.01	-0.1	0.91	-0.6	0.58	DPP4	-1.2	0.24	0.2	0.85	-0.5	0.62	DPP4	1.7	0.09	1.1	0.28	-0.1	0.91
	MMP14	2.1	0.04	1.2	0.24	1.0	0.33	MMP14	0.9	0.39	-0.1	0.96	-0.8	0.42	MMP14	-1.4	0.17	-1.0	0.34	-1.2	0.25
	MMP2	0.4	0.70	0.8	0.44	-0.2	0.81	MMP2	1.8	0.07	0.0	1.00	0.0	1.00	MMP2	1.2	0.25	-0.4	0.71	0.0	0.97
	MMP9	-1.3	0.18	1.2	0.22	0.2	0.80	MMP9	-0.8	0.45	2.4	0.02	1.1	0.26	MMP9	0.5	0.62	1.0	0.33	1.4	0.17
		GBM vs MI							GBM vs HC							MI vs HC					
		HPCs		CD34		KDR			HPCs		CD34		KDR			HPCs		CD34		KDR	
	MF	Z	p	Z	p	Z	p	MF	Z	p	Z	p	Z	p	MF	Z	p	Z	p	Z	p
MF	CSF2	-0.3	0.73	0.3	0.74	0.9	0.39	CSF2	-2.0	0.05	0.3	0.78	0.3	0.79	CSF2	-1.4	0.16	-0.2	0.85	-0.5	0.62
	CSF3	1.5	0.13	0.5	0.65	0.8	0.44	CSF3	-0.2	0.87	0.4	0.70	0.4	0.71	CSF3	-1.6	0.12	-0.1	0.94	-0.6	0.52
	CXCL12	2.8	0.01	3.3	0.00	0.1	0.93	CXCL12	0.6	0.53	1.3	0.19	-0.6	0.56	CXCL12	-1.7	0.08	-1.8	0.07	-0.8	0.41
		GBM vs MI							GBM vs HC							MI vs HC					
		HPCs		CD34		KDR			HPCs		CD34		KDR			HPCs		CD34		KDR	
	ITG	Z	p	Z	p	Z	p	ITG	Z	p	Z	p	Z	p	ITG	Z	p	Z	p	Z	p
ITG	ITGA4	-0.5	0.64	-0.1	0.91	-1.6	0.10	ITGA4	0.4	0.68	0.7	0.49	-0.9	0.37	ITGA4	1.2	0.22	0.6	0.56	0.9	0.35
	ITGA5	3.1	0.00	3.3	0.00	1.6	0.12	ITGA5	1.7	0.08	1.1	0.29	0.2	0.84	ITGA5	-2.1	0.04	-2.0	0.04	-1.9	0.05
	ITGA6	0.7	0.48	2.1	0.04	-0.3	0.76	ITGA6	1.2	0.25	2.3	0.02	0.1	0.89	ITGA6	1.2	0.21	0.2	0.83	0.2	0.81
	ITGAV	-1.2	0.21	-0.2	0.85	-1.3	0.20	ITGAV	0.9	0.37	0.7	0.45	0.2	0.82	ITGAV	2.0	0.04	1.0	0.29	1.4	0.16
	ITGB1	-0.8	0.42	-0.2	0.83	-1.2	0.21	ITGB1	0.1	0.89	0.3	0.78	0.1	0.92	ITGB1	1.5	0.13	0.5	0.64	1.1	0.25
	ITGB2	0.6	0.54	0.3	0.76	-0.6	0.54	ITGB2	0.6	0.55	1.1	0.26	-1.0	0.32	ITGB2	0.0	0.98	1.2	0.24	-0.2	0.85
	ITGB3	0.0	0.96	-1.4	0.16	-0.1	0.90	ITGB3	2.3	0.02	-0.6	0.57	1.7	0.08	ITGB3	1.7	0.09	0.9	0.39	1.4	0.17
	ITGB5	0.1	0.88	-0.9	0.38	0.0	0.98	ITGB5	0.9	0.36	-0.8	0.40	1.3	0.21	ITGB5	0.9	0.35	0.0	0.98	1.1	0.28
		GBM vs MI							GBM vs HC							MI vs HC					
		HPCs		CD34		KDR			HPCs		CD34		KDR			HPCs		CD34		KDR	
	Other	Z	p	Z	p	Z	p	Other	Z	p	Z	p	Z	p	Other	Z	p	Z	p	Z	p
Other	POSTN	0.0	1.00	1.9	0.05	0.0	1.00	POSTN	0.0	1.00	1.6	0.10	0.0	1.00	POSTN	0.0	1.00	-0.4	0.67	0.0	1.00
	TNC	-0.7	0.47	0.7	0.51	-1.6	0.11	TNC	-1.0	0.32	0.7	0.48	-1.6	0.10	TNC	0.0	0.97	0.3	0.78	0.1	0.93
	CD133	0.1	0.88	1.4	0.17	-1.3	0.18	CD133	0.5	0.62	0.5	0.60	1.1	0.27	CD133	0.2	0.81	-0.6	0.52	2.0	0.04

GBM>MI	GBM vs MI					
MI>GBM	HPCs		CD34		KDR	
PAF	Z	p	Z	p	Z	p
APLN	-2.4	0.02	-1.9	0.05	-1.7	0.09
CXCL12	2.8	0.01	3.3	0.00	0.1	0.93
CXCL8	-0.2	0.82	-1.3	0.20	-0.8	0.40
EGF	0.8	0.45	-1.0	0.30	0.2	0.83
EPO	0.0	1.00	-1.8	0.07	-1.3	0.20
FGF2	0.8	0.40	-0.2	0.87	0.6	0.55
HGF	-1.8	0.08	0.2	0.82	-1.3	0.19
IGF1	-2.9	0.00	-1.3	0.18	0.2	0.82
JAG1	3.5	0.00	1.0	0.31	1.2	0.23
KITL	2.2	0.03	2.7	0.01	3.0	0.00
PDGFB	1.0	0.31	1.7	0.08	1.6	0.11
PGF	0.1	0.96	1.2	0.22	-0.3	0.76
TGFB	1.0	0.33	-0.2	0.81	-0.2	0.88
VEGFA	1.0	0.30	0.4	0.70	-1.4	0.17
	GBM vs MI					
	HPCs		CD34		KDR	
GFR	Z	p	Z	p	Z	p
ADA2	0.3	0.74	0.3	0.74	-1.1	0.28
APLR	0.0	1.00	0.0	1.00	0.0	1.00
CXCR4	3.1	0.00	2.4	0.02	1.9	0.06
EGFR	0.2	0.81	1.1	0.29	1.4	0.15
FLT1	0.0	1.00	-1.1	0.26	-0.4	0.71
IGF1R	1.7	0.09	1.9	0.05	0.5	0.60
KDR	1.0	0.30	-0.8	0.43	-0.4	0.66
KIT	1.6	0.11	0.1	0.91	0.3	0.80
PDGFRB	-1.1	0.27	1.6	0.11	0.8	0.44
TEK	0.4	0.70	1.0	0.30	0.2	0.81
TGFBR2	2.7	0.01	1.0	0.30	-0.2	0.88
TIE1	0.4	0.72	0.5	0.58	-0.7	0.51
	GBM vs MI					
	HPCs		CD34		KDR	
CR	Z	p	Z	p	Z	p
ACKR3	0.6	0.54	2.0	0.04	1.5	0.14
CCR2	2.0	0.04	0.7	0.48	0.2	0.83
CX3CR1	0.7	0.46	-0.1	0.96	-0.8	0.44
CXCR2	0.4	0.70	1.4	0.16	1.3	0.18
CXCR4	3.1	0.00	2.4	0.02	1.9	0.06
SELPLG	0.1	0.94	0.7	0.48	0.4	0.71
	GBM vs MI					
	HPCs		CD34		KDR	
DIF	Z	p	Z	p	Z	p
DPP4	-2.8	0.01	-0.1	0.91	-0.6	0.58
MMP14	2.1	0.04	1.2	0.24	1.0	0.33
MMP2	0.4	0.70	0.8	0.44	-0.2	0.81
MMP9	-1.3	0.18	1.2	0.22	0.2	0.80
	GBM vs MI					
	HPCs		CD34		KDR	
MF	Z	p	Z	p	Z	p
CSF2	-0.3	0.73	0.3	0.74	0.9	0.39
CSF3	1.5	0.13	0.5	0.65	0.8	0.44
CXCL12	2.8	0.01	3.3	0.00	0.1	0.93
	GBM vs MI					
	HPCs		CD34		KDR	
ITG	Z	p	Z	p	Z	p
ITGA4	-0.5	0.64	-0.1	0.91	-1.6	0.10
ITGA5	3.1	0.00	3.3	0.00	1.6	0.12
ITGA6	0.7	0.48	2.1	0.04	-0.3	0.76
ITGAV	-1.2	0.21	-0.2	0.85	-1.3	0.20
ITGB1	-0.8	0.42	-0.2	0.83	-1.2	0.21
ITGB2	0.6	0.54	0.3	0.76	-0.6	0.54
ITGB3	0.0	0.96	-1.4	0.16	-0.1	0.90
ITGB5	0.1	0.88	-0.9	0.38	0.0	0.98
	GBM vs MI					
	HPCs		CD34		KDR	
Other	Z	p	Z	p	Z	p
POSTN	0.0	1.00	1.9	0.05	0.0	1.00
TNC	-0.7	0.47	0.7	0.51	-1.6	0.11
CD133	0.1	0.88	1.4	0.17	-1.3	0.18

GBM>HC	GBM vs HC					
HC>GBM	HPCs		CD34		KDR	
PAF	Z	p	Z	p	Z	p
APLN	-0.6	0.54	-1.3	0.20	-1.4	0.15
CXCL12	0.6	0.53	1.3	0.19	-0.6	0.56
CXCL8	1.0	0.34	0.1	0.91	0.2	0.83
EGF	1.4	0.17	-0.9	0.37	1.7	0.09
EPO	0.0	1.00	0.9	0.35	-2.2	0.02
FGF2	1.4	0.15	-0.2	0.88	0.5	0.64
HGF	-0.6	0.56	1.4	0.17	-0.3	0.74
IGF1	-3.3	0.00	-1.3	0.21	1.7	0.08
JAG1	1.4	0.15	0.6	0.52	0.5	0.64
KITL	2.3	0.02	1.1	0.29	2.0	0.05
PDGFB	-0.4	0.68	0.3	0.74	1.6	0.11
PGF	1.1	0.28	1.2	0.23	-1.3	0.18
TGFB	0.2	0.82	-0.1	0.92	-1.1	0.28
VEGFA	0.6	0.56	1.2	0.22	-1.1	0.28
	GBM vs HC					
	HPCs		CD34		KDR	
GFR	Z	p	Z	p	Z	
ADA2	-1.0	0.29	-0.3	0.80	-1.4	0.18
APLR	-0.9	0.35	0.0	1.00	-0.9	0.36
CXCR4	2.7	0.01	-0.1	0.90	0.9	0.39
EGFR	0.0	0.98	0.5	0.64	0.2	0.88
FLT1	0.0	1.00	0.0	1.00	1.1	0.27
IGF1R	1.8	0.07	1.2	0.25	0.6	0.57
KDR	0.2	0.88	-0.2	0.86	-0.1	0.94
KIT	0.7	0.50	0.4	0.72	0.5	0.58
PDGFRB	-0.5	0.65	0.6	0.55	-0.1	0.95
TEK	1.2	0.22	1.2	0.25	1.2	0.22
TGFBR2	2.1	0.04	0.3	0.78	-0.7	0.47
TIE1	1.3	0.18	1.1	0.28	-1.3	0.21
	GBM vs HC					
	HPCs		CD34		KDR	
CR	Z	p	Z	p	Z	p
ACKR3	0.3	0.80	2.2	0.03	1.6	0.11
CCR2	1.0	0.32	0.8	0.40	0.6	0.55
CX3CR1	0.4	0.71	0.8	0.44	-0.5	0.60
CXCR2	0.4	0.68	2.6	0.01	1.5	0.13
CXCR4	2.7	0.01	-0.1	0.90	0.9	0.39
SELPLG	1.2	0.24	0.3	0.80	-1.1	0.29
	GBM vs HC					
	HPCs		CD34		KDR	
DIF	Z	p	Z	p	Z	p
DPP4	-1.2	0.24	0.2	0.85	-0.5	0.62
MMP14	0.9	0.39	-0.1	0.96	-0.8	0.42
MMP2	1.8	0.07	0.0	1.00	0.0	1.00
MMP9	-0.8	0.45	2.4	0.02	1.1	0.26
	GBM vs HC					
	HPCs		CD34		KDR	
MF	Z	p	Z	p	Z	p
CSF2	-2.0	0.05	0.3	0.78	0.3	0.79
CSF3	-0.2	0.87	0.4	0.70	0.4	0.71
CXCL12	0.6	0.53	1.3	0.19	-0.6	0.56
	GBM vs HC					
	HPCs		CD34		KDR	
ITG	Z	p	Z	p	Z	p
ITGA4	0.4	0.68	0.7	0.49	-0.9	0.37
ITGA5	1.7	0.08	1.1	0.29	0.2	0.84
ITGA6	1.2	0.25	2.3	0.02	0.1	0.89
ITGAV	0.9	0.37	0.7	0.45	0.2	0.82
ITGB1	0.1	0.89	0.3	0.78	0.1	0.92
ITGB2	0.6	0.55	1.1	0.26	-1.0	0.32
ITGB3	2.3	0.02	-0.6	0.57	1.7	0.08
ITGB5	0.9	0.36	-0.8	0.40	1.3	0.21
	GBM vs HC					
	HPCs		CD34		KDR	
Other	Z	p	Z	p	Z	p
POSTN	0.0	1.00	1.6	0.10	0.0	1.00
TNC	-1.0	0.32	0.7	0.48	-1.6	0.10
CD133	0.5	0.62	0.5	0.60	1.1	0.27

MI>HC	MI vs HC					
HC>MI	HPCs		CD34		KDR	
PAF	Z	p	Z	p	Z	p
APLN	2.4	0.02	0.4	0.66	0.8	0.45
CXCL12	-1.7	0.08	-1.8	0.07	-0.8	0.41
CXCL8	1.4	0.15	1.7	0.09	1.3	0.20
EGF	0.3	0.74	0.4	0.71	0.5	0.64
EPO	0.1	0.94	2.2	0.03	-1.7	0.09
FGF2	0.6	0.57	-0.1	0.95	-0.1	0.93
HGF	1.3	0.21	1.1	0.25	0.7	0.51
IGF1	-1.0	0.30	0.5	0.64	1.1	0.27
JAG1	-1.6	0.12	-0.4	0.67	-1.0	0.34
KITL	0.4	0.73	-0.7	0.48	-0.9	0.35
PDGFB	-1.3	0.19	-1.2	0.23	0.2	0.85
PGF	1.0	0.32	0.1	0.95	-1.1	0.26
TGFB	-0.6	0.54	-0.1	0.95	-0.8	0.40
VEGFA	-0.6	0.58	0.8	0.42	0.4	0.70
	MI vs HC					
	HPCs		CD34		KDR	
GFR	Z	p	Z	p	Z	p
ADA2	-1.2	0.25	-0.9	0.39	0.2	0.87
APLR	-1.0	0.33	0.0	1.00	-1.0	0.30
CXCR4	-0.7	0.50	-2.1	0.03	-1.1	0.29
EGFR	-0.2	0.82	-0.7	0.48	-1.2	0.25
FLT1	0.0	1.00	1.0	0.30	1.4	0.17
IGF1R	0.1	0.91	-0.4	0.69	-0.1	0.91
KDR	-1.0	0.33	0.7	0.47	0.6	0.57
KIT	-0.5	0.63	0.0	1.00	0.1	0.93
PDGFRB	1.6	0.10	-1.1	0.28	-2.6	0.01
TEK	1.0	0.34	-0.2	0.85	1.1	0.27
TGFBR2	0.0	0.98	-0.6	0.55	-1.0	0.34
TIE1	1.2	0.21	0.5	0.60	-0.5	0.58
	MI vs HC					
	HPCs		CD34		KDR	
CR	Z	p	Z	p	Z	p
ACKR3	-0.6	0.53	0.9	0.38	0.9	0.37
CCR2	-1.2	0.25	0.4	0.67	0.8	0.43
CX3CR1	-0.2	0.86	1.5	0.13	0.7	0.46
CXCR2	0.2	0.86	1.9	0.06	0.0	1.00
CXCR4	-0.7	0.50	-2.1	0.03	-1.1	0.29
SELPLG	-1.3	0.20	-0.2	0.85	-2.0	0.05
	MI vs HC					
	HPCs		CD34		KDR	
DIF	Z	p	Z	p	Z	p
DPP4	1.7	0.09	1.1	0.28	-0.1	0.91
MMP14	-1.4	0.17	-1.0	0.34	-1.2	0.25
MMP2	1.2	0.25	-0.4	0.71	0.0	0.97
MMP9	0.5	0.62	1.0	0.33	1.4	0.17
	MI vs HC					
	HPCs		CD34		KDR	
MF	Z	p	Z	p	Z	p
CSF2	-1.4	0.16	-0.2	0.85	-0.5	0.62
CSF3	-1.6	0.12	-0.1	0.94	-0.6	0.52
CXCL12	-1.7	0.08	-1.8	0.07	-0.8	0.41
	MI vs HC					
	HPCs		CD34		KDR	
ITG	Z	p	Z	p	Z	p
ITGA4	1.2	0.22	0.6	0.56	0.9	0.35
ITGA5	-2.1	0.04	-2.0	0.04	-1.9	0.05
ITGA6	1.2	0.21	0.2	0.83	0.2	0.81
ITGAV	2.0	0.04	1.0	0.29	1.4	0.16
ITGB1	1.5	0.13	0.5	0.64	1.1	0.25
ITGB2	0.0	0.98	1.2	0.24	-0.2	0.85
ITGB3	1.7	0.09	0.9	0.39	1.4	0.17
ITGB5	0.9	0.35	0.0	0.98	1.1	0.28
	MI vs HC					
	HPCs		CD34		KDR	
Other	Z	p	Z	p	Z	p
POSTN	0.0	1.00	-0.4	0.67	0.0	1.00
TNC	0.0	0.97	0.3	0.78	0.1	0.93
CD133	0.2	0.81	-0.6	0.52	2.0	0.04

and improve endothelial recovery.[33] In MI strategies to increase the expression of *CXCR4* by circulating progenitor cells lead to improved homing to ischemic myocardium resulting in restoration of the blood flow and a reduction of cardiac damage following the infarction.[24] MMP9 not only induces mobilization of HPCs by cleaving the CXCL12–CXCR4 interaction,[34] but also increases the expression of CXCR4 by bone marrow progenitor cells.[35,36] The increased plasma levels of MMP9 in GBM patients found in the present study corroborate the literature.[37] The elevated levels of tumor-derived MMP9 could cause upregulation of *CXCR4* in CACs of GBM patients. Furthermore, the reduced expression of *DPP4* in GBM HPCs is also associated with a more efficient homing of HPCs to CXCL12-expressing target tissue.[38] It is therefore likely that the elevated expression of *CXCR4* and the reduced expression of *DPP4* by GBM CACs, combined with the high GBM tissue-to-plasma CXCL12 gradient, translate into a highly efficient homing process of CXCR4$^+$ CACs to GBM tumor. Interference with the MMP9/DPP4/CXCR4/CXCL12 axis in CACs in GBM patients seems a very promising therapeutic option for targeting CAC-mediated neovascularization.

In GBM CACs, gene expression of *KITL* was significantly higher than in MI and HC. *KIT* was expressed higher in GBM than in MI HPCs. KITL is a cytokine that binds to the KIT receptor; the KIT/KITL receptor/ligand pair is important for hematopoiesis and for the mobilization, chemotaxis/homing, and maintenance of HPCs,[39,40] as well as for angiogenesis.[41–43] The KIT/KITL axis is also essential for neovascularization in glial tumors.[41] In GBM tissue, KITL is not only produced by glial tumor cells, but also by neurons.[41] Silencing of *KITL* in glioma cells leads to a decrease in angiogenesis and tumor growth and improved survival.[41] The KIT receptor is widely expressed in GBM endothelial cells and in tumor cells present around foci of necrosis.[44] KITL exists in a soluble (sKITL) and membrane bound (mKITL) form.[45] sKITL results from proteolytic cleavage of mKITL.[42] Transmembrane KITL is formed by alternative mRNA splicing. The proteolytic cleavage of mKITL to sKITL by MMPs (in particular MMP9) is crucial for the mobilization of HPCs from the bone marrow in a similar fashion as for CXCR4/CXCL12.[46,47] Indeed, we previously found a strong correlation between plasma MMP9 levels and circulating levels of HPCs in GBM patients.[14] In the present study, the primer set used to determine *KITL* mRNA levels did not distinguish between the soluble and transmembrane forms. Hence, we do not yet know if the increased *KITL* gene expression translates to higher levels of sKITL, mKITL, or both in GBM CACs. Importantly, mKITL can act as a chemotactic membrane bound ligand to KIT$^+$ cells in the target tissue,[48] mediating the homing of mKITL$^+$ cells to KIT$^+$ target tissue. Reversely, KIT$^+$ circulating progenitor cells home to KITL$^+$ target tissue.[49] Hence, the high *KITL* expression by GBM CACs, and the high *KIT* expression by GBM HPCs, is expected to facilitate homing to KIT$^+$/KITL$^+$ GBM tissue and stimulate tumor angiogenesis. The role of KIT/KITL in GBM CACs therefore deserves further investigations in the search for targets for CACs-induced neovascularization in GBM.

The functional meaning of our findings should be explored further using in vitro and ex vivo experimental systems, in animal models and finally in clinical trials on humans. FACS or immunomagnetic bead-isolated CACs could be used in chemotaxis/invasion assays (transwell) to determine the potential of GBM versus MI/HC CACs to migrate along gradients of chemoattractants (eg, CXCL12, CCL2, sKITL, sKIT, and sVCAM1) and/or to GBM cells. Silencing of *CXCR4, KIT/KITL*, and *ITGA5/ITGA4* in CACs or the addition of CXCR4 blockers (such as AMD3100) or KITL/KIT/Intα5β1/Intα4β1 inhibitors could be used to validate the importance of these factors in the chemoattraction/homing response. Additionally, CACs could be treated with MMP9 to determine its effect on CAC CXCR4 expression and chemotaxis. The angiogenic function of GBM CACs in GBM could be confirmed using 3D angiogenesis assays.[50] Labeled CACs (GBM vs MI/HC) could be injected into the circulation and tumor tissue of a GBM xenograft orthotopic mouse model to determine their tumor-homing capacity and their effect on tumor neovascularization and growth. CACs could be isolated from GBM tissue after having homed to tumor, and their expression profile compared to the original CACs to determine the effect of the GBM microenvironment on CAC gene expression. Inhibition of homing molecules like CXCR4, KITL/KIT, and Intα5β1/Intα4β1 prior to peripheral administration of CACs would validate the function of these molecules in vivo. Finally, clinical trials can be developed investigating the effect of blocking the mobilization and/or tumor homing of CACs on GBM neovascularization and growth (eg, by blocking circulating MMP9 or VCAM1, both elevated in GBM patient plasma and correlating positively with levels of HPCs and KDR$^+$ cells, respectively[14]). Lowering the levels of plasma MMP9 would reduce CAC CXCR4 expression[35,36] and diminish their homing capacity to tumor CXCL12. Similarly, blockage of CXCR4 using, eg, AMD3100 could abrogate the homing potential of CACs.[51] Since AMD3100 also mobilizes CACs from the bone marrow, alternative homing mechanisms than the CXCR4/CXCL12 axis may need to be targeted simultaneously to prevent CACs from reaching GBM tissue using alternative routes (eg, KIT/KITL, Intα4β1/VCAM1).

Our results can eventually be translated toward developing disease-specific therapies targeting CAC-induced neovascularization. Crucial to the development of these targeted therapies is maintaining the balance between effective anti-angiogenic therapy and preservation of the necessary regenerative capacities of the organism.

Figure 5. Differential gene expression between GBM, MI, and control groups. *Z*-scores and *P*-values of CAC subset gene expression (–dCt values) differences in patients and controls (Mann–Whitney *U*-test; SPSS version 25). Comparisons are made for each CAC subset included (HPCs, CD34$^+$ cells, KDR$^+$ cells) between patients (GBM, MI) and controls (HC, UCB). Genes are organized based on their function: PAFs, proangiogenic factors; GFRs, growth factor receptors; CRs, chemotactic receptors; DIFs, de-adhesion and invasion factors; MFs, mobilization factors; ITG, integrins (adhesion factors); Other, matricellular modulators of angiogenesis (*POSTN/TNC*) and the progenitor cell marker *CD133*.

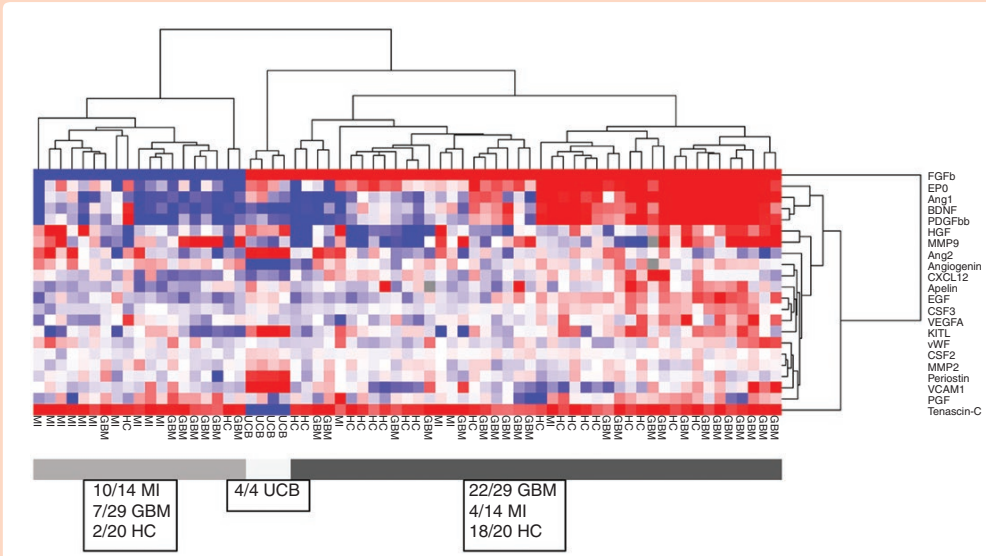

Figure 6. Plasma factors: unsupervised hierarchical cluster analysis and *Z*-scores. (A) Unsupervised hierarchical cluster analysis of plasma factors. GBM and MI samples are divided into different clusters. GBM patients have higher levels of many plasma factors. (B) *Z*-scores and *P*-values of plasma factors with significantly different levels in GBM, MI, and HC ($P \leq .05$).

Supplementary Data

Supplementary data are available at *Neuro-Oncology Advances* online.

Keywords

angiogenesis | circulating angiogenic cell | endothelial progenitor cell | glioma | hematopoietic progenitor cell | myocardial infarction | neovascularization.

Funding

The funding for this project was provided by the Department of Pathology of the Erasmus Medical Center.

Acknowledgments

Dr A. M. Sieuwerts† for her expertise and help with setting up and validating the rare-cell RT-PCR experiments; Dr R. J. M. van Geuns, Department of Cardiology for collection of the MI patients' blood samples; Prof. Dr R. Fodde for granting access to the FACS facility; Mr F. van der Panne for his assistance with creating the figures.

Conflict of interest statement. None of the authors have any conflicts of interest to disclose.

Authorship Statement. K.H., J.M.K., D.A.M., and A.S. contributed to formation of hypotheses, experimental design, implementation and interpretation of the data, and writing the manuscript. S.S. and P.J.v.d.S. contributed to data analysis. W.D. contributed to experimental design, implementation, and data interpretation regarding Luminex assays.

References

1. Xiao Q, Yang S, Ding G, Luo M. Anti-vascular endothelial growth factor in glioblastoma: a systematic review and meta-analysis. *Neurol Sci.* 2018;39(12):2021–2031.
2. Carmeliet P. Mechanisms of angiogenesis and arteriogenesis. *Nat Med.* 2000;6(4):389–395.

3. Drake CJ. Embryonic and adult vasculogenesis. *Birth Defects Res C Embryo Today.* 2003;69(1):73–82.
4. Fang S, Salven P. Stem cells in tumor angiogenesis. *J Mol Cell Cardiol.* 2011;50(2):290–295.
5. Wojakowski W, Landmesser U, Bachowski R, Jadczyk T, Tendera M. Mobilization of stem and progenitor cells in cardiovascular diseases. *Leukemia.* 2012;26(1):23–33.
6. Aragona CO, Imbalzano E, Mamone F, et al. Endothelial progenitor cells for diagnosis and prognosis in cardiovascular disease [published online ahead of print December 29, 2015]. *Stem Cells Int.* 2016;2016:8043792. doi:10.1155/2016/8043792.
7. Zheng PP, Hop WC, Luider TM, Sillevis Smitt PA, Kros JM. Increased levels of circulating endothelial progenitor cells and circulating endothelial nitric oxide synthase in patients with gliomas. *Ann Neurol.* 2007;62(1):40–48.
8. Lau KK, Chan YH, Yiu KH, et al. Burden of carotid atherosclerosis in patients with stroke: relationships with circulating endothelial progenitor cells and hypertension. *J Hum Hypertens.* 2007;21(6):445–451.
9. Regueiro A, Cuadrado-Godia E, Bueno-Betí C, et al. Mobilization of endothelial progenitor cells in acute cardiovascular events in the PROCELL study: time-course after acute myocardial infarction and stroke. [published online ahead of print January 22, 2015] *J Mol Cell Cardiol.* 2015;80:146–155. doi:10.1016/j.yjmcc.2015.01.005.
10. Moccia F, Zuccolo E, Poletto V, et al. Endothelial progenitor cells support tumour growth and metastatisation: implications for the resistance to anti-angiogenic therapy. *Tumour Biol.* 2015;36(9):6603–6614.
11. Jeevanantham V, Butler M, Saad A, Abdel-Latif A, Zuba-Surma EK, Dawn B. Adult bone marrow cell therapy improves survival and induces long-term improvement in cardiac parameters: a systematic review and meta-analysis. *Circulation.* 2012;126(5):551–568.
12. Lyden D, Hattori K, Dias S, et al. Impaired recruitment of bone-marrow-derived endothelial and hematopoietic precursor cells blocks tumor angiogenesis and growth. *Nat Med.* 2001;7(11):1194–1201.
13. Caiado F, Dias S. Endothelial progenitor cells and integrins: adhesive needs. *Fibrogenesis Tissue Repair.* 2012;5:4. doi:10.1186/1755-1536-5-4.
14. Huizer K, Sacchetti A, Dik WA, Mustafa DA, Kros JM. Circulating proangiogenic cells and proteins in patients with glioma and acute myocardial infarction: differences in neovascularization between neoplasia and tissue regeneration. *J Oncol.* 2019;2019:3560830. doi:10.1155/2019/3560830. eCollection 2019.
15. Mazo IB, Massberg S, von Andrian UH. Hematopoietic stem and progenitor cell trafficking. *Trends Immunol.* 2011;32(10):493–503.
16. Steidl U, Kronenwett R, Haas R. Differential gene expression underlying the functional distinctions of primary human CD34+ hematopoietic stem and progenitor cells from peripheral blood and bone marrow. *Ann N Y Acad Sci.* 2003;996:89–100. PMID: 12799287. doi:10.1111/j.1749-6632.2003.tb03237.x.
17. Larsson J, Scadden D. Nervous activity in a stem cell niche. *Cell.* 2006;124(2):253–255.
18. Ugarte F, Forsberg EC. Haematopoietic stem cell niches: new insights inspire new questions. *EMBO J.* 2013;32(19):2535–2547.
19. Forsberg EC, Smith-Berdan S. Parsing the niche code: the molecular mechanisms governing hematopoietic stem cell adhesion and differentiation. *Haematologica.* 2009;94(11):1477–1481.
20. Dar A, Kollet O, Lapidot T. Mutual, reciprocal SDF-1/CXCR4 interactions between hematopoietic and bone marrow stromal cells regulate human stem cell migration and development in NOD/SCID chimeric mice. *Exp Hematol.* 2006;34(8):967–975.
21. Salmaggi A, Gelati M, Pollo B, et al. CXCL12 in malignant glial tumors: a possible role in angiogenesis and cross-talk between endothelial and tumoral cells. *J Neurooncol.* 2004;67(3):305–317.
22. Zagzag D, Esencay M, Mendez O, et al. Hypoxia- and vascular endothelial growth factor-induced stromal cell-derived factor-1alpha/CXCR4 expression in glioblastomas: one plausible explanation of Scherer's structures. *Am J Pathol.* 2008;173(2):545–560.
23. Jiang Z, Zhou W, Guan S, Wang J, Liang Y. Contribution of SDF-1α/CXCR4 signaling to brain development and glioma progression. *Neurosignals.* 2013;21(3–4):240–258.
24. Takahashi M. Role of the SDF-1/CXCR4 system in myocardial infarction. *Circ J.* 2010;74(3):418–423.
25. Stellos K, Ruf M, Sopova K, et al. Plasma levels of stromal cell-derived factor-1 in patients with coronary artery disease: effect of clinical presentation and cardiovascular risk factors. *Atherosclerosis.* 2011;219(2):913–916.
26. Greenfield JP, Jin DK, Young LM, et al. Surrogate markers predict angiogenic potential and survival in patients with glioblastoma multiforme. *Neurosurgery.* 2009;64(5):819–826; discussion 826–817.
27. Chatterjee M, Gawaz M. Platelet-derived CXCL12 (SDF-1α): basic mechanisms and clinical implications. *J Thromb Haemost.* 2013;11(11):1954–1967.
28. Döring Y, Pawig L, Weber C, Noels H. The CXCL12/CXCR4 chemokine ligand/receptor axis in cardiovascular disease. *Front Physiol.* 2014;5:212. doi:10.3389/fphys.2014.00212. eCollection 2014.
29. Berahovich RD, Zabel BA, Lewén S, et al. Endothelial expression of CXCR7 and the regulation of systemic CXCL12 levels. *Immunology.* 2014;141(1):111–122.
30. Madlambayan GJ, Butler JM, Hosaka K, et al. Bone marrow stem and progenitor cell contribution to neovasculogenesis is dependent on model system with SDF-1 as a permissive trigger. *Blood.* 2009;114(19):4310–4319.
31. Stellos K, Gawaz M. Platelets and stromal cell-derived factor-1 in progenitor cell recruitment. *Semin Thromb Hemost.* 2007;33(2):159–164.
32. Yong K, Fahey A, Reeve L, et al. Cord blood progenitor cells have greater transendothelial migratory activity and increased responses to SDF-1 and MIP-3beta compared with mobilized adult progenitor cells. *Br J Haematol.* 1999;107(2):441–449.
33. Chen L, Wu F, Xia WH, et al. CXCR4 gene transfer contributes to in vivo reendothelialization capacity of endothelial progenitor cells. *Cardiovasc Res.* 2010;88(3):462–470.
34. Klein G, Schmal O, Aicher WK. Matrix metalloproteinases in stem cell mobilization. [published online ahead of print January 21, 2015] *Matrix Biol.* 2015;44–46:175–183. doi:10.1016/j.matbio.2015.01.011.
35. Kawai K, Xue F, Takahara T, et al. Matrix metalloproteinase-9 contributes to the mobilization of bone marrow cells in the injured liver. *Cell Transplant.* 2012;21(2–3):453–464.
36. Lapid K, Glait-Santar C, Gur-Cohen S, Canaani J, Kollet O, Lapidot T. Egress and mobilization of hematopoietic stem and progenitor cells: a dynamic multi-facet process. *StemBook.* Cambridge, MA: Harvard Stem Cell Institute;2008.
37. Lin Y, Wang JF, Gao GZ, Zhang GZ, Wang FL, Wang YJ. Plasma levels of tissue inhibitor of matrix metalloproteinase-1 correlate with diagnosis and prognosis of glioma patients. *Chin Med J (Engl).* 2013;126(22):4295–4300.
38. Christopherson KW 2nd, Hangoc G, Mantel CR, Broxmeyer HE. Modulation of hematopoietic stem cell homing and engraftment by CD26. *Science.* 2004;305(5686):1000–1003.
39. Dutt P, Wang JF, Groopman JE. Stromal cell-derived factor-1 alpha and stem cell factor/kit ligand share signaling pathways in hemopoietic progenitors: a potential mechanism for cooperative induction of chemotaxis. *J Immunol.* 1998;161(7):3652–3658.
40. Fazel SS, Chen L, Angoulvant D, et al. Activation of c-kit is necessary for mobilization of reparative bone marrow progenitor cells in response to cardiac injury. *FASEB J.* 2008;22(3):930–940.
41. Sun L, Hui AM, Su Q, et al. Neuronal and glioma-derived stem cell factor induces angiogenesis within the brain. *Cancer Cell.* 2006;9(4):287–300.

42. Lennartsson J, Rönnstrand L. Stem cell factor receptor/c-Kit: from basic science to clinical implications. *Physiol Rev.* 2012;92(4):1619–1649.
43. Kim KL, Meng Y, Kim JY, Baek EJ, Suh W. Direct and differential effects of stem cell factor on the neovascularization activity of endothelial progenitor cells. *Cardiovasc Res.* 2011;92(1):132–140.
44. Sihto H, Tynninen O, Bützow R, Saarialho-Kere U, Joensuu H. Endothelial cell KIT expression in human tumours. *J Pathol.* 2007;211(4):481–488.
45. Smith MA, Court EL, Smith JG. Stem cell factor: laboratory and clinical aspects. *Blood Rev.* 2001;15(4):191–197.
46. Grünwald B, Vandooren J, Gerg M, et al. Systemic ablation of MMP-9 triggers invasive growth and metastasis of pancreatic cancer via deregulation of IL6 expression in the bone marrow. *Mol Cancer Res.* 2016;14(11):1147–1158.
47. Heissig B, Hattori K, Dias S, et al. Recruitment of stem and progenitor cells from the bone marrow niche requires MMP-9 mediated release of kit-ligand. *Cell.* 2002;109(5):625–637.
48. Wang Y, Luther K. Genetically manipulated progenitor/stem cells restore function to the infarcted heart via the SDF-1α/CXCR4 signaling pathway. *Prog Mol Biol Transl Sci.* 2012;111:265–284. doi:10.1016/B978-0-12-398459-3.00012-5.
49. Lutz M, Rosenberg M, Kiessling F, et al. Local injection of stem cell factor (SCF) improves myocardial homing of systemically delivered c-kit + bone marrow-derived stem cells. *Cardiovasc Res.* 2008;77(1):143–150.
50. Zhu C, Chrifi I, Mustafa D, et al. CECR1-mediated cross talk between macrophages and vascular mural cells promotes neovascularization in malignant glioma. *Oncogene.* 2017;36(38):5356–5368.
51. Gagner JP, Sarfraz Y, Ortenzi V, et al. Multifaceted C-X-C chemokine receptor 4 (CXCR4) inhibition interferes with anti-vascular endothelial growth factor therapy-induced glioma dissemination. *Am J Pathol.* 2017;187(9):2080–2094.

CHAPTER 4

PERIOSTIN IS EXPRESSED BY PERICYTES AND IS CRUCIAL FOR ANGIOGENESIS IN GLIOMA

J Neuropathol Exp Neurol
Vol. 00, No. 0, 2020, pp. 1–10
doi: 10.1093/jnen/nlaa067

ORIGINAL ARTICLE

Periostin Is Expressed by Pericytes and Is Crucial for Angiogenesis in Glioma

Karin Huizer, MD, Changbin Zhu, MD, PhD, Ihsan Chirifi, PhD, Bart Krist, PhD, Denise Zorgman, Marcel van der Weiden, Thierry P. P. van den Bosch, PhD, Jasper Dumas, Caroline Cheng, PhD, Johan M. Kros, MD, PhD, and Dana A. Mustafa, PhD

Abstract

The expression of the matricellular protein periostin has been associated with glioma progression. In previous work we found an association of periostin with glioma angiogenesis. Here, we screen gliomas for *POSTN* expression and identify the cells that express periostin in human gliomas. In addition, we study the role of periostin in an in vitro model for angiogenesis. The expression of periostin was investigated by RT-PCR and by immunohistochemistry. In addition, we used double labeling and in situ RNA techniques to identify the expressing cells. To investigate the function of periostin, we silenced *POSTN* in a 3D in vitro angiogenesis model. Periostin expression was elevated in pilocytic astrocytoma and glioblastoma, but not in grade II/III astrocytomas and oligodendrogliomas. The expression of periostin colocalized with PDGFRβ^+ cells, but not with OLIG2$^+$/SOX2$^+$ glioma stem cells. Silencing of periostin in pericytes in coculture experiments resulted in attenuation of the numbers and the length of the vessels formation and in a decrease in endothelial junction formation. We conclude that pericytes are the main source of periostin in human gliomas and that periostin plays an essential role in the growth and branching of blood vessels. Therefore, periostin should be explored as a novel target for developing anti-angiogenic therapy for glioma.

Key Words: Angiogenesis, Glioblastoma, Glioma, Matricellular protein, Periostin, Vasculogenesis.

INTRODUCTION

In order to find new targets for effective anti-angiogenic therapy for gliomas, the identification of molecules that play key roles in neovascularization is crucial. In spite of the fact that gliomas are among the tumors with highest degree of vascularization, anti-angiogenic therapies have not yielded major improvements in clinical outcome (1). It remains unclear why anti-angiogenic therapies largely fail, and whether the currently used drugs address all players in the complex process of angiogenesis. Levels of vascular endothelial growth factor (VEGF) are associated with tumor hypoxia that increases with tumor progression. VEGF inhibitors like bevacizumab are only used in patients with high-grade gliomas/glioblastomas (GBM) (2). The blood vessels in GBM show proliferation of endothelial cells, pericytes, and other mural cells, altogether designated as microvascular proliferation. However, notable changes in protein expression patterns of the vessel walls of gliomas that do not yet show microvascular proliferation have been recorded (3, 4). Given the notion that shifts in protein expression patterns have been recorded in the vasculature of low-grade gliomas, new targets for anti-angiogenic therapies in glioma should be explored.

In a previous study, we identified some proteins that are specifically upregulated in tumor angiogenesis (3). Among the proteins identified were αV-integrin and the matricelluar proteins tenascin-C and, most prominently, periostin. Matricellular proteins are expressed during development, tissue repair and cancer and contribute to angiogenesis by making the extracellular matrix permissive for new vascular sprouts (5–11). In various epithelial tumors increased levels periostin were found (5, 12–15) and a prominent role of periostin at sites of metastasis was reported (16). Periostin has been associated with glioma invasion and vasculature (3, 17–19), and recently its interference with anti-angiogenic therapies was highlighted (20). Most data were obtained in mouse models and data on the expression site of *POSTN* in human glioma are sketchy. In addition, the direct effects of periostin expression on glioma angiogenesis have not yet been investigated.

In this study, we explored the expression of periostin in human glioma samples by immunohistochemical detection of

From the Laboratory for Tumor Immunopathology, Department of Pathology (KH, CZ, BK, DZ, MvdW, TPPvdB, JD, JMK, DAM); and; Laboratory for Experimental Cardiology (IC, CC), Erasmus Medical Center, Rotterdam, The Netherlands.
Send correspondence to: Johan M. Kros, MD, PhD, Laboratory for Tumor Immunopathology, Department of Pathology, Erasmus Medical Center, Room Be-230-c, Wytemaweg 80, 3015 CE Rotterdam, The Netherlands; E-mail: j.m.kros@erasmusmc.nl
Karin Huizer and Changbin Zhu contributed equally to this work.
This study was partly sponsored by the China Scholarship Council (CSC) at the Erasmus Medical Center, Rotterdam, The Netherlands.
The authors have no duality or conflicts of interest to declare.

co-expression patterns and RNA in situ hybridization and found expression of periostin by PDGFRβ$^+$ pericytes without overlap with SOX2$^+$/OLIG2$^+$ glioma stem cells. Silencing of the *POSTN* gene in cultured pericytes resulted in a reduction of angiogenic capacity, proving the importance of periostin for glioma angiogenesis.

MATERIALS AND METHODS

Tissue Samples

Tissue samples of 21 GBM, 10 pilocytic astrocytomas (PA), 19 grade II and III astrocytoma (A II/III), and 9 oligodendrogliomas grade II/III (O II/III) were obtained from the Department of Pathology, Erasmus Medical Center, Rotterdam (Table 1). Pathology diagnoses were in accordance with the WHO criteria including the molecular criteria. IDH1 mutation was present in 2/21 GBMs, in 18/19A II/III, and in all O II/III. All oligodendrogliomas had 1p/19q codeletion (Table 1). In order to make comparisons with normal brain and other vascular lesions, we included 11 normal brain samples, 5 cavernous hemangiomas (CH), 10 arteriovenous malformations (AVM), and 10 hemangioblastomas (HB). The age and gender distributions of the patients are shown in Table 1. All patients had given consent for using their biomaterials and the study was approved by the medical ethical committee of the Erasmus Medical Center.

RNA Isolation and RT-PCR

Fresh-frozen samples (n = 67) and formalin-fixed paraffin-embedded (FFPE) samples (n = 28) were used for RNA isolation. For each fresh-frozen sample, 10–15 sections of 20-μm thickness were cut by a cryostat. Sections were collected in RNase free Eppendorf tubes, snap frozen on dry ice, and stored at –80°C until RNA isolation. To verify the presence of tumor in all the sections used for RNA isolation, 5-μm sections before and after sampling for RNA isolation were collected, H&E-stained and studied by a pathologist (J.M.K.). Total RNA was isolated using RNA-Bee (Campro, Veenendaal, The Netherlands) according to the instructions supplied by the manufacturer. For FFPE samples, RNA isolation and quality control was performed as described previously (3, 4).

Following isolation, RNA samples were diluted in nuclease-free water, snap frozen on dry ice and subsequently stored at –80°C. Total RNA quantity was determined by Nanodrop and RNA integrity was checked using gel electrophoresis. To generate cDNA, 1 μg of total RNA was reverse transcribed using the RevertAid cDNA synthesis kit (Fermentas, Waltham, MA). cDNA samples were stored at –20°C until they were measured by RT-PCR. siPOSTN sequences were purchased from Dharmacon (Cambridge, UK) (siPOSTN 1: catalogue #: J-020118-05-0005; siPOSTN 2: catalogue #: J-020118-06-0005). Exon-spanning TaqMan Gene Expression Assays of periostin (Hs00170815_m1, Applied Biosystems, Foster City, CA) was used to measure the expression of periostin. Expression of HPRT1 (Hs01003267_m1) and ACTB (Hs99999903_m1) were used as reference genes. RT-PCR to the endothelial marker CD31 was performed in order to correct for blood vessel density in a selection of samples (n = 67). PCR was performed in a 20 μL reaction volume in the Applied Biosystems 7500 Fast Real-Time PCR System. Negative controls using H_2O only samples were included and showed to be negative in all cases.

Mann-Whitney *U* test was used to perform statistical analysis. All glioma subgroups were compared with each other, and p value <0.01 was considered statistically significant.

Immunohistochemistry

FFPE samples corresponding to the same sample used for RNA isolation were used for immunohistochemistry. Antibodies for periostin, CD31, PDGFRβ, SOX2, and OLIG2 were used as previously described (2) (Table 2).

Confocal Imaging

A confocal laser-scanning microscope (LSM510; Carl Zeiss MicroImaging, Inc., Thornwood, NY) was used. A diode laser was used for excitation of DAPI at 405 nm, an argon laser for FITC at 488 nm and a HeNe-laser for Cy5 at 633 nm. For DAPI an emission bandpass filter of 420–480 nm, for FITC the bandpass filter of 500–530 nm, and for Cy5 a bandpass filter of 650 nm were used.

In Situ Hybridization

The RNAscope 1 2.0 HD Brown Chromogenic Reagent Kit and Hs-*POSTN* probe (#409181) were used, according to

TABLE 1. Patient and Tumor Characteristics

	Mean Age(SD)	Sex(m/f)	IDH1wt/mut	1p/19q CodelYes/No	Total
Glioblastoma	47.4 (12.7)	15/6	19/2	0/21	21
Pilocytic astrocytoma	23.4 (18.6)	3/7			10
Astrocytoma (grade II/III)	43.2 (14.8)	7/12	1/18	0/19	19
Oligodendroglioma (grade II/III)	50.7 (7.8)	6/3	0/9	9/0	9
Normal brain	49.3 (14.8)	5/6			11
Cavernous hemangioma	19.4 (11.2)	1/4			5
Hemangioblastoma	1.3 (21.2)	6/4			10
Arterio-venous malformation	39.8 (18.3)	8/2			10

SD, standard deviation; m, male; f, female; IDH1, isodehydrogenase 1; wt, wild type; mut., mutation; codel, codeletion.

TABLE 2. *Z* Scores of Periostin Expression Tumors, Malformations and Normal Brain and p Values of Differences in Expression Between Tissues

			GBM	PA	AII/III	Oligo	n.b.	CH	HB	AVM
GBM	POSTN (–dCt)	Z		−1.10	**−3.50**	**−2.86**	**−2.98**	−0.81	−0.19	−0.82
		p		0.27	0.00	0.00	0.00	0.42	0.85	0.41
	POSTN/CD31 (–dCt)	Z		−0.39	**−2.22**		**−2.69**	−0.06	−1.80	−1.13
		p		0.70	0.03		0.01	0.95	0.07	0.26
PA	POSTN (–dCt)	Z	−1.10		**−3.30**	**−3.03**	**−3.39**	−0.25	**−1.66**	−1.74
		p	0.27		0.00	0.00	0.00	0.81	0.10	0.08
	POSTN/CD31 (–dCt)	Z	−0.39		**−2.72**		**−3.59**	−0.55	**−2.88**	−1.78
		p	0.70		0.01		0.00	0.58	0.00	0.08
AII/III	POSTN (–dCt)	Z	**−3.50**	**−3.30**		−0.49	−0.18	**−2.19**	**−3.60**	**−2.12**
		p	0.00	0.00		0.62	0.86	0.03	0.00	0.03
	POSTN/CD31 (–dCt)	Z	**−2.22**	**−2.72**			−0.32	−1.53	−1.29	−1.10
		p	0.03	0.01			0.75	0.13	0.20	0.27
Oligo	POSTN (–dCt)	Z	**−2.86**	**−3.03**	−0.49		−0.38	−1.91	**−3.56**	**−1.96**
		p	0.00	0.00	0.62		0.71	0.06	0.00	0.05
	POSTN/CD31 (–dCt)	Z								
		p								
n.b.	POSTN (–dCt)	Z	**−2.98**	**−3.39**	−0.18	−0.38		**−2.34**	**−3.43**	**−1.92**
		p	0.00	0.00	0.86	0.71		0.02	0.00	0.05
	POSTN/CD31 (–dCt)	Z	**−2.69**	**−3.59**	−0.32			**−2.15**	−1.76	−1.41
		p	0.01	0.00	0.75			0.03	0.08	0.16
CH	POSTN (–dCt)	Z	−0.81	−0.25	**−2.19**	−1.91	**−2.34**		−0.86	−1.47
		p	0.42	0.81	0.03	0.06	0.02		0.39	0.14
	POSTN/CD31 (–dCt)	Z	−0.06	−0.55	−1.53		**−2.15**		−1.47	−1.04
		p	0.95	0.58	0.13		0.03		0.14	0.30
HB	POSTN (–dCt)	Z	−0.19	−1.66	**−3.60**	**−3.56**	**−3.43**	−0.86		−1.10
		p	0.85	0.10	0.00	0.00	0.00	0.39		0.27
	POSTN/CD31 (–dCt)	Z	−1.80	**−2.88**	−1.29		−1.76	−1.47		−0.68
		p	0.07	0.00	0.20		0.08	0.14		0.50
AVM	POSTN (–dCt)	Z	−0.82	−1.74	**−2.12**	**−1.96**	**−1.92**	−1.47	−1.10	
		p	0.41	0.08	0.03	0.05	0.05	0.14	0.27	
	POSTN/CD31 (–dCt)	Z	−1.13	−1.78	−1.10		−1.41	−1.04	−0.68	
		p	0.26	0.08	0.27		0.16	0.30	0.50	

Abbreviations: GBM = glioblastoma; PA = pilocytic astrocytoma; A II/III = astrocytoma WHO grades II and III; OLIGO = oligodendroglioma WHO grades II and III; n.b. = normal brain; CH = cavernous hemangioma; HB = hemangioblastoma; AVM = arteriovenous malformation; POSTN = periostin. P < 0.05 highlighted.

the manufacturer's instruction (Advanced Cell Diagnostics, Hayward, CA). Briefly, prepared slides were baked for 1 hour at 60°C prior to use. After deparaffinization and hydration, tissue and cells were air-dried and treated with a peroxidase blocker before heating in a target retrieval solution (#320043) for 20 minutes at 95–100°C. Protease (#320045) was then applied for 30 minutes at 40°C. *POSTN* probe was hybridized for 2 hours at 40°C, followed by a series of signal amplification and washing steps. Hybridization signals were detected by chromogenic reaction using DAB chromogen followed by 1:1 (vol/vol)-diluted hematoxylin (Fisher Scientific, Pittsburg, PA) counterstaining.

Cell Culture Experiments

In order to investigate the main source of periostin, various cell lines were used. HUVEC (ScienCell-1800), human brain vascular pericytes (ScienCell-1200), and human astrocytes (ScienCell-8000) were cultured following the manual protocols. Periostin expression in cell lysates was measured by Western blotting using Periostin antibody (HPA012306, 1:50, Sigma Life Sciences, St. Louis, MO). In addition, GBM cell line U87 was cultured for 3 days. After that, U87-conditioned media was added to the cultures of HUVECs, pericytes and astrocytes for 3 days. The expression of periostin in the cell lysate and the media was measured in the 3 cells lines by Western blot.

Silencing of POSTN

Two different siRNA sequences of periostin were used (Dharmacon, GE Health Care, Eindhoven, The Netherlands). A mix of nontargeting siRNA (referred to as siSham) were also obtained from Dharmacon and used as a negative control for silencing. Silencing experiments were performed using transfection buffer 1, following the manufacturer's instructions. Human

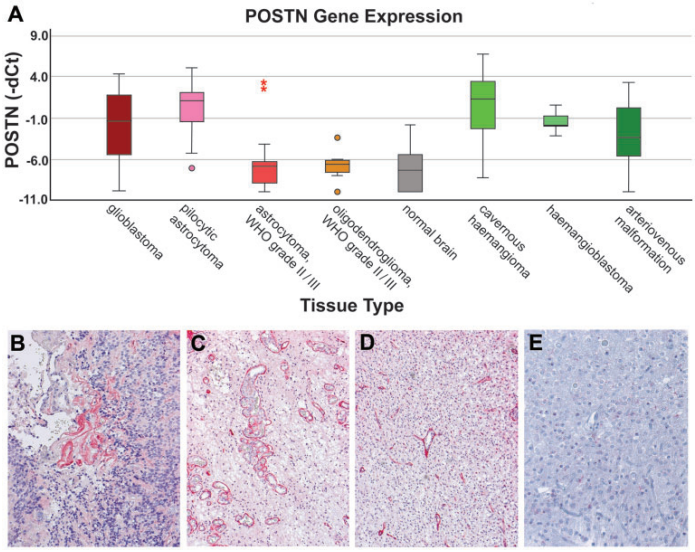

FIGURE 1. Results of RT-PCR to *POSTN* and immunohistochemistry to periostin. **(A)** Box plots of RT-PCR to *POSTN*. Highest expression levels of *POSTN* were found in GBM and PA. Significantly lower levels of expression are encountered in A II/III and O II/III. In HB and cerebral vascular malformations (CH and AVM), *POSTN* expression levels are high relative to A II/III and O II/III. In normal brain (n.b.) samples, lowest expression was recorded. **(B–E)** Periostin immunohistochemistry in GBM. Expression is concentrated around areas of MVP **(B)**. The expression is confined to the proliferated vessels in PA **(C)**. In A II/III **(D)** and O II/III **(E)**, periostin expression is found in around scattered blood vessels (×100).

brain vascular pericytes were transfected for 24 and 48 hours. RNA and proteins were isolated subsequently. The silencing efficiency was evaluated by RT-PCR and by Western blotting, following the protocols that were previously described.

3D In Vitro Angiogenesis Model

Pericytes were stained with DsRed and mixed with GFP labeled HUVECs at 1:5 ratio as described previously (21). To create a 3D in vitro angiogenesis model, bovine collagen type 1 was used. The parameters of angiogenesis, namely: number of tubule formation, length of tubule formation, and number of junctions were measured following 3 days of coculturing. These experiments were repeated 6 times.

RESULTS

POSTN Expression Is Associated With Angiogenesis in the Glial Tumors

The RNA expression of *POSTN* was corrected for vessel density by relating it to the expression of the endothelial marker CD31. *POSTN* expression was strongly elevated in PA and GBM as compared with that in normal brain (Fig. 1A). *POSTN* expression was also high in CH, HB, and AVM. The expression was low in A II/III and O II/III. The absolute expression and expression relative to vessel density (CD31 expression) are shown in Table 2. The results of immunohistochemistry were in line with those of the RT-PCR (Fig. 1B–E). In GBM, the expression of periostin was present in the perivascular area of hypertrophic and glomeruloid vessels, with dissemination in the neuropil (Fig. 1B). In the PAs expression was confined to the hypertrophied vasculature (Fig. 1C). The expression levels of periostin in A II/III and O II/III were comparable to those found in control brain samples (Fig. 1D, E). In AVM and CH, periostin was variably expressed in arteries and veins. In the HB, only a minority of capillaries was surrounded by perivascular periostin.

POSTN Is Expressed by Pericytes

In order to characterize the cells that express periostin, we performed double labeling fluorescent IHC. Periostin expression colocalized with PDGFRβ^+ pericytes (Fig. 2A). RNA in situ hybridization revealed that periostin protein expression localized with *POSTN* expression in scattered cells present just outside the cells expressing CD31 (Fig. 2B). GFAP-positive cells did not express *POSTN* (data not shown). IHC to the stem cell markers SOX2 and OLIG2 revealed that the expression of periostin does not colocalize with SOX2 and OLIG2-positive cells (Fig. 2C).

Pericytes Are the Main Source of POSTN

In order to study the function of *POSTN*, we first identified the periostin expressing cells in vitro. Western blotting using a periostin specific antibody confirmed that pericytes are the main source of expression. In addition, periostin expres-

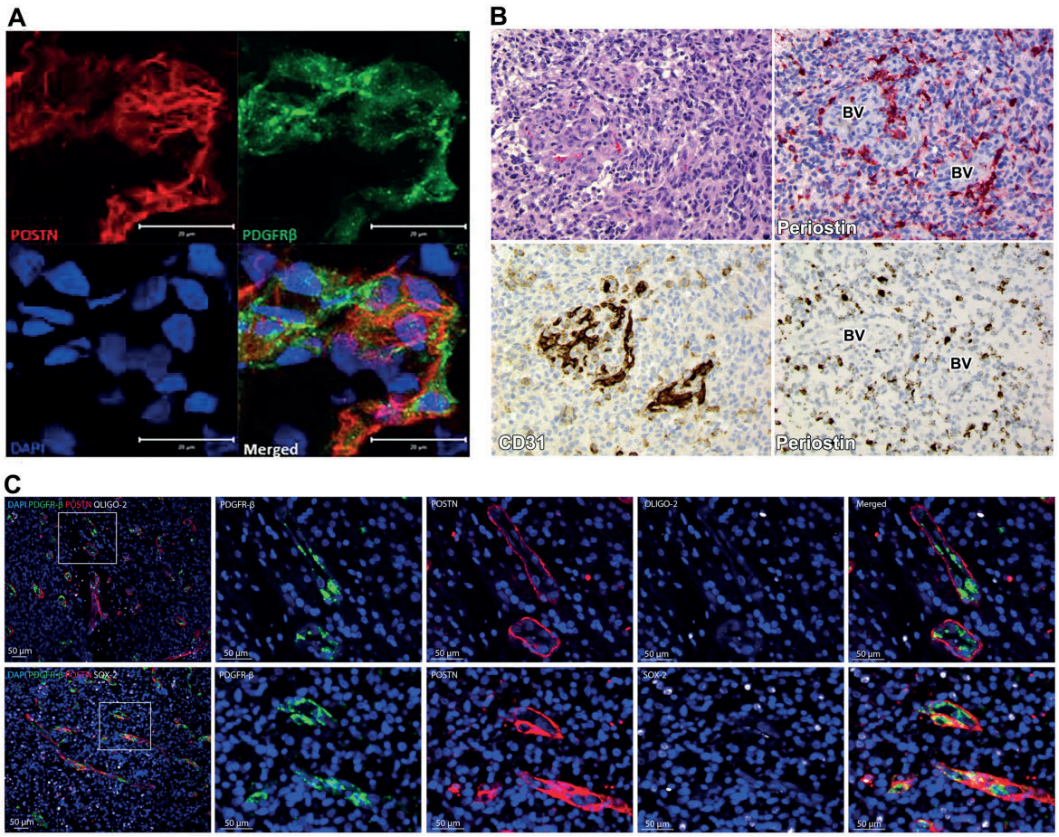

FIGURE 2. Periostin is expressed by pericytes. **(A)** Glioblastoma tissue immunostained for periostin and the pericyte marker PDGFRβ. There is overlapping expression of PDGFRβ and periostin (×400). **(B)** RNA in situ hybridization to *POSTN* in glioblastoma (lower right panel) reveals expression in scattered cells just outside of the endothelial layer. The CD31-positive endothelial cells (lower left panel) do not overlap with this RNA expression of *POSTN* (×40). **(C)** Cells expressing the stem cell transcription markers SOX2 and OLIG-2 do not overlap with the cells expressing periostin (IHC; ×40; DAPI counterstaining).

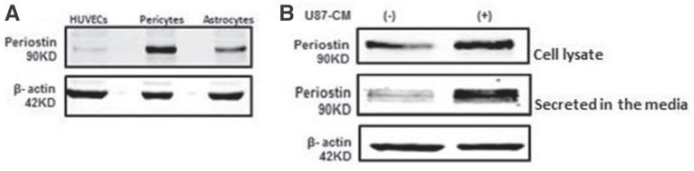

FIGURE 3. Western blotting to *POSTN* in cell cultures of various lineages. **(A)** Western blots for periostin in cell cultures of HUVEC (endothelial cells), pericytes, and normal astrocytes. *POSTN* expression is high in pericytes while expression is lower in astrocytes and absent from HUVEC. **(B)** Periostin protein expression by cultured pericytes w/wo cell lysates of the glioma cell line U87, or U87-conditioned media (U87-CM). Increased expression of periostin is observed following the addition of U87-CM, and after culturing the pericytes in the presence of U87 cell lysates.

sion was found in astrocytes also, but to a lesser extent than in pericytes. No expression was detected in endothelial cells (Fig. 3A). To investigate periostin expression in the presence of glial tumor cells, we added the conditioned media of U87 cells to the cultured pericytes and measured the expression of periostin after 24 hours. Glioma-conditioned media stimulated pericytes to express higher level of periostin (Fig. 3B). Increased periostin expression was also obtained following cul-

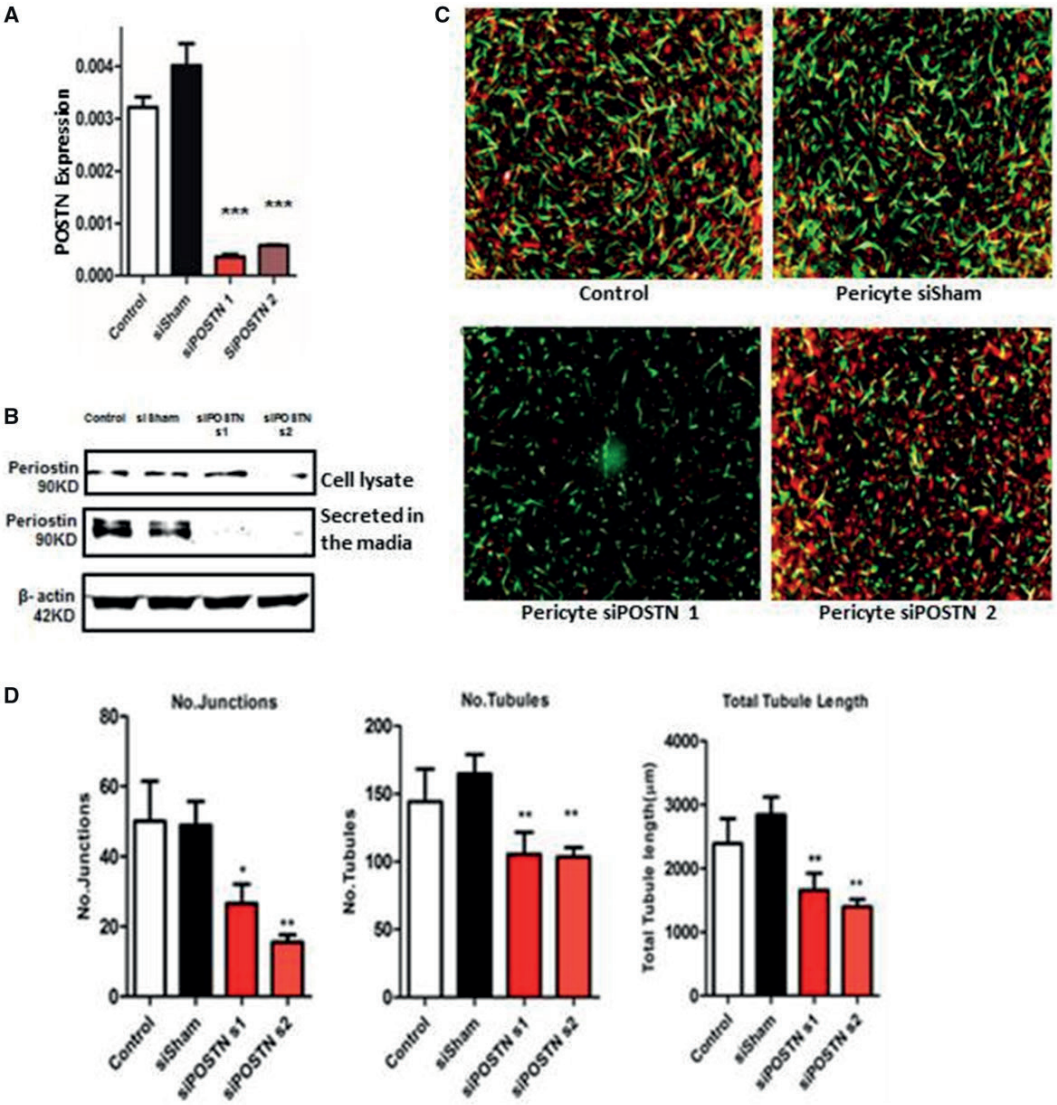

FIGURE 4. In vitro angiogenesis following silencing of *POSTN*. **(A)** Bar diagram of RT-PCR results showing the successful silencing of *POSTN* by 2 siRNAs. **(B)** Western blots showing levels of periostin in pericyte cell lysates and conditioned media, following silencing of *POSTN* in the pericytes. Silencing by sequence #2 resulted in significant reduction of periostin expression in the pericyte cell lysates and conditioned media. Silencing by sequence #1 resulted in reduced expression only in the conditioned media, not in the cell lysates. **(C)** Images of the 3D angiogenesis culture assay (pericytes stained with DsRed, HUVEC expressing GFP) using different conditions: Off-target silencing sequences (siSham) did not affect the formation of the blood vessels (upper panel right); effective silencing of *POSTN* resulted in significant reduction of formation of angiogenesis for both sequences (lower panels). **(D)** Bar diagrams showing the results of *POSTN* silencing in the pericytes on angiogenesis. For both silencing sequences, significant reductions in numbers of tubules (middle panel), tubular lengths (right panel), and number of vascular junctions (left panel) was achieved.

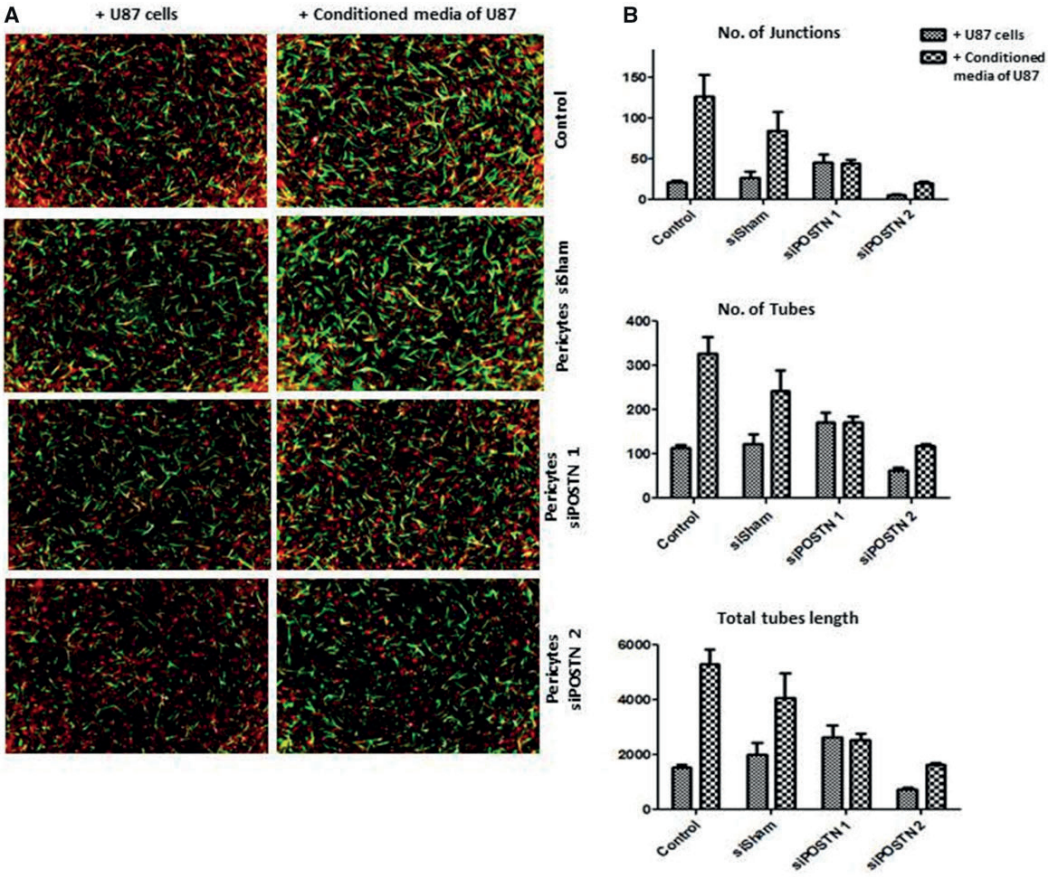

FIGURE 5. In vitro angiogenesis following silencing of *POSTN* in the presence of U87 cells or U87-conditioned medium. **(A)** Images of the angiogenesis culture assay following silencing of *POSTN* (using 2 different sequences) combined with U87 cells or U87 condition medium. **(B)** Quantification of the numbers and lengths of tubes and junctions. The effects of silencing *POSTN* on the number of vascular tubes, their length and the number of junctions were reduced in the presence of U87 cells or U87-conditioned medium.

turing the pericytes in the presence of U87 cell lysates (Fig. 3B).

POSTN Effect on In Vitro Angiogenesis

In functional assays, we silenced *POSTN* in pericytes and used a 3D in vitro angiogenesis assay. Silencing *POSTN* was achieved by 2 different siRNA sequences and *POSTN* was successfully downregulated using si*POSTN* for both sequences ($n = 3$; mean ± SEM; $p = 0.005$) (Fig. 4A). Effective downregulation of periostin protein in conditioned media and cell lysates of the cultured pericytes was achieved by using sequence #2. Following the use of sequence #1, downregulation of *POSTN* expression was only detected in the conditioned media, not in the cell lysates (Fig. 4B). The pericyte cultures silenced for *POSTN* were cocultured with endothelial cells in the 3D in vitro angiogenesis model. The number and length of the tubules and the number of junctions formed in the assay revealed significant differences for both silencing sequences (Fig. 4C, D).

In Vitro Angiogenesis Following Silencing of POSTN Partially Restored in the Presence of U87 Cells or U87 Conditioned Medium

The effects of silencing of periostin on angiogenesis was measured following the introduction of U87 (glioma) cells and following the addition of U87-conditioned media to the culture system. The angiogenesis-inhibiting effect of *POSTN* silencing in pericytes was partially saved by the addition of U87 cells or conditioned medium (Fig. 5A, B). The effects of silencing were stronger by using sequence #2.

DISCUSSION

In this study, we investigated the expression of periostin in gliomas of various malignancy grades and found the highest levels of expression in gliomas with proliferated microvasculature, that is, GBM and PA. Periostin expression appeared also to be high in other cerebral lesions with angiogenic activity, like HB and vascular malformations. In gliomas of lower malignancy grade, in which no visible changes of the vessel walls exist, the expression levels were comparable to those in normal brain. Both in the tissue samples of the patients and in the cell cultures, periostin was expressed by PDGFRβ$^+$ pericytes. However, in the cell cultures low-level expression by astrocytes was also observed. In the functional studies, we showed that periostin expression is necessary for proper formation of vasculature and that the presence of glioma cells (or their secretome) positively influences the angiogenesis-promoting effects of periostin.

Periostin is a matricellular protein and member of the tumor growth factor (TGF) family and its expression is induced by TGF-β and BMP-2 (22). Periostin promotes the incorporation of tenascin-C into the extracellular matrix (23) and interacts with bone morphogenic proteins 1/2 (BMP1/2) for the regulation of collagen cross-linking (24). Periostin interacts with various matricellular proteins in reparative processes and plays a role in the epithelial-mesenchymal transition in the context of neoplasia (2, 23–27). In recent years, it became clear that periostin plays roles in the proliferation, migration and the epithelial-mesenchymal transition of cancer (28–31). In breast cancer, periostin is expressed by tumor associated fibroblasts and promotes the proliferation and metastatic capacities of the tumor cells (32, 33). The N-terminal region of the molecule binds to integrins αVβ3, αVβ5, and α6β4 through its FAS domain (28), thereby promoting migration of tumor cells via the activation of Akt/PKB and focal adhesion kinase-mediated signaling pathways (14). In accordance, knock-down of *POSTN* in the ErbB2/Neu-driven murine breast tumor model results in reduced activity of the Notch signaling pathway and deceleration of tumor growth (34, 35). In breast and colonic cancer, it was shown that the expression of periostin by stromal cells is induced by tumor cells and is associated with cell proliferation, immune evasion, migration and genomic instability and decreases apoptosis of cancer cells (14, 36, 37). Periostin was associated with angiogenesis in wound healing and vascular heart disease, and also in neoplasia (38–44). In breast cancer-associated angiogenesis, the endothelial cells that navigate the branching of newly formed vessels, the vascular tip cells, also transiently express periostin (45).

To date, only few studies have focused on the expression of periostin in glial neoplasms and its expression was associated with tumor cell invasion (3, 17, 20, 46, 47). In contrast to periostin, the matricellular proteins tenascin-C and integrin-αV have been strongly associated with glioma angiogenesis (48–52). It is likely that endothelial cells and pericytes are responsible for the perivascular expression of tenascin-C while the proliferating glial tumor cells are the extravascular source of this protein (53, 54). The expression of tenascin-C is induced by several angiogenic factors, including VEGF, acidic and basic fibroblast growth factors (FGF), platelet-derived growth factor (PDGF), and tumor necrosis factor (TNF) (55). The perivascular presence of tenascin-C correlates with microvessel density and tumor cell proliferation (49, 50, 52, 53). Therefore, tenascin-C was selected as target for experimental tumor therapy with the use of radio-labeled anti-tenascin-C monoclonal antibodies (55). Integrin-αV is another molecule that interacts with periostin and not only plays a role in angiogenesis, but also in the proliferation, migration and invasion of the tumor cells (56). Integrins coordinate the interaction of the extracellular matrix with the cytoskeleton. Tenascin-C preferentially binds to integrin-αVβ3 (56). The expression of integrin-αV is increased during physiological angiogenesis (56, 57) and has been found upregulated in vascular malformations just as we found to be the case with respect to periostin (58). In the CNS, VEGF triggers the expression of integrin-αV by pericytes and endothelial and glial cells. The expression of integrin $\alpha_V\beta_3$ parallels the progression from low-grade to high-grade tumors (5, 59–61). Literature data point to upregulation of periostin expression by hypoxia and VEGF-driven angiogenesis (62–66). However, the expressional regulation seems more complex from the present findings. We found high expression of periostin in GBM as opposed to low expression in the lower-grade gliomas in which hypoxia is not yet dominant. However, hypoxia certainly drives angiogenesis in GBM, but the vascular proliferation in PA seems not essentially hypoxia-driven while the hypertrophied vasculature differs in architecture and protein expression patterns (67). We conclude that periostin expression contributes to aberrant angiogenesis, both in malformations and in gliomas, and that the formation and structure of the malformed blood vessels is a result of the cellular and environmental context of its expression.

Recently, it was suggested that periostin plays a role in the maintenance of stem cells in normal bone marrow and in the maintenance of leukemia-initiating cells (68). Among various extracellular matrix proteins, periostin was identified as important for the glioma stem cell niche (69). A similar effect of periostin on breast cancer stem cells has been described (32). In mice, it was shown that glioma stem cells defined by expression of SOX2 and OLIG2 produce periostin that stimulates the recruitment of tumor-associated macrophages through $\alpha_V\beta_3$ integrin signaling. In addition, periostin remodels the tumor micro-environment in concert with osteopontin and proteins of the CNN family by interaction with tumor-associated macrophages and other immune cells (69). Following their arrival in the brain, monocytes differentiate into M2-like macrophages that promote tumor progression and counteract the antitumor effects of T lymphocytes. In GBM the secretion of periostin was preferentially seen around cells marked by OLIG2 and SOX2 (69). In this study, we identified the PDGFRβ$^+$ pericytes as the source of periostin production. The perivascular RNA expression and the overlap with the protein by scattered cells corroborate this finding. In another recent paper, periostin secretion has been associated with glioma cell invasion, adhesion, migration and stem cell survival in gliomas, and correlates directly with glioma grade (70). Periostin expression was reportedly found in tumor cells but no double labeling for GFAP or other markers was provided.

The association between the expression levels of periostin on the one hand, and glioma grade and patient survival on the other, was explained by the increase in angiogenesis during glioma progression (70). Although we found expression of periostin in cultured astrocytes, we were unable to detect any expression in astrocytic tumor cells in the human glioma samples. We are, however, unable to confirm expression of periostin by any of the numerous cells expressing OLIG2 or SOX2, and we did not observe its overlap with the expression of SOX2 or OLIG2. Unfortunately, Zhou et al did not include immunohistochemistry to PDGFR in their study, which might have identified the true origin of periostin in their GBM samples. Therefore, we are unable to confirm expression of periostin by glioma tumor cells or glioma stem cells. The data indicate that the periostin expression in mice is only partly recapitulated in man.

In conclusion, periostin expression in gliomas serves a variety of functions that relate to neo-angiogenesis, an association that is also present in cerebral vascular malformations. The expression is significant in gliomas with microvascular proliferation (GBM and PA). We identified $PDGFR^{+}$ pericytes as the source of periostin, a finding that is relevant to new anti-angiogenic strategies in glioma.

ACKNOWLEDGMENTS

The authors thank Mr. F. van der Panne for his assistance with the photography, and the laboratory staff of the Department of Experimental Cardiology of the Erasmus Medical Center for their help and provision of the blood vessel culture systems. Mrs. Vanja de Weerd is thanked for her technical assistance.

REFERENCES

1. Van Meir EG, Hadjipanayis CG, Norden AD, et al. Exciting new advances in neuro-oncology: The avenue to a cure for malignant glioma. CA Cancer J Clin 2010;60:166–93
2. Ferrara N, Hillan KJ, Gerber HP, et al. Discovery and development of bevacizumab, an anti-VEGF antibody for treating cancer. Nat Rev Drug Discov 2004;3:391–400
3. Mustafa DA, Dekker LJ, Stingl C, et al. A proteome comparison between physiological angiogenesis and angiogenesis in glioblastoma. Mol Cell Proteomics 2012;11:M111.008466
4. Mustafa D, van der Weiden M, Zheng P, et al. Expression sites of colligin 2 in glioma blood vessels. Brain Pathol 2010;20:50–65
5. Tabatabai G, Weller M, Nabors B, et al. Targeting integrins in malignant glioma. Targ Oncol 2010;5:175–81
6. Llera AS, Girotti MR, Benedetti LG, et al. Matricellular proteins and inflammatory cells: A task force to promote or defeat cancer? Cytokine Growth Factor Rev 2010;21:67–76
7. Midwood KS, Orend G. The role of tenascin-C in tissue injury and tumorigenesis. J Cell Commun Signal 2009;3:287–310
8. Orend G. Potential oncogenic action of tenascin-C in tumorigenesis. Int J Biochem Cell Biol 2005;37:1066–83
9. Hsia HC, Schwarzbauer JE. Meet the tenascins: Multifunctional and mysterious. J Biol Chem 2005;280:26641–4
10. Bornstein P, Sage EH. Matricellular proteins: Extracellular modulators of cell function. Curr Opin Cell Biol 2002;14:608–16
11. Matsui Y, Morimoto J, Uede T. Role of matricellular proteins in cardiac tissue remodeling after myocardial infarction. World J Biol Chem 2010;1:69–80
12. Bao S, Ouyang G, Bai X, et al. Periostin potently promotes metastatic growth of colon cancer by augmenting cell survival via the Akt/PKB pathway. Cancer Cell 2004;5:329–39
13. Carnemolla B, Castellani P, Ponassi M, et al. Identification of a glioblastoma-associated tenascin-C isoform by a high affinity recombinant antibody. Am J Pathol 1999;154:1345–52
14. Ruan K, Bao S, Ouyang G. The multifaceted role of periostin in tumorigenesis. Cell Mol Life Sci 2009;66:2219–30
15. Baril P, Gangeswaran R, Mahon PC, et al. Periostin promotes invasiveness and resistance of pancreatic cancer cells to hypoxia-induced cell death: Role of the beta4 integrin and the PI3k pathway. Oncogene 2007;26:2082–94
16. Oskarsson T, Massague J. Extracellular matrix players in metastatic niches. EMBO J 2012;31:254–6
17. Broudy VC, Kovach NL, Bennett LG, et al. Human umbilical vein endothelial cells display high-affinity c-kit receptors and produce a soluble form of the c-kit receptor. Blood 1994;83:2145–52
18. Lal A, Lash AE, Altschul SF, et al. A public database for gene expression in human cancers. Cancer Res 1999;59:5403–7
19. Tso CL, Shintaku P, Chen J, et al. Primary glioblastomas express mesenchymal stem-like properties. Mol Cancer Res 2006;4:607–19
20. Park SY, Piao Y, Jeong KJ, et al. Periostin (*POSTN*) regulates tumor resistance to antiangiogenic therapy in glioma models. Mol Cancer Ther 2016;15:2187–97
21. Koh W, Stratman AN, Sacharidou A, et al. In vitro three dimensional collagen matrix models of endothelial lumen formation during vasculogenesis and angiogenesis. Methods Enzymol 2008;443:83–101
22. Horiuchi K, Amizuka N, Takeshita S, et al. A. Identification and characterization of a novel protein, periostin, with restricted expression to periosteum and periodontal ligament and increased expression by transforming growth factor beta. J Bone Miner Res 1999;14:1239–49
23. Kii I, Nishiyama T, Li M, et al. Incorporation of tenascin-C into the extracellular matrix by periostin underlies an extracellular meshwork architecture. J Biol Chem 2010;285:2028–39
24. Hwang EY, Jeong MS, Park EK, et al. Structural characterization and interaction of periostin and bone morphogenetic protein for regulation of collagen cross-linking. Biochem Biophys Res Commun 2014;449:425–31
25. Kii I, Nishiyama T, Kudo A. Periostin promotes secretion of fibronectin from the endoplasmic reticulum. Biochem Biophys Res Commun 2016;470:888–93
26. Conway SJ, Izuhara K, Kudo Y, et al. The role of periostin in tissue remodeling across health and disease. Cell Mol Life Sci 2014;71:1279–88
27. Kudo A. Periostin in fibrillogenesis for tissue regeneration: Periostin actions inside and outside the cell. Cell Mol Life Sci 2011;68:3201–7
28. Morra L, Moch H. Periostin expression and epithelial-mesenchymal transition in cancer: A review and an update. Virchows Arch 2011;459:465–75
29. Moniuszko T, Wincewicz A, Koda M, et al. Role of periostin in esophageal, gastric and colon cancer. Oncol Lett 2016;12:783–7
30. Xu X, Chang W, Yuan J, et al. Periostin expression in intra-tumoral stromal cells is prognostic and predictive for colorectal carcinoma via creating a cancer-supportive niche. Oncotarget 2016;7:798–813
31. Sato-Matsubara M, Kawada N. New player in tumor-stromal interaction: Granulin as a novel therapeutic target for pancreatic ductal adenocarcinoma liver metastasis. Hepatology 2017;65:374–6
32. Malanchi I, Santamaria-Martinez A, Susanto E, et al. Interactions between cancer stem cells and their niche govern metastatic colonization. Nature 2012;481:85–9
33. Ghajar CM, Peinado H, Mori H, et al. The perivascular niche regulates breast tumour dormancy. Nat Cell Biol 2013;15:807–17
34. Tanabe H, Takayama I, Nishiyama T, et al. Periostin associates with Notch1 precursor to maintain Notch1 expression under a stress condition in mouse cells. PLoS One 2010;5:e12234
35. Sriram R, Lo V, Pryce B, et al. Loss of periostin/OSF-2 in ErbB2/Neu-driven tumors results in androgen receptor-positive molecular apocrine-like tumors with reduced Notch1 activity. Breast Cancer Res 2015;17:7
36. Contie S, Voorzanger-Rousselot N, et al. Increased expression and serum levels of the stromal cell-secreted protein periostin in breast cancer bone metastases. Int J Cancer 2011;128:352–60
37. Kikuchi Y, Kashima TG, Nishiyama T, et al. Periostin is expressed in pericryptal fibroblasts and cancer-associated fibroblasts in the colon. J Histochem Cytochem 2008;56:753–64

38. Hill JJ, Tremblay TL, Pen A, et al. Identification of vascular breast tumor markers by laser capture microdissection and label-free LC-MS. J Proteome Res 2011;10:2479–93
39. Hakuno D, Kimura N, Yoshioka M, et al. Periostin advances atherosclerotic and rheumatic cardiac valve degeneration by inducing angiogenesis and MMP production in humans and rodents. J Clin Invest 2010;120: 2292–306
40. Zhu M, Fejzo MS, Anderson L, et al. Periostin promotes ovarian cancer angiogenesis and metastasis. Gynecol Oncol 2010;119:337–44
41. Takanami I, Abiko T, Koizumi S. Expression of periostin in patients with non-small cell lung cancer: Correlation with angiogenesis and lymphangiogenesis. Int J Biol Markers 2008;23:182–6
42. Roy S, Patel D, Khanna S, et al. Transcriptome-wide analysis of blood vessels laser captured from human skin and chronic wound-edge tissue. Proc Natl Acad Sci USA 2007;104:14472–7
43. Gillan L, Matei D, Fishman DA, et al. Periostin secreted by epithelial ovarian carcinoma is a ligand for alpha(V)beta(3) and alpha(V)beta(5) integrins and promotes cell motility. Cancer Res 2002;62:5358–64
44. Sun F, Hu Q, Zhu Y, et al. High-level expression of periostin is significantly correlated with tumor angiogenesis in prostate cancer. Int J Clin Exp Pathol 2018;11:1569–74
45. Shao R1, Bao S, Bai X, et al. Acquired expression of periostin by human breast cancers promotes tumor angiogenesis through up-regulation of vascular endothelial growth factor receptor 2 expression. Mol Cell Biol 2004;24:3992–4003
46. Formolo CA, Williams R, Gordish-Dressman H, et al. Secretome signature of invasive glioblastoma multiforme. J Proteome Res 2011;10:3149–59
47. Zinn PO, Majadan B, Sathyan P, et al. Radiogenomic mapping of edema/cellular invasion MRI-phenotypes in glioblastoma multiforme. PLoS One 2011;6:e25451
48. Kulla A, Liigant A, Piirsoo A, et al. Tenascin expression patterns and cells of monocyte lineage: Relationship in human gliomas. Mod Pathol 2000;13:56–67
49. Behrem S, Zarkovic K, Eskinja N, et al. Distribution pattern of tenascin-C in glioblastoma: Correlation with angiogenesis and tumor cell proliferation. Pathol Oncol Res 2005;11:229–35
50. Maris C, Rorive S, Sandras F, et al. Tenascin-C expression relates to clinicopathological features in pilocytic and diffuse astrocytomas. Neuropathol Appl Neurobiol 2008;34:316–29
51. Zagzag D, Friedlander DR, Miller DC, et al. Tenascin expression in astrocytomas correlates with angiogenesis. Cancer Res 1995;55: 907–14
52. Leins A, Riva P, Lindstedt R, et al. Expression of tenascin-C in various human brain tumors and its relevance for survival in patients with astrocytoma. Cancer 2003;98:2430–9
53. Zagzag D, Shiff B, Jallo GI, et al. Tenascin-C promotes microvascular cell migration and phosphorylation of focal adhesion kinase. Cancer Res 2002;62:2660–8
54. Zagzag D, Friedlander DR, Dosik J, et al. Tenascin-C expression by angiogenic vessels in human astrocytomas and by human brain endothelial cells in vitro. Cancer Res 1996;56:182–9
55. Midwood KS, Hussenet T, Langlois B, et al. Advances in tenascin-C biology. Cell Mol Life Sci 2011;68:3175–99
56. Weis SM, Cheresh DA. alphav integrins in angiogenesis and cancer. Cold Spring Harb Perspect Med 2011;1:a006478
57. Reardon DA, Zalutsky MR, Bigner DD. Antitenascin-C monoclonal antibody radioimmunotherapy for malignant glioma patients. Expert Rev Anticancer Ther 2007;7:675–87
58. Seker A, Yildirim O, Kurtkaya O, et al. Expression of integrins in cerebral arteriovenous and cavernous malformations. Neurosurgery 2006;58: 159–68. discussion 159–68
59. Schnell O, Krebs B, Wagner E, et al. Expression of integrin alphavbeta3 in gliomas correlates with tumor grade and is not restricted to tumor vasculature. Brain Pathol 2008;18:378–86
60. D'Abaco GM, Kaye AH. Integrins: Molecular determinants of glioma invasion. J Clin Neurosci 2007;14:1041–8
61. Hashimoto T, Lawton MT, Wen G, et al. Gene microarray analysis of human brain arteriovenous malformations. Neurosurgery 2004;54:410–23. discussion 23–5
62. Liang X, Shen D, Huang Y, et al. Molecular pathology and CXCR4 expression in surgically excised retinal hemangioblastomas associated with von Hippel-Lindau disease. Ophthalmology 2007;114:147–56
63. Takagi Y, Kikuta K, Moriwaki T, et al. Expression of thioredoxin-1 and hypoxia inducible factor-1alpha in cerebral arteriovenous malformations: Possible role of redox regulatory factor in neoangiogenic property. Surg Neurol Int 2011;2:61
64. Zhu Y, Wu Q, Fass M, et al. In vitro characterization of the angiogenic phenotype and genotype of the endothelia derived from sporadic cerebral cavernous malformations. Neurosurgery 2011;69:722–31. discussion 31–2
65. Shimamura M, Taniyama Y, Katsuragi N, et al. Role of central nervous system periostin in cerebral ischemia. Stroke 2012;43:1108–14
66. Ouyang G, Liu M, Ruan K, et al. Upregulated expression of periostin by hypoxia in non-small-cell lung cancer cells promotes cell survival via the Akt/PKB pathway. Cancer Lett 2009;281:213–9
67. Bouwens van der Vlis TAM, Kros JM, Mustafa DAM, et al. The complement system in glioblastoma multiforme. Acta Neuropathol Commun 2018;6:91
68. Khurana S, Schouteden S, Manesia JK, et al. Outside-in integrin signalling regulates haematopoietic stem cell function via Periostin-Itgav axis. Nat Commun 2016;7:13500
69. Zhou W, Ke SQ, Huang Z, et al. Periostin secreted by glioblastoma stem cells recruits M2 tumour-associated macrophages and promotes malignant growth. Nat Cell Biol 2015;17:170–82
70. Mikheev AM, Mikheeva SA, Trister AD, et al. Periostin is a novel therapeutic target that predicts and regulates glioma malignancy. Neuro Oncol 2015;17:372–82

CHAPTER 5

SUMMARY

The overall aim of our project was to elucidate the role of both the tumor microenvironment and macro-environment (the blood) in glioblastoma (GBM) neovascularization, with a focus on circulating angiogenic cells (CACs). More specifically, we aimed to answer the following questions:

1) Which subtypes of CACs are mainly involved in GBM neovascularization compared to regenerative neovascularization (as represented by myocardial infarction, MI; Chapter 3)?

2) Do qualitative (gene expression) differences exist within CAC subsets between GBM and regenerative (MI) and developmental (fetal) neovascularization. If so, which (treatment-targetable) genes are predominantly involved (Chapter 4)?

3) What is the cellular source and the role of the matricellular protein periostin in GBM vessel formation (Chapter 5)?

To answer questions 1 and 2, we formulated the additional research question:

4) How can CAC subsets be best identified, characterized and isolated using Fluorescence-Activated Cell Sorting (FACS; Chapter 2)?

Since the definitions of "endothelial progenitor cells" EPCs and CACs are used promiscuously and confusingly in the literature, we will explain what we consider to be CACs versus EPCs for this chapter. In our technical paper [1], we used the term EPC as an overarching denotation describing both circulating pro-angiogenic cell types able to fully differentiate into mature endothelial cells and partake in the vessel wall and circulating cell types without endothelial differentiation capacity, stimulating target tissue neovascularization by paracrine pro-angiogenic factor secretion. The term EPC is widely used in the literature in this fashion. However, using this definition of 'EPC' does not allow for a separation between cells able as opposed to unable to differentiate into endothelial cells. For that reason, we later moved to a stricter definition of EPC, more in line with recent literature: cells able to fully differentiate into endothelial cells only (thus driving actual vasculogenesis), while we reserved the overarching term CAC to include the kaleidoscopic mixture of all cell types able to stimulate neovascularization in target tissue, regardless of their lineage or endothelial differentiation capacity. In the Introduction chapter, we furthermore specified a CAC subset with hematopoietic origin as 'pro-angiogenic hematopoietic cells' (PAHCs), which are usually acting by paracrine factor secretion to stimulate neovascularization (and therefore do not fit the definition of EPC used here). That having said, cells tend to not stick to the delimited functions we want to impose on them for the sake of categorization: there is large overlap between the groups. As an example: in the Introduction chapter we discovered that (the progeny of) hematopoietic stem cells (HSCs) usually stimulate target tissue neovascularization through paracrine factor secretion as bystander cells, but in the right circumstances can and will fully differentiate into endothelial cells

and partake in the target tissue vessel wall to an impressive degree (thus in most circumstances acting as PAHCs and in some as EPCs).
For our experiments, we included blood from treatment-naïve glioblastoma (GBM) patients, using healthy subjects (HC), acute myocardial infarction (MI) patients and umbilical cord blood (UCB) as controls representing steady state adult, acute ischemia and developmental CAC-induced neovascularization respectively. With this approach, we intended to unravel GBM-specific alterations in CAC-induced neovascularization. Pinpointing specific changes in GBM CAC-induced neovascularization may allow for the development of tailor-made therapies targeting GBM-specific vessel formation mediated by CACs.

CHAPTER 2: IMPROVING THE CHARACTERIZATION OF ENDOTHELIAL PROGENITOR CELL SUBSETS BY AN OPTIMIZED FACS PROTOCOL

To investigate the role of CACs in any disease, their careful and reliable characterization and isolation from the circulation are primary prerequisites. To meet these prerequisites, we developed an improved Fluorescence-Activated Cell Sorting (FACS)-based protocol for the simultaneous characterization and isolation of the CAC subset of hematopoietic progenitor cells (HPCs) and of circulating endothelial cells (CECs) [1]. We succeeded in establishing a better definition of HPCs based on selection of the lympho/mono gate in the FSC/SSC plot and gating for dim expression of CD45. HPCs were thus defined as CD34+CD133+/-$CD45^{dim}$ lympho/mono. By combining CD34, CD133, CD45 and c-kit staining, we discovered 4 new HPC subgroups in UCB and adult blood: $CD133^{neg}$c-kit^{high}, $CD133^{low}$c-$kit^{med/high}$, $CD133^{high}$c-$kit^{med/high}$ and $CD133^{high}$c-$kit^{neg/low}$, the latter only present in adult blood, not in UCB. We also found a very small subset of HPCs expressing KDR (0.0 - 0.3% of HPCs), indicating that the commonly used definition of circulating 'EPC' in the literature (i.e. $CD34^{+}CD133^{+}KDR^{+}$ cells) could be a very rare subset of HPCs.

In contrast to the assumption that CECs are apoptotic endothelial cells released into the circulation upon vascular damage, we discovered a fully viable subset of CECs. Viable CECs expressed c-kit more often than apoptotic CECs. Phenotypic FACS characterization of HPCs, CECs and outgrowth endothelial cells (OECs) revealed that marker expression of early passage OECs and HUVECs is almost identical and highly comparable to CECs, while HPCs exhibit essentially different expression of phenotypic markers than OECs, HUVECs and CECs.
Moreover, CECs, OECs and HUVECs have comparably high gene expression levels of angiogenic factors such as *APLN, VEGFA, PDGFB, FGF* and *KITL* (low expression in HPCs).
We thus hypothesized that OECs are derived from viable c-kit^{+} CECs and that viable CECs should be considered as EPCs, not merely as a passive marker of vascular damage. Determining the OEC formation capacity of c-kit^{+} versus c-kit^{-} viable CECs would be required to prove our hypothesis. However, we and others were unable to grow OECs from exclusively FACS-isolated cells, be it CECs or PBMCs.

Future directions of research could include investigating the functional meaning of the newly described subpopulations of HPCs based on variable expression of CD133 and c-kit, as well as the functional meaning of viable c-kit$^+$ CECs.

CHAPTER 3: CIRCULATING PROANGIOGENIC CELLS AND PROTEINS IN PATIENTS WITH GLIOMA AND ACUTE MYOCARDIAL INFARCTION: DIFFERENCES IN NEOVASCULARIZATION BETWEEN NEOPLASIA AND TISSUE REGENERATION

We next investigated which subtypes of CACs were mainly involved in GBM as compared to MI neovascularization [2]. Healthy adults and patients with grade II/III astrocytoma were included as controls. CAC subsets were picked based on different combinations of 3 to 4 markers (CD34, KDR, CD133, CD45) and their involvement in neovascularization in ischemic disease and/or cancer as previously described in the literature. HPCs (CD34$^+$CD133$^+$CD45^{dim} lympho/mono), CECs (CD34$^+$KDR$^+$CD45$^-$), KDR$^+$CD133$^+$*(CD34$^-$)* cells, CD34$^+$(CD133$^-$KDR$^-$) and KDR$^+$(CD34$^-$CD133$^-$) cells were included in the study. In addition, we measured the levels of 21 plasma factors involved in the mobilization, chemoattraction and homing of CACs, as well as pro-angiogenic factors secreted by CACs.

Although in both contexts all CAC subsets measured were elevated compared to HC, specific subsets were prominently increased in GBM: KDR$^+$(CD34$^-$CD133$^-$) and HPCs, in contrast to other subsets in MI: CD133$^+$(KDR$^-$CD34$^-$) and KDR$^+$CD133$^+$*(CD34$^-$)*. CAC frequencies were similar between patients with grade II/III astrocytoma and healthy controls.

Both in GBM and MI patients, the factors MMP9 (mobilization and tissue invasion of CACs), HGF and vWF (angiogenic factors) were elevated in plasma relative to HC. VCAM1 (angiogenesis & chemoattraction of CACs) was specifically elevated in GBM, while angiogenin and tenascin-c (angiogenesis) were specifically elevated in MI. The concentrations of plasma factors in astrocytoma grade II and grade III (AII/III) patients were overall similar to HC. A strong positive correlation was found between plasma MMP9 and HPC levels, and between plasma VCAM1 and KDR$^+$ cell levels in GBM patients. Since plasma MMP9 can mobilize HPCs from the bone marrow, this positive correlation could imply causation. In MI patients, tenascin-c concentration correlated positively with both KDR$^+$CD133$^+$ levels and CD133$^+$ levels.

These findings indicate that although neovascularization induced by CACs is paramount in both GBM (malignant high-grade neoplasia) and MI (acute ischemia), each elicits a disease-specific pattern of elevation of CAC subsets and CAC-related plasma factors. Grade II and III astrocytoma patients had equivalent levels of CACs and plasma factors as HC, suggesting that the role of CACs becomes pronounced in glioma when the amount of tumor neovascularization increases. We propose that disease-specific, tailor-made therapies targeting CACs can optimize treatment outcome in GBM and MI patients.

CHAPTER 4: CIRCULATING ANGIOGENIC CELLS IN GLIOBLASTOMA: TOWARDS DEFINING CRUCIAL FUNCTIONAL DIFFERENCES IN CAC-INDUCED NEOPLASTIC VERSUS REACTIVE NEOVASCULARIZATION

After having established numerical differences in CAC subsets, we next examined potential qualitative differences within CACs between GBM and MI patients [3]. CACs from umbilical cord (representing developmental neovascularization) and healthy subjects served as controls. Expression analysis of a panel of 48 genes selected based on their function in CAC mobilization, chemo-attraction, homing, tissue invasion and angiogenesis was performed in 3 CAC subtypes (HPCs, $CD34^{+}KDR^{-}CD133^{-}$ cells, $KDR^{+}CD34^{-}CD133^{-}$ cells) using CECs and peripheral blood mononuclear cells (PBMCs) as controls. This revealed a unique and distinct pattern of expression in each disease state. Compared to MI, GBM CACs showed higher expression of chemotactic receptors (esp. *CXCR4* and *CCR2*) and integrins (*ITGA5* and *ITGA6*); pro-angiogenic factors (esp. *KITL*, *CXCL12* and *JAG1*) and growth factor receptors (e.g. *IGF1R*, *TGFBR2*) and the matricellular factor *POSTN*. These findings suggest that CAC-mediated neovascularization in GBM is characterized by more efficient CAC homing to target tissue and a more potent pro-angiogenic response than in reactive tissue repair in MI. A strong positive correlation between plasma MMP9 levels and expression of *CXCR4* in HPCs was found in GBM patients, illustrating that GBM tissue (the source of elevated MMP9 levels) appears capable of pre-programming circulating angiogenic cells to home more efficiently to tumor tissue. GBM, though non-metastatic, should thus be considered a systemic disease requiring systemic treatment.

Our study is the first to show that GBM CACs are qualitatively different from non-neoplastic CACs (i.e. in reactive (myocardial infarction), developmental (umbilical cord blood) and steady-state adult (healthy control) neovascularization). Our findings can aid in selecting targets for therapeutic strategies acting against GBM-specific CACs.

CHAPTER 5: PERIOSTIN IS EXPRESSED BY PERICYTES AND IS CRUCIAL FOR ANGIOGENESIS IN GLIOMA

In a previous study [4] we discovered periostin protein was elevated in glioblastoma perivascular tissue. In our current project, we found periostin gene (*POSTN*) gene expression was increased in GBM CACs ($CD34^{+}$) compared to MI, HC and UCB CACs [3], again highlighting the role of this matricellular protein in glioblastoma neovascularization.

We aimed to identify the cellular source of periostin expression in human gliomas and to clarify the role of periostin in an *in vitro* model of angiogenesis [5]. Periostin gene and protein expression was increased in tissue of both glioblastoma (grade IV glioma) and pilocytic astrocytoma (grade I glioma), but not in grade II and III gliomas (where expression was comparable to normal brain samples), corresponding to the degree of microvascular proliferation present in gliomas. Immunohistochemistry confirmed the presence of periostin protein in the perivascular tissue of glomeruloid and hypertrophic blood vessels in glioblastoma and pilocytic astrocytomas.

To determine the cellular source of periostin in gliomas, we set up RNA *in situ* hybridization (ISH) and double labelling immunohistochemistry (IHC) experiments, which indicated periostin protein expression co-localized with PDGFRβ$^+$ perivascular cells (pericytes). Periostin was neither expressed by putative glioblastoma stem cells (Sox-2$^+$ and/or Olig-2$^+$ tumor cells), nor by CD31$^+$ endothelial cells or GFAP$^+$ cells (astrocytes and GBM tumor cells).

In vitro studies confirmed that brain pericytes were the main source of periostin (HUVECs did not produce periostin, astrocytes at very low levels). Furthermore, pericytes increased production of periostin when glioblastoma (U87) cell conditioned medium (CM) or cell lysate was added to cell cultures. Measures of angiogenesis in a 3D angiogenesis model coculturing HUVECs and pericytes were greatly enhanced after the addition of GBM U87 CM. Silencing *POSTN* in pericytes led to an attenuation of angiogenesis in the same model. The addition of GBM U87 CM could only partially save the effect of pericytic *POSTN* silencing on measures of angiogenesis. The level of angiogenesis remained strikingly decreased compared with the normal pericytes with added GBM U87 CM.

To conclude, periostin is highly expressed by PDGFRβ$^+$ pericytes in cerebral lesions with abundant angiogenic activity and vascular remodeling (glioblastoma, pilocytic astrocytoma), not in grade II/III gliomas where neovascularization is present at low to normal levels. From the sum of our *in vitro* experiments it can be surmised that the angiogenesis-boosting effect of the GBM secretome is predominantly mediated by increasing the expression of periostin in pericytes.

NEDERLANDSE SAMENVATTING

Middels onze studies wilden we de rol verhelderen van zowel de tumor micro-omgeving als de macro-omgeving (het bloed) in de vaatnieuwvorming van glioblastomen (GBM), met een focus op circulerende angiogene cellen (CACs). Meer in het bijzonder richtten we ons op het beantwoorden van de volgende vragen:

1) Welke subtypen CACs zijn vooral betrokken bij de vaatnieuwvorming van GBM vergeleken met regeneratieve vaatnieuwvorming (myocardinfarct, MI; Hoofdstuk 3)?

2) Bestaan er kwalitatieve verschillen tussen CAC-subsets in vaatnieuwvorming in het kader van GBM, regeneratie (MI) en ontwikkeling (navelstrengbloed, UCB), gemeten middels genexpressie? Zo ja, welke genen spelen met name een rol (Hoofdstuk 4)?

3) Wat is de cellulaire bron en de rol van het matricellulaire eiwit periostine in GBM-vaatnieuwvorming (Hoofdstuk 5)?

Om vraag 1 en 2 te beantwoorden formuleerden we de aanvullende vraag:

4) Hoe kunnen CAC-subsets het best geïdentificeerd, gekarakteriseerd en geïsoleerd worden middels Fluorescence-Activated Cell Sorting (FACS; Hoofdstuk 2)?

Daar de definitie van de celtypen 'endotheliale voorlopercellen' (EPCs) en CACs in de literatuur sterk varieert en de termen tot verwarrends toe door elkaar gebruikt worden zullen we starten met de door ons gebruikte definitie van beide celtypen voor dit hoofdstuk. In onze technische publicatie [1] gebruikten we de term 'EPCs' als een overkoepelende naam voor circulerende pro-angiogene cellen die in staat zijn te differentiëren naar volwassen endotheelcellen alsmede voor cellen zonder endotheliaal differentiatievermogen. Het laatste type stimuleert vaatnieuwvorming middels het aanzwengelen van de angiogenese door secretie van pro-angiogene factoren en is perivasculair gesitueerd. In de literatuur is deze allesomvattende definitie van 'EPCs' wijdverbreid. Het nadeel hiervan is dat een onderscheid tussen beide type cellen niet evident is. Om deze reden hanteerden we later een striktere definitie van EPCs, die meer in lijn is met de recentere literatuur: namelijk uitsluitend celtypen die in staat zijn volledig te differentiëren naar endotheelcellen en te integreren in de bloedvatwand (daarmee in staat tot daadwerkelijke vasculogenese). We reserveerden de term CACs voor het caleidoscopische mengsel van alle type circulerende cellen die de vaatnieuwvorming stimuleren in het doelwitweefsel, ongeacht hun 'lineage' of vermogen te differentiëren tot endotheelcellen. In **hoofdstuk 1** (Introductie) beschreven we een CAC-subtype van hematopoietische origine, genaamd 'pro-angiogene hematopoietische cellen' (PAHCs). Celtypen uit deze groep maken veelal gebruik van het paracriene pro-angiogene mechanisme zonder in staat

te zijn tot vasculogenese. Zij voldoen hiermee niet aan de definitie 'EPCs'. Echter, cellen hebben niet de neiging zich te houden aan door ons opgestelde definities voor het gemak van classificatie en overzicht: er is grote overlap tussen beide groepen. Als voorbeeld zagen we in **hoofdstuk 1** (Introductie) dat HSCs veelal de vaatnieuwvorming bevorderen door paracrien de angiogenese te stimuleren, maar onder de juiste omstandigheden tevens differentiëren naar endotheelcellen en in indrukwekkende mate integreren in nieuwgevormde bloedvaten. HSCs handelen hiermee veelal als PAHCs, maar soms als EPCs.

Voor onze experimenten includeerden we bloed van patiënten met een glioblastoom voordat behandeling was ingezet. Als controles gebruikten we bloed van gezonde volwassenen (HC), patiënten met een myocardinfarct (MI) en navelstrengbloed (UCB). Respectievelijk dienden deze controles als reflectie van vaatnieuwvorming in gezonde volwassenen ('steady state'), in acute ischemie en tijdens de foetale ontwikkeling. Met deze insteek was onze intentie om specifieke veranderingen in CAC-gemedieerde vaatnieuwvorming in GBM-patiënten te ontdekken. Het vinden van GBM-specifieke veranderingen in CAC-gemedieerde vaatnieuwvorming kan helpen bij het ontwikkelen van ziekte-specifieke behandelingen gericht op bloedvatvorming door CACs.

Voorwaarden voor het bestuderen van de rol van CACs in om het even welke aandoening zijn een betrouwbare karakterisering en isolatie uit de circulatie. Om aan deze voorwaarden te voldoen ontwikkelden we een "Fluorescence-Activated Cell Sorting" (FACS)-protocol voor de gelijktijdige karakterisering en isolatie van de volgende CAC-subsets: hematopoietische voorlopercellen (HPCs) en circulerende endotheelcellen (CECs). De resultaten zijn beschreven in **hoofdstuk 2** [1]. Middels dit geoptimaliseerde protocol zijn we erin geslaagd een betere definitie van HPCs te formuleren, gebaseerd op selectie van de lymfo/mono gate in de FSC/SSC grafiek, alsmede door te gaten op een zwakke expressie van CD45. Zodoende definieerden we HPCs als $CD34^{+}CD133^{+/-}CD45^{dim}$ lymfo/mono. Voorts ontdekten we door het combineren van de markers CD34, CD133, CD45 en c-kit 4 nieuwe subtypen HPCs in navelstrengbloed en volwassen bloed: $CD133^{-}$c-kit^{high}, $CD133^{low}$c-$kit^{med/high}$, $CD133^{high}$c-$kit^{med/high}$ en $CD133^{high}$c-$kit^{neg/low}$; de laatste was slechts aanwezig in volwassen bloed, niet in navelstrengbloed. Daarnaast bracht een zeer lage frequentie HPCs de endotheelcelmarker KDR tot expressie (0.0-0.3% van de totale HPCs), waaruit blijkt dat de veel gebruikte definitie van circulerende 'EPCs' in de literatuur (namelijk $CD34^{+}CD133^{+}KDR^{+}$ cellen) een zeldzaam subtype HPCs kan betreffen.

In de literatuur worden CECs vaak beschreven als apoptotische endotheelcellen, die zodoende slechts als afspiegeling zouden dienen van de mate van vaatschade in het organisme. Wij vonden echter dat een aanzienlijk deel van de CECs levend was. Levende CECs brachten bovendien vaker c-kit tot expressie dan apoptotische CECs. Verdere fenotypische karakterisering middels FACS van vroege passage 'outgrowth endothelial cells' (OECs) en HUVECs toonde een vrijwel identiek patroon, dat bovendien overkwam met dat van CECs. HPCs echter waren fenotypisch sterk

afwijkend van OECs, HUVECs en CECs. De genexpressie van angiogene factoren zoals *APLN*, *VEGFA*, *PDGFB*, *FGF* en *KITL* was wederom vergelijkbaar in OECs, HUVECs en CECs, in tegenstelling tot HPCs.

Gebaseerd op deze data formuleren we de hypothese dat OECs ontstaan uit levende, c-kit$^+$ CECs en dat CECs als zodanig beschouwd dienen te worden als daadwerkelijke EPCs, niet slechts als een passieve indicator van vaatschade. De isolatie van levende c-kit$^+$ versus c-kit$^-$ CECs en het vaststellen van het vermogen van deze subtypen CECs om OECs te generen zou noodzakelijk zijn om deze hypothese te bewijzen. Zowel wijzelf als andere groepen zijn er echter niet in geslaagd om OECs te kweken uit cellen die uitsluitend middels FACS geïsoleerd zijn.
Verder toekomstig onderzoek kan zich richten op het onthullen van de functionele betekenis van de door ons beschreven subpopulaties HPCs gebaseerd op variabele expressie van CD133 en c-kit, alsmede op de functionele betekenis van levende, c-kit$^+$ CECs.

Na het optimaliseren van ons protocol voor de identificatie en isolatie van CACs onderzochten we welke CAC-subtypen voornamelijk een rol speelden in de vaatnieuwvorming in GBM vergeleken met MI (**hoofdstuk 3**) [2]. Gezonde volwassenen en patiënten met een graad II/III astrocytoom dienden als controles. De CAC-subsets werden geselecteerd op basis van verschillende combinaties van 3 tot 4 veel beschreven markers (CD34, KDR, CD133 en CD45) en op basis van beschikbare literatuur over CAC-subtypen in neoplasie en ischemie. We analyseerden de frequentie van HPCs (CD34$^+$CD133$^+$CD45^{dim} lymfo/mono gate), CECs (CD34$^+$KDR$^+$CD45$^-$), KDR$^+$CD133$^+$(*CD34*$^-$), CD34$^+$(*CD133*$^-$*KDR*$^-$) en KDR$^+$(*CD34*$^-$*CD133*$^-$) cellen. Hiernaast analyseerden we de concentratie van 21 plasmafactoren die een rol spelen in CAC-mobilisatie, -chemoattractie, -homing en -angiogenese.

De frequentie van alle CAC-subsets was verhoogd in zowel GBM als MI vergeleken met gezonde controles. Echter, specifieke subtypen van CACs waren in het bijzonder aanwezig in het bloed van GBM-patiënten: KDR$^+$(*CD34*$^-$*CD133*$^-$) en HPCs. Daarentegen waren juist CD133$^+$(*KDR*$^-$*CD34*$^-$) en KDR$^+$CD133$^+$(*CD34*$^-$) cellen sterker verhoogd in MI patiënten. De CAC-frequenties waren gelijk tussen de patiënten met graad II/III astrocytomen en gezonde controles.

Wat betreft plasmafactoren waren zowel MMP9 (mobilisatie van CACs en weefselinvasie), HGF en vWF (pro-angiogenese) in concentratie verhoogd in GBM en MI patiënten vergeleken met gezonde controles. VCAM1 (angiogenese en chemoattractie) was uitsluitend verhoogd in GBM-patiënten, terwijl er een specifieke stijging was van angiogenine en tenascine-c in MI-patiënten. Er werd geen verschil gezien in de concentratie van de plasmafactoren tussen graad II/III gliomen en gezonde controles. De MMP9 concentratie correleerde positief en sterk met de HPC-frequentie in GBM-patiënten. Gezien MMP9 tot mobilisatie kan leiden van HPCs betreft dit een mogelijk causaal verband. In MI-patiënten werd een positieve correlatie gezien tussen de plasmaconcentratie van tenascine-c en de frequentie van zowel KDR$^+$CD133$^+$ als CD133$^+$ cellen.

Onze bevindingen duiden erop dat GBM (hooggradige neoplasie) en MI (acute ischemie) ieder een unieke respons geven wat betreft de frequentie van specifieke subsets van CACs, alsmede van bij CAC betrokken plasma factoren. Dit ondanks dat in beide ziektebeelden een cruciale rol is weggelegd voor neovascularisatie geïnduceerd door CACs. Graad II/III astrocytoom patiënten hadden vergelijkbare niveaus van CACs en plasmafactoren als gezonde controles, waaruit blijkt dat de rol van CACs toeneemt met het vaatrijker worden van gliomen bij een stijgende tumorgraad.

We stellen derhalve op basis van onze bevindingen voor dat ziekte-specifieke behandelingen gericht op CACs de uitkomst kunnen verbeteren van patiënten met GBM en MI.

Na het vaststellen van numerieke verschillen in CAC-subsets onderzochten we de aanwezigheid van kwalitatieve verschillen in CACs tussen GBM- en MI-patiënten (**hoofdstuk 4**) [3]. CACs uit navelstrengbloed en van gezonde proefpersonen dienden als controles. Navelstrengbloed werd geïncludeerd om een indruk te krijgen van CACs gedurende vaatnieuwvorming tijdens de foetale ontwikkeling. We selecteerden 48 genen voor genexpressieanalyse op basis van hun functie in de mobilisatie, chemoattractie, homing, weefselinvasie en angiogenese van en door CACs. Genexpressieanalyse werd verricht in 3 CAC subtypen (HPCs, $CD34^{+}KDR^{-}CD133^{-}$ cells, $KDR^{+}CD34^{-}CD133^{-}$ cellen). CECs en PBMCs dienden als controles. Voor elk ziektebeeld alsmede voor navelstrengbloed bleek het genexpressieprofiel van CACs zeer onderscheidend. Vergeleken met MI vertoonden GBM CACs een hogere expressie van chemotactische receptoren (in het bijzonder *CXCR4* en *CCR2*), integrines (*ITGA5* en *ITGA6*), pro-angiogene factoren (in het bijzonder *KITL*, *CXCL12* en *JAG1*), groeifactorreceptoren (bijvoorbeeld *IGF1R*, *TGFBR2*) en van de matricellulaire factor *POSTN*. Deze bevindingen suggereren dat CAC-gemedieerde vaatnieuwvorming in GBM wordt gekenmerkt door een efficiëntere homing van CACs naar het weefsel en een krachtigere pro-angiogene respons dan bij myocardischemie. In GBM-patiënten bestond een sterke positieve correlatie tussen plasma MMP9 concentraties en expressie van *CXCR4* in HPCs. Dit illustreert dat GBM-weefsel (de bron van de verhoogde MMP9 plasmaconcentratie) in staat lijkt om CACs voor te programmeren in het bloed om efficiënter naar tumorweefsel te migreren en aldaar een sterkere pro-angiogene respons op te wekken. Ondanks dat GBM niet uitzaait dient deze vorm van kanker daarom toch beschouwd te worden als een systemische ziekte, die een systemische behandeling behoeft.

Onze studie toont aan dat GBM CACs kwalitatief verschillen van niet-neoplastische CACs (in reactieve/ischemische, ontwikkelings- en 'steady-state' volwassen vaatnieuwvorming). Onze bevindingen kunnen helpen bij het ontwikkelen van therapeutische strategieën die zich richten op GBM-specifieke CACs.

In **hoofdstuk 5** beschrijven we de rol van periostine in vaatnieuwvorming in glioblastomen [5]. In een eerdere studie [2] ontdekten we dat het matricellulaire eiwit periostine verhoogd aanwezig was

in het perivasculaire weefsel van glioblastomen. In ons huidige project vonden we een verhoogde periostine (*POSTN*) genexpressie in circulerende angiogene cellen ($CD34^+$) van patiënten met een glioblastoom vergeleken met controles. Deze bevinding benadrukt opnieuw de rol van dit matricellulaire eiwit in de vaatnieuwvorming van glioblastomen.

In de huidige studie onderzochten we de cellulaire bron van periostine-expressie in glioblastomen, alsmede de rol van periostine in vaatnieuwvorming. Periostine gen- en eiwitexpressie waren verhoogd in weefsel van zowel glioblastomen (graad IV gliomen) als pilocytaire astrocytomen (graad I gliomen). De expressie was echter vergelijkbaar tussen graad II/III gliomen en normaal hersenweefsel. Dit suggereert dat verhoogde expressie van periostine uitsluitend voorkomt in gliomen met microvasculaire proliferatie. Immunohistochemie bevestigde de aanwezigheid van periostine-eiwit in het perivasculaire weefsel van glomeruloïde en hypertrofische bloedvaten in glioblastomen en pilocytaire astrocytomen.

Om de cellulaire bron van periostine in gliomen te bepalen, verrichten we RNA *in situ*-hybridisatie (ISH) en dubbel-kleuring immunohistochemie (IHC). Periostine eiwitexpressie co-gelokaliseerde met pericyten ($PDGFR\beta^+$ perivasculaire cellen). Periostine werd niet tot expressie gebracht door glioblastoom stamcellen ($Sox\text{-}2^+$ en/ of $Olig\text{-}2^+$ tumorcellen), noch door $CD31^+$ endotheelcellen of $GFAP^+$ cellen (astrocyten en GBM-tumorcellen). *In vitro* onderzoeken bevestigden dat humane brein pericyten de belangrijkste bron van periostine waren (HUVECs produceerden geen periostine, astrocyten in zeer lage concentraties). Bovendien verhoogden pericyten de productie van periostine wanneer GBM (U87) geconditioneerd medium of cel-lysaat werd toegevoegd aan celkweken.

Voorts onderzochten we of periostine de mate van angiogenese beïnvloedt door gebruik te maken van een 3D-angiogenese-model bestaande uit co-culturen van HUVECs en humane brein pericyten. De mate van angiogenese nam significant toe na additie van GBM (U87) geconditioneerd medium. 'Silencing' van *POSTN* in pericyten zorgde daarentegen voor een flinke afname van alle maten van angiogenese in hetzelfde model. De toevoeging van GBM (U87) geconditioneerd medium kon deze afname van angiogenese bij pericytaire 'silencing' van *POSTN* beperkt compenseren. De mate van angiogenese bleef sterk verlaagd vergeleken met normale pericyten en additie van GBM (U87) geconditioneerd medium.

Concluderend tonen onze bevindingen dat periostine verhoogd tot expressie wordt gebracht door pericyten in cerebrale neoplasmata gekenmerkt door veel vaatnieuwvorming en vasculaire omvorming (glioblastoom, pilocytair astrocytoom), niet in graad II/III gliomen, waarin neovascularisatie nog beperkt aanwezig is. Uit de som van onze *in vitro* experimenten blijkt dat het stimulerende effect van het GBM-secretoom op de angiogenese hoofdzakelijk wordt gemedieerd door de expressie van periostine in pericyten te verhogen.

REFERENCES

1. Huizer, K., et al., *Improving the characterization of endothelial progenitor cell subsets by an optimized FACS protocol.* PLoS One, 2017. **12**(9): p. e0184895.
2. Huizer, K., et al., *Circulating Proangiogenic Cells and Proteins in Patients with Glioma and Acute Myocardial Infarction: Differences in Neovascularization between Neoplasia and Tissue Regeneration.* J Oncol, 2019. **2019**: p. 3560830.
3. Huizer, K., et al., *Circulating Angiogenic Cells in Glioblastoma: Towards Defining Crucial Functional Differences in CAC-induced Neoplastic versus Reactive Neovascularization.* Neuro-Oncology Advances, 2020. **2**(1): p. 1-12.
4. Mustafa, D.A., et al., *A proteome comparison between physiological angiogenesis and angiogenesis in glioblastoma.* Mol Cell Proteomics, 2012. **11**(6): p. M111 008466.
5. Huizer, K., et al., *Periostin Is Expressed by Pericytes and Is Crucial for Angiogenesis in Glioma.* Journal of Neuropathology & Experimental Neurology, 2020. **79**(8): p. 863-872.

PORTFOLIO

Erasmus MC
Universitair Medisch Centrum Rotterdam

PhD Portfolio

Summary of PhD training and teaching

Name PhD student: Karin Huizer	PhD period: 2011 – 2020
Erasmus MC Department: Pathology	Promotor: prof. dr. J.M. Kros
Research School: MGC	Supervisor: prof. dr. J.M. Kros, dr. D.A. Mustafa

1. PhD training

(total 30 ECTS: courses, seminars etc, teaching)	**Year**	**Workload**	
		Hours	**ECTS**
General courses			
- Research Management for PhD students (MolMed)	2011	28	1
- Course Molecular Diagnostics (MolMed)	2011	28	1
- Biomedical Research Techniques (MolMed)	2012	44.8	1.6
- Biomedical English Writing and Communication	2012	56	2
- Coding in 'PALGA' course	2015	10	0.4
- BOP course Immunology	2015	28	1
- BOP course Molecular Pathology	2015	28	1
- BOP course Oncology	2016	28	1
- BOP course Pathophysiology	2016	28	1
- Coursera course Systems Biology and Biotechnology	2018	112	4
Total:		390.8	14
Specific courses (e.g. Research school, Medical Training)			
- Confocal Microscopy (Alex Nigg)	2011	8	0.3
- In vivo imaging	2012	50.4	1.8
- RT-PCR Workshop Life Technologies	2012	9	0.3
Total:		67.4	2.4
Seminars and workshops			
- PhD Day (Workshops: "Portfolio and PhD training", "There's no excuse for writing unreadable scientific articles"	2011	8	0.3

Presentations			
- poster presentation ECNP	2012	42	1.5
- Research meeting Obstetrics & Gynecology	2012	42	1.5
- presentation JNI meeting	2012	42	1.5
- presentation Neuro-Oncology meeting	2012	42	1.5
- presentation JNI meeting	2013	42	1.5
- presentation Neuro-Oncology meeting	2013	42	1.5
- poster presentation SNO conference	2014	42	1.5
- presentation 'Pathologendagen'	2015	42	1.5
Total:		328	12
(Inter)national conferences			
- ECNP	2012	42	1.5
- SNO	2014	42	1.5
- Pathologendagen	2015	42	1.5
Total:		126	4.5
Other			
- seminar series: JNI meetings	2011-2014	150	5.4
- seminar series: Neuro-Oncology meetings	2011-2014	100	3.6
Total:		250	9
2. Teaching			
	Year	**Workload**	
		Hours	**ECTS**
- Teaching HLO student (9 month final internship)	2012-2013	400	14.3
- Teaching Pathology classes to medical students	2014-2017	80	2.9
Total:		480	17.2
Lecturing			
n/a			

ACKNOWLEDGEMENTS


ΝΤΑΝΑ ΜΟΥΣΤΑΦΑ ΜΑΞ ΚΡΟΣ ΑΝΝΤΡΕΑ ΣΑΚΕΤΗ ΕΛΛΗ ΜΠΟΧΑΡΤΣ ΤΑΛ ΜΠΡΙΤ ΜΠΛΟΚΕΡ ΚΑΣΠΕΡ ΒΑΝ ΑΗΚ
ΕΒΑ ΜΠΟΟΥΝ
ΧΡΙΣ ΝΟΛΤΟΣ ΚΑΛΚΑΝΗΣ
ΝΤΡΚ ΓΙΑΝ ΝΤΟΥΝΚΕΡ
ΜΕΡΑΕ ΓΙΑΑΝΤΕΝ
ΜΑΤΙΑΣ ΣΚΕΗΒΕ
ΣΕΡΑΦΕΙΜ ΚΑΛΚΑΝΗΣ
ΧΑΝΝΕΚΕ ΜΠΟΟΥΝ
ΚΛΑΡΙΣΣΑ ΣΠΕΛΤ
ΣΕΡΑΦΕΙΜ ΚΑΛΚΑΝΗΣ
ΑΝΝΑ ΜΑΡΙΑ ΦΕΡΝΑΝΤΕΖ
ΠΑΤΡΙΣΙΑ ΓΙΟΥΝΓΚ

ΡΕΝΕ ΒΑΝ ΛΙΡ
ΑΛΙΤΑ ΣΙΒΕΡΤΣΤ
ΣΥΓΡΙΝΤ ΣΒΑΧΕΜΑΚΕΡΣ
ΜΑΡΣΕΛ ΒΑΝ ΝΤΕΡ ΒΑΙΝΤΕΝ ΙΕΗΤΕΡ ΒΑΝ ΝΤΕΡ ΣΠΕΚ ΒΙΜ ΝΤΚ ΑΞΕΝ ΝΙΧ
ΦΡΑΝΖΙΝ ΒΑΝ ΝΕΝΤΕΡΒΕΗΝ
ΜΑΡΣΕΛ ΒΑΝ ΝΤΕΡ ΒΑΙΝΤΕΝ ΙΕΗΤΕΡ ΒΑΝ ΝΤΕΡ ΣΠΕΚ ΒΙΜ ΝΤΚ ΑΞΕΝ ΝΙΧ
ΦΡΕΝΤΕΡΚ ΒΑΝ ΝΤΕΝ ΜΙΤΕΡΧ
ΧΟΥΛΙΟ ΦΕΡΝΑΝΤΕΖ
ΧΟΥΛΙΟ ΦΕΡ ΝΑΝΤΕΖ
ΦΕΡΝΑΝΤΕΖ ΖΟΡΙΑΝΟ ΒΕΡΤΖΝΤΑΝΑΜΟΥΣΤΑ
ΦΕΡΝΑΝΤΕΖ ΖΟΡΙΑΝΟ ΒΕΡΤΖΝΤΑΝΑΜΟΥΣΤΑ
ΝΙΚΟ ΒΑΝ ΜΠΕΗΒΕΡ ΕΝ
ΦΑΜΑΞΚΡΟΣΑΝΝΤΡΕΑΣΑΚΕΤΗΕΛΛΗΜΠΟΧΑΡΤΣΤΑΛΜΠΡΙΤΜΠΛΟΚΕΡΧΡΙΣΤΟΣΚΑΛΚΑΝΗΣΝΤΕΝΙΣΣΕΝΤΟ
ΜΑΡΤΑΗΝ ΜΙΤΟΧΑΡΤΣ
ΜΑΡΤΑΗΝ ΜΙΤΟΧΑΡΤΣ ΝΤΟΥΡΚ ΦΕΚΕΖ
ΜΑΡΣΕΛ ΧΟΡΣΤΜΑΝ
ΝΙΚΟ ΒΑΝ ΜΠΕΗΒΕΡ ΕΝ ΣΕΝΑΝΤΑ ΚΟΛΙΕΝΟΒΙΤΣ
ΡΟΝΑΛΤ ΧΑΟΥΖΕΡ ΧΙΛΝΤΑ ΧΑΟΥΖΕΡ
ΓΙΑΠ ΜΠΟΝΓΚΕΡΣ
ΧΑΝΝΕΚΕ ΜΠ ΟΟΥΝ
ΚΟΡΑ ΣΑΝΝΤΕΡΣ ΣΟΦΙΑ ΚΑΛΚΑΝΗ
ΣΑΝΝΤΕΡΣ ΑΝΝΤΡΕ Χ ΕΝΓ ΒΑΝ ΝΤΑΙΚΕ
ΧΑΟΥΖΕΡ
ΝΤΑΝΥ ΒΑΝ Ν ΤΕΡ ΒΑΗΚ
ΡΟΜΕΡΛΕΠΛΑΝΤΕΝΑΝΙ ΤΑΣΙΒΕΡΤΣΤ ΣΟΥΖΑΝΝΕ ΣΠΟΡΜΑΝΣ
ΜΠΑΟΥΝΤΕΒΑΗΝ ΚΛΟΠ
ΑΟΥΡΟΡΑ ΜΕΝΕΝΝΤΕΖ
ΑΟΥΤΕΟ ΛΑΟΥΝΤΕΡ
ΦΡΕΝΤΕΡΚ ΒΑΝ ΜΙΤΕΡΧ
ΜΑΡΣΕΛ ΧΟΡΣΤΜΑΝ
ΑΜΠΡΙΤΜΑΟΚΕΡΧΡΙΣΤΟΣΚΑΛΚΑΝΗΣΝΤΕΝΙΣΣΕΝΤΟ
ΡΕΝΕ ΒΑΝ ΛΙΡ ΝΤΙΡΚ ΓΙΑΝ ΝΤΟΥΝΚΕΡ
ΝΤΑΝΑΜΟΥΣΤΑΦΑΜΑΞΚΡΟΣΑΝΝΤ ΡΕΑΣΑΚΕΤΗΕΛΛΗΜΠΟΧΑΡΤΣ
ΡΟΠ ΒΙΛΕΜΣΕΝ
ΚΑΡΟΛΙΝΕ ΤΖΕΝ ΡΟΜΙΕΡΤ ΒΑΝ ΧΟΟΤΝΖ
ΚΑΕΜΕΝΣ ΝΤΙΡΒΕΝ

ABOUT THE AUTHOR

ABOUT THE AUTHOR

Karin was born in Ridderkerk, the Netherlands on April 24, 1981. She finished grammar school summa cum laude at the "Erasmiaans Gymnasium" in Rotterdam in 1999. At the age of 15 she read "The Man Who Mistook his Wife for a Hat" by Oliver Sacks, which set the stage for the rest of her career.

She started studying Biology at University College Utrecht with the aim of becoming a neuroscientist. During her studies there, she enrolled in Medical School and was accepted for the newly started Neuroscience Research Master-program of academic excellence at Erasmus Medical Center. Her interest in how neuro(patho)physiology drives experience and behavior motivated her to do research at the intersection of Neuroscience and Psychiatry. After finishing her Neuroscience degree successfully, she worked as a junior researcher at the department of Clinical Genetics in Erasmus Medical Center before starting her internships. As a new medical doctor, Karin embarked on a PhD program in Neuropathological Oncology in 2011, combined with her Pathology residency. Although her curiosity regarding the biological foundation of (brain) diseases was fully satiated in the field of Pathology, she increasingly missed patient care and the link between pathophysiology and human experience. Karin therefore started her Psychiatry residency in 2019 at Antes/Parnassia Groep.

She aims to become a psychiatrist and researcher focusing on the neuropathology of psychiatric diseases.

Glioma Neovascularization

THE PLOT THICKENS

KARIN HUIZER